IJAE

Italian Journal of Anatomy and Embryology

Official Organ of the Italian Society
of Anatomy and Histology

Vol. 129
N. 1
2025
ISSN 1122-6714

FIRENZE
UNIVERSITY
PRESS

IJAE
Italian Journal of Anatomy and Embryology
Official Organ of the Italian Society of Anatomy and Histology

Founded by Giulio Chiarugi in 1901

Editor-in-Chief
Domenico Ribatti, University of Bari, Italy

Managing Editor
Ferdinando Paternostro, University of Firenze, Italy

Editorial Board
Gianfranco Alpini, Indiana University, USA
Giuseppe Anastasi, University of Messina, Italy
Juan Arechaga, University of Leioa, Spagna
Erich Brenner, University of Innsbruck, Austria
Marina Bentivoglio, University of Verona, Italy
Anca M. Cimpean, University of Timisoara, Romania
Lucio I. Cocco, University of Bologna, Italy
Bruna Corradetti, Houston Methodist Hospital, USA
Raffaele De Caro, University of Padova, Italy
Valentin Djonov, University of Berne, Switzerland
Amelio Dolfi, University of Pisa, Italy
Roberto di Primio, University of Ancona, Italy
Gustavo Egea, University of Barcellona, Spagna
Antonio Filippini, University "La Sapienza", Roma, Italy
Eugenio Gaudio, University of Roma "La Sapienza", Italy
Paolo Mazzarello, University of Pavia, Italy
Thimios Mitsiadis, University of Zurich, Switzerland
John H. Martin, City University New York, USA
Stefania Montagnani, University of Napoli, Italy
Michele Papa, University of Napoli, Italia
Jeroen Pasterkamp, University of Utrecht, The Netehrlands
Francesco Pezzella, University of Oxford, UK
Marco Presta, University of Brescia, Italy
Jose Sañudo, University of Madrid, Spain
Gigliola Sica, University "Cattolica", Roma, Italy
Michail Sitkovsky, Harvard University, Boston, USA
Carlo Tacchetti, University "Vita-Salute San Raffaele", Milano, Italy
R. Shane Tubbs, Tulane University, New Orleans USA
Sandra Zecchi, University of Firenze, Italy

Past-Editors
I. Fazzari; E. Allara; G.C. Balboni; E. Brizzi; G. Gheri; P. Romagnoli

Journal e-mail: ijae@unifi.it – Web site: https://www.fupress.com/ijae

Firenze University Press
via Cittadella, 7
I-50144 Firenze, Italy
E-mail: journals@fupress.com
Available online at
https://www.fupress.com/ijae

Copyright: © 2025 The Author(s). This is an open access, peer-reviewed issue published by Firenze University Press and distribuited under the terms of the Creative Commons Attribution License, which permits unrestricted use, distribution, and reproduction in any medium, provided the original author and source are credited.

Italian Journal of Anatomy and Embryology

IJAE

Vol. 129, n. 1 – 2025

Firenze University Press

Italian Journal of Anatomy and Embryology
https://www.fupress.com/ijae
ISSN 1122-6714 (print) | ISSN 2038-5129 (online)

Direttore responsabile: **Ferdinando Paternostro, University of Firenze, Italy**
Direttore scientifico: **Domenico Ribatti, University of Bari, Italy**

© 2025 Author(s)

Content license: except where otherwise noted, the present work is released under Creative Commons Attribution 4.0 International license (CC BY 4.0: https://creativecommons.org/licenses/by/4.0/legalcode). This license allows you to share any part of the work by any means and format, modify it for any purpose, including commercial, as long as appropriate credit is given to the author, any changes made to the work are indicated and a URL link is provided to the license.

Metadata license: all the metadata are released under the Public Domain Dedication license (CC0 1.0 Universal: https://creativecommons.org/publicdomain/zero/1.0/legalcode).

Published by Firenze University Press

Firenze University Press
Università degli Studi di Firenze
via Cittadella, 7, 50144 Firenze, Italy
www.fupress.com

IJAE
ITALIAN JOURNAL OF ANATOMY AND EMBRYOLOGY

Firenze University Press
www.fupress.com/ijae

OPEN ACCESS

Citation: Lippi, D., Cammelli, D., Zucchini, E., Vignozzi, L., Galassi, F. M., Belviso, I., Paternostro, F. & Varotto, E. (2025). Visual Thinking Strategies for medico-anatomical teaching and rheumatological diagnostics: the case of M. L. Greville Cooksey's *Maria Virgo* (1915). *Italian Journal of Anatomy and Embryology* 129(1): 3-8. doi: 10.36253/ijae-16176

© 2024 Author(s). This is an open access, peer-reviewed article published by Firenze University Press (https://www.fupress.com) and distributed, except where otherwise noted, under the terms of the CC BY 4.0 License for content and CC0 1.0 Universal for metadata.

Data Availability Statement: All relevant data are within the paper and its Supporting Information files.

Competing Interests: The Author(s) declare(s) no conflict of interest.

Visual Thinking Strategies for medico-anatomical teaching and rheumatological diagnostics: the case of M. L. Greville Cooksey's *Maria Virgo* (1915)

Donatella Lippi[1], Daniele Cammelli[1], Elisa Zucchini[2], Linda Vignozzi[3], Francesco M. Galassi[4,6], Immacolata Belviso[5], Ferdinando Paternostro[1,*], Elena Varotto[6,7]

[1] *Department of Experimental and Clinical Medicine, University of Florence, Florence, Italy*
[2] *Department of History, Archaeology, Geography, Fine and Performing Art, University of Florence, Florence, Italy*
[3] *Department of Biomedical, Experimental and Clinical Sciences "Mario Serio", University of Florence, Florence, Italy*
[4] *Department of Anthropology, Faculty of Biology and Environmental Protection, University of Lodz, Łódź, Poland*
[5] *Department of Psychology and Health Sciences, Telematic University Pegaso*
[6] *School of Biomedicine, The University of Adelaide, Adelaide, SA, Australia*
[7] *Archaeology, College of Humanities, Arts and Social Sciences, Flinders University, Adelaide, SA, Australia*
*Corresponding author. E-mail: ferdinando.paternostro@unifi.it

Abstract. The paper exemplifies the use of Visual Thinking Strategies method in the biomedical area as implemented in the degree course in Medicine and Surgery at the University of Florence through the analysis of the Pre-Raphaelite painting *Maria Virgo* by May Louise Greville Cooksey. The team includes an art historian, a medical historian, two palaeopathologists, a rheumatologist, an endocrinologist and two anatomist, who have adopted their disciplines' diagnostic methodologies. The nodose hands of the Virgin Mary in the painting remind the art historian of Botticelli's and Filippino Lippi's Madonne, models for the Pre-Raphaelites, whereas the rheumatologist conjectures that she suffers from knuckle pads.

Keywords: Visual Thinking Strategies, fictopathography, medical didactics, rheumatology, art and medicine, anatomy.

INTRODUCTION

Visual Thinking Strategies (VTS) are an educational strategy that trains students, using works of art, counting through inclusive discussions, supporting critical thinking, visual literacy, communication and collaboration skills. The VTS were born in the USA, developed by Abigail Housen, Pro-

fessor of Art Education and Director of the Graduate Program at Massachusetts College of Art, and Philip Yenawine, when he was Director of Education at the Museum of Modern Art, New York (Housen 1987). Their longitudinal research studies on the impact of VTS have demonstrated that, in addition to growth in aesthetic understanding, VTS support the development of creative and critical thinking skills (Yenawine 2013). In front of a work of art, in which possible signs of illness are detected, the intention is not to set up a pathographic interpretation, but to solicit the students' attention to the details and signs, in the absence of symptoms (Hailey et al. 2015).

The interpretative ways that are offered are innumerable, thus we are not looking for the definitive answer, but rather training in observation, which will become an acquired posture in the clinical exercise of the profession. The literature on these topics has increased significantly, in parallel with illness stories, which do not belong to scientific texts, but are the expression of the patients' voices.

In this way, alongside the biologically identifiable disease, ample space is given to illness – as the subjective experience of being unwell – and to sickness, understood as its social dimension within a network of relationships.

Therefore, VTS represent an original interpretation for students in the biomedical area, in this way they know how to develop the clinical eye, highlighting the signs, the ability to discuss a differential diagnosis and highlight the elements that escape the untrained eye (Housen 1997).

Every year, 5th year students of the degree course in Medicine and Surgery of the University of Florence (Florence, Italy) are accompanied to the Uffizi Gallery to carry out this exercise, accompanied by a medical doctor and an art historian: in this manner, the work of art is analysed, going deep into the students' reactions and their capacity of highlighting possible signs of disease.

The work of art is silent in a certain sense: virtual patients do not report their symptoms and, for this reason, students must sharpen their eyes and highlight the possible signs.

A similar exercise is performed with reading: looking to learn to see, reading to learn to listen (Lippi 2014).

The VTS method proposes some questions to which the observer is asked to answer:

What's going on in this picture?
What do you see that makes you say that?
What else can you find?
To these, others can be added, aimed at the medical student, who can practice suggesting hypotheses and rejecting them, hypothesizing a clinical history, listing the possible tests to formulate a diagnosis:
What is the most likely history from this patient?
What would you find on further examination?
What else could you do in the clinic to further confirm the diagnosis? (Lippi et al. 2019)

This is what was called Fictopathography, "to refer to the diagnoses which are pronounced about characters who aren't real" and can be based on literature, cinema and television characters (Jutel & Russell 2023).

We have broadened this concept to works of art, broadening the fictional approach to works of art and therefore integrating VTS, through a series of more purely medical and clinical questions.

The examples we could propose are countless, but we have chosen a work recently showcased at the Exhibition *Pre-Raphaelites-Modern Renaissance*, which was held in Forlì from February to June 2024.

MATERIALS AND METHODS

The title of the artwork in question is *Maria Virgo* and the author is May Louise Greville Cooksey (Birmingham, 1878-Freshfield, Lancashire, 1943), a British painter of ecclesiastical subjects, figures and landscapes in Pre-Raphaelite style. The work is an oil on panel from the Russell-Cotes Art Gallery and Museum in Bournemouth (GB) (Russel-Cotes Museum 2024) – Link to museum's webpage: Photo credit: Bournemouth, Russell-Cotes Art Gallery & Museum, licensed under CC BY-NC-ND (https://artuk.org/discover/artworks/maria-virgo-58583). Cooksey, an alumna of the Leamington School of Arts, the Liverpool School of Arts and the South Kensington School of Arts (where she later taught), converted to Catholicism in 1899, then went to Italy on a scholarship in 1903. After her return from Italy, she devoted herself to religious paintings such as this, which was exhibited at the Royal Academy of Arts in 1915 (Cooksey 1999).

The team involved in this case study includes an art historian (E.Z.), a medical historian (D.L.), two palaeopathologists (F.M.G., E.V.), a rheumatologist (D.C.) two anatomists (I.B., F.P.) and the president of the degree course in medicine and surgery at the University of Florence, responsible for the training project, who also serves as an academic endocrinologist (L.V.). When retrospectively diagnosing artworks, the methodologies applied in retrospective diagnoses in palaeopathology are implemented (Traversari et al. 2017; Galassi et al. 2023; Varotto & Ballestriero 2018).

RESULTS AND DISCUSSION

The Virgin Mary is portrayed in profile against a brocade background – a possible reminiscence of Gentile da Fabriano's *Madonna* at the San Matteo National Museum in Pisa – holding a lily, a symbol of purity associated with the Madonna, moreover because the Archangel Gabriel usually brings a lily to Mary in the iconography of the Annunciation; indeed, this lily looks like the one in Leonardo da Vinci's *Annunciation* (1475, Florence, Uffizi). The type of the Virgin recalls examples by Botticelli and Filippino Lippi, from her delicate features to the transparent veil on her hair, as does the sombre palette, in line with the Pre-Raphaelite tenet of looking up to 14th and 15th century Italian painters preceding Raphael, especially Botticelli and other Florentines. In fact, her nodose hands remind an art historian of those visible in works from Botticelli's later years (e. g. *Lamentation over the dead Christ,* Milan, Poldi Pezzoli Museum), in works by Filippino Lippi (e. g. *Annunciation,* San Gimignano, City Museum), Piero di Cosimo (e. g. *Madonna and Child with angels,* Venice, Fondazione Giorgio Cini), all artists imitated by later Pre-Raphaelites (Acidini 2024; Catalogue entry XV.31 2024).

The hands of the Virgin Mary show nodosities at the metacarpophalangeal (MCP) and proximal interphalangeal (PIP) joints (Fig. 1). The pathology that first catches our attention is primary nodular arthrosis of the hand. Arthrosis (the osteoarthritis of the Anglo-Saxon Authors) is a degenerative joint disease characterized by erosion of articular cartilage, hypertrophy of the bones at the margins (the so-called osteophytes), sclerosis of the subchondral bone, and a series of biochemical and morphological changes in the synovial membrane and joint capsule. The sequence of pathological changes in osteoarthritis includes softening, ulceration, and focal disintegration of articular cartilage, which is followed by inflammation of the synovial membrane. Typical clinical symptoms are pain and stiffness, especially after prolonged activity (Di Cesare et al. 2017).

It is known that this disease is significantly more common in women than in men and that it generally occurs in the climacteric or perimenopausal period. The disease characteristically affects the PIP (Bouchard's nodes) and distal interphalangeal (DIP) joints (Heberden's nodes), rarely the MCPs. The female figure depicted in the picture is that of a young woman who has joint swellings in both the PIPs and MCPs. The involvement of the latter (MCPs) and the young age of the virgin make this diagnostic hypothesis unlikely, although suggestive. In fact, cases of osteoarthritis are described in the literature even at ages < 40 years (Culvenor et al. 2019).

Figure 1. Details of the Virgin's hands. Full image at the official museum's website: https://artuk.org/discover/artworks/maria-virgo-58583.

Another disease that we need to differentially diagnose is undoubtedly rheumatoid arthritis, which is known to be a chronic inflammatory disease that characteristically affects the small joints of the hands and feet symmetrically. In our picture we note that while symmetricity is respected, another key detail is present, namely sparing of DIPs. The absence of involvement of the DIPs is a peculiar feature of RA that differentiates this disease from arthrosis on the one hand and from other inflammatory rheumatisms on the other, especially psoriatic arthritis. However, if we look closely at Virgo's hands, the swellings of the fingers give the impression of having a nodular, solid, hard appearance, whereas in RA the joint inflammation is localized at the level of the synovial

membrane, where it causes a thickening of the same, the so-called synovial cloth, giving the fingers a spindle-like, soft, doughy appearance, and not hard as in arthrosis.

If we move on to consider not the joint itself, but the skin overlying the small joints of the hands, it opens up a range of diagnostic hypotheses that we will have to examine, that is it is necessary to make a differential diagnosis of the various nodosities that may occur at the DIP, PIP and MCP.

A rheumatologist would say to consider the following pathological conditions:

1. Rheumatoid nodules

They are observed that in some forms of RA, usually those with high titers of rheumatoid factor, are predominantly located at the extensor surface of the fingers.

2. Meynet nodules

They are characteristic of rheumatic fever or acute articular rheumatism (AAR), a disease of pediatric age, but also observable in adults, characterized by migrating arthritis following streptococcal angina. In AAR there is possible involvement of the heart and nervous system. Solid, painless, roundish nodules may develop in the subcutaneous tissue, the diameter of which may vary from a few millimeters to 1 or 2 cm. The skin over the lesions is not inflamed. They are found at bony surfaces or bumps or near tendons. Subcutaneous Meynet nodules generally appear only after the first few weeks of disease, usually only in patients with carditis (Guilherme et al. 2016).

3. Xanthomatosis

Xanthomatosis is characterized by the presence of yellowish nodular formations, called xanthomas, appearing in various locations (particularly in the skin and tendons), which result from the accumulation of histiocytic cells engulfing lipid substances. Tendon xanthomatosis often accompanies familial hypercholesterolemia. The Achilles tendon is the most commonly affected tendon due to xanthomatosis. Regarding hand involvement, it is known that xanthomas can occur at the level of the flexor tendons and, more rarely, at the extensor tendons. In the literature, rare are the descriptions concerning bilateral xanthomatosis involving the extensor tendons of the hand and, at the same time, causing reduced range of motion of the fingers (Brenn et al. 2019).

4. Multicentric reticulohistiocytosis

Multicentric reticulohistiocytosis (MRH) is a rare multisystem disease of unknown etiology, occurring most frequently in women characterized by localized erythematous-nodular lesions in the skin, mucous membranes, and subcutaneous tissue. There is a predilection for the hands followed by the face, extremities, and trunk. The skin lesions are multiple, symmetrical papules and nodules, ranging from several millimeters to a few centimeters. The skin lesions are often accompanied by progressive, symmetrical erosive arthritis, which is often the onset symptom. The joints of the hand, wrist, and knee are predominantly affected, followed by the shoulder and ankles. The clinical course is characterized by remission and recurrence, which in most cases results in erosive, disfiguring, and disabling arthritis. The disease is often accompanied by generalized systemic symptoms, such as weight loss, fever, malaise, myalgia, and lymphadenopathy.

Of considerable clinical importance is the frequent association of MRH with cancerous conditions such as melanoma, breast, stomach, lung, ovarian, colon, and pancreatic carcinoma, and with noncancerous conditions such as thyroid disease, diabetes mellitus, and tuberculosis.

Histological examination showed the presence of a dermal infiltrate consisting of histiocytes and multinucleated giant cells containing abundant eosinophilic cytoplasm with the characteristic “ground glass” appearance (Brenn et al. 2019; Richetta et al. 2000).

5. Knuckle pads (also known as heloderma)

These are benign, round, plaque-like, smooth, firm, well-circumscribed subcutaneous fibrotic nodules localized mainly at the dorsal portion of the proximal interphalangeal (PIP) joints and, less frequently, the metacarpophalangeal (MCP) joints of the hands; the thumbs and toes are less frequently involved. They are sometimes associated with Dupuytren’s contracture and camptodactyly. Knuckle pads are mostly asymptomatic, painless, and have a progressive growth, reaching sizes up to 40 mm in diameter. They also do not cause any functional impact on the joints, such as decreased flexibility or tendon disruption. Histologically, epidermal abnormalities such as hyperkeratosis and acanthosis can be observed, whereas at the dermal level, a proliferative stage can be distinguished, in which fibroblasts immersed in collagen bands to form an unencapsulated dermal nodule and a less cellular fibrotic stage, with spindle-shaped fibroblasts and thickened, irregular col-

lagen bundles are recognizable. The histologic picture is similar to that found in Dupuytren's contracture or Ledderhose disease, with which knuckle pads are often associated (Lagier et al. 1975).

They were first described by Garrod in 1893 (Garrod 1893). Some authors have identified knuckle pads in some of Michelangelo's works such as the David, the Moses, the statue of Victory and that of Giuliano de Medici (Allison & Allison 1966).

Knuckle pads have been associated with repetitive friction or pressure (e.g., habitual chewing or sucking of the fingers, repetitive work activities, athletic activities such as boxing and surfing, and bulimia nervosa with self-induced vomiting), fibrosing disorders (Dupuytren's contracture, Ledderhose syndrome/plantar fascial fibromatosis, and Peyronie's disease), and autosomal dominant syndrome (Bart-Pumphrey syndrome), but idiopathic cases have also been described (Giovannini et al. 2021).

CONCLUSIONS

In conclusion, the careful observation of the nodular lesions on the hands of Maria Virgo portrayed by May Louise Greville Cooksey led us to undertake a differential diagnostic exercise and to formulate several diagnostic hypotheses, each of them suggestive and possible, while emphasizing the differences that distinguish them from each other. Of all the diagnostic hypotheses examined, the most plausible is, in the rheumatologist's opinion, the knuckle pads hypothesis.

REFERENCES

Acidini C. (2024) L'amore e l'esilio. Firenze nello specchio preraffaellita fra Dante e Botticelli, in: Preraffaelliti. Rinascimento moderno. Dario Cimorelli editore, Milan, pp. 59-73.

Allison J.R. Jr, Allison J.R. Sr. (1966) Knuckle pads. Arch. Dermatol. 93:311-316.

Brenn T., Jason L., Hornick J.L. (2019) Cutaneous Mesenchymal Tumors. In: Practical Soft Tissue Pathology: a Diagnostic Approach, Second Edition. Elsevier, Philadelphia, pp. 403-457.

Catalogue entry XV.31. In: Preraffaelliti. Rinascimento moderno. Milan: Dario Cimorelli editore, 2024.

Cooksey M.L.G. (1999) In: SaurAllgemeines Künstlerlexikon. K.G. Saur Verlag, Munich-Leipzig: 1999, p. 21.

Culvenor A.G., Øiestad B.E., Hart H.F., Stefanik J.J., Guermazi A., Crossley K.M. (2019) Prevalence of knee osteoarthritis features on magnetic resonance imaging in asymptomatic uninjured adults: a systematic review and meta-analysis. Br. J. Sports Med. 53:1268-1278. doi: 10.1136/bjsports-2018-099257.

Di Cesare P.E., et al. (2017) Pathogenesis of Osteoarthritis. In: Kelley & Firestein's Textbook of Rheumatology, Tenth Edition. Elsevier, Philadelphia, pp. 1685-1704.

Galassi F.M., Lippi D., Zucchini E., Bianucci R., Varotto E. (2023) Palaeodermatological exposé on the historical case of Ferdinando II de' Medici (AD 1610-1670). J. Eur. Acad. Dermatol. Venereol. 37:2415-2418. https://doi.org/10.1111/jdv.19436.

Garrod A.E. (1893) On an unusual form of nodule upon joints of the fingers. St. Bartholomew's Hosp. Rep. 1893;29:157-161.

Giovannini I., Zandonella Callegher S., Errichetti E., De Vita S., Zabotti A. (2021) Knuckle pads mimic early psoriatic arthritis. Reumatismo 73:67-69 https://doi.org/10.4081/reumatismo.2021.1354.

Guilherme L. et al. (2016) Rheumatic Fever and Poststreptococcal Arthritis. In: Kelley & Firestein's Textbook of Rheumatology. Tenth Edition. Elsevier, Philadelphia, pp. 1956-1972.

Hailey D, Miller A, Yenawine P. (2015) Understanding Visual Literacy: The Visual Thinking Strategies Approach. In: Baylen D., D'Alba A. (eds). Essentials of Teaching and Integrating Visual and Media Literacy. Springer, New York, pp. 49-73.

Housen A. (1983) The eye of the Beholder: Measuring Aesthetic Development. Dissertation. Harvard Graduate School of Education.

Housen A. (1997) The Eye of the Beholder: Research, Theory and Practice. https://VTShome.org/wp-content/uploads/2016/08/Eye-of-the-Beholder.pdf (accessed April 5, 2020).

Huri G., Joachim N. (2013) An unusual case of hand xanthomatosis. Case Rep. Orthop. 2013; 183018. https://doi.org/10.1155/2013/183018.

Jutel A. Russell G. (2023) Past, present and imaginary: Pathography in all its forms. Health. 27: 886-902. https://doi.org/10.1177/13634593211060759.

Lagier R., Meineeke R. (1975) Pathology of "Knuckle Pads". Study of Four Cases. Virchows Arch. A. Pathol. Anat. Histol. 365:185-191.

Lippi D. (2014) Reading different literature helps one to learn to listen. Intern. Emerg. Med. 2014;9:493-495. https://doi.org/10.1007/s11739-014-1078-3.

Lippi D, Bianucci R, Donell S. (2019) The visual arts and medical education. Knee Surg. Sports Traumatol. Arthrosc. 27:3397-3399. https://doi.org/10.1007/s00167-019-05744-4.

Richetta A., Faiola R., Divona L., Calabretta F., Sansolini T., Innocenzi D., Bottoni U., Calvieri S. (2000) Multicentric reticulocytosis (Description of a case). Ital. J. Dermatol. Venereol. 135: 501-504.

Russell-Cotes Museum. Maria Virgo. https://russellcotes.com/collection-piece/maria-virgo/ (accessed on 18 September 2024).

Traversari M., Ballestriero R., Galassi F.M. (2017) A likely case of goiter in the Madonna col Bambino dormiente (1465/1470) by Andrea Mantegna (1431-1506). J. Endocrinol. Invest. 40:237-238. https://doi.org/10.1007/s40618-016-0548-z.

Varotto E., Ballestriero R. (2018) 17th-century sculptural representation of leprosy in Perugia's Cathedral. Infection. 46:893-895. https://doi.org/10.1007/s15010-018-1237-y.

Yenawine P. (2013) Visual Thinking Strategies: Using Art to Deepen Learning Across School Disciplines. Harvard Education Press, Cambridge (MA).

IJAE
ITALIAN JOURNAL OF ANATOMY AND EMBRYOLOGY

Firenze University Press
www.fupress.com/ijae

OPEN ACCESS

Citation: Maigne, J.-Y. (2025). An anatomical drawing by Leonardo as the matrix for the landscape of his Monna Lisa? An anatomical analysis. *Italian Journal of Anatomy and Embryology* 129(1): 9-16. doi: 10.36253/ijae-16064

© 2024 Author(s). This is an open access, peer-reviewed article published by Firenze University Press (https://www.fupress.com) and distributed, except where otherwise noted, under the terms of the CC BY 4.0 License for content and CC0 1.0 Universal for metadata.

Data Availability Statement: All relevant data are within the paper and its Supporting Information files.

Competing Interests: The Author(s) declare(s) no conflict of interest.

An anatomical drawing by Leonardo as the matrix for the landscape of his Monna Lisa? An anatomical analysis

Jean-Yves Maigne, MD

Department of Physical Medicine, University Hospital Hôtel-Dieu de Paris, France
E-mail: maigne@wanadoo.fr
ORCID ID: 0000-0002-7926-0790

Abstract. The landscape behind the Monna Lisa has always intrigued art historians. It is difficult to understand it and there are great differences of interpretation among Leonardo scholars. In this study, we suggest that the source of inspiration for this landscape could be an anatomical drawing by Leonardo himself, entitled the Coition of a Hemisectioned Man and Woman. Far beyond a simple coitus, it illustrates the anatomy of the mechanisms of human generation as they were understood at that time. To test this hypothesis, we compared different elements in the anatomical drawing with the landscape in the painting: respectively the left part of the drawing (female side) with the left part of the landscape and the right part of the drawing (male side) with the right part of the landscape. Indeed, the anatomical elements involved in the reproduction process and appearing in the drawing can be found in the painting as well and with the same arrangement, with more or less marked camouflage. We conclude that the landscape behind the Monna Lisa is a composite landscape with a double meaning, natural and anatomical. This stratagem may have allowed Leonardo to have his drawing admired by those who admire the portrait of a Florentine lady, without anyone knowing.

Keywords: Monna Lisa, Mona Lisa, Joconde, Leonardo Da Vinci.

INTRODUCTION

The Monna Lisa (ML) by Leonardo da Vinci is the most famous painting in the world. The portrait was commissioned by Francesco del Giocondo in 1503 to represent his spouse and to celebrate the birth of two healthy children. The painting was never delivered to its sponsor, for unknown reasons, and remained in Leonardo's hands until his death in 1519.

Beside the famous mysterious smile, the landscape appearing in the background of the painting has always remained intriguing for art historians (fig. 1). It is described as a chaotic landscape of desolation, without human presence.[1,11] The right and left parts do not match because the horizon is not at the same level on both sides and the features of the landscape are independent although very similar (mountains, lakes, rivers). The right side is in a dominant position. There is no perspective.[3,8] The lake on the left does not flow

into the valley, despite the presence of a communication point (see fig. 4).[15] The lake on the right appears slightly inclined below the horizontal. Just next to the right shoulder, there is a half hidden, perfectly spherical shaped rock, incongruous in this environment of high mountains (see fig. 3). Finally, a reddish rectangle at the bottom left (fig. 2) and a double rock at the bottom right (see fig. 7) are not understood.[8] No explanation for these anomalies has ever been given. Most art historians note that they are "not clear" [15], that they are maybe unfinished parts[8,13] or that the landscape does not obey the rules of traditional perspective.[8] They refer to the traditional explanation that Monna Lisa represents the human microcosm and embodies the macrocosm-landscape[7,12] or that it is an evocation of the passing of time.[1,11]

A careful examination of the painting allows us to present a new analysis. In this paper, we bring evidence that the landscape behind the ML might be based on a famous anatomical drawing by Leonardo, entitled "Coition of a Hemisected Man and Woman" (1492) which represents the carnal union of a man and a woman (Fig. 1).[4]

This drawing goes much further than just sexual intercourse. It illustrates the classical doctrine of Hippocrates and Galen that semen consisted of a mixture of white matter and CSF that collected and mixed at the base of the skull ("the fundamental bone of the brain"[14], according to Leonardo). Then, it followed the flow of CSF along the spinal cord where it gradually concentrated. Arriving at the very bottom of the thecal sac, it reached the testicles via hypothetical canals (which in fact were nerves).[4,9] The female brain played no role in this process, hence probably the absence of a woman's

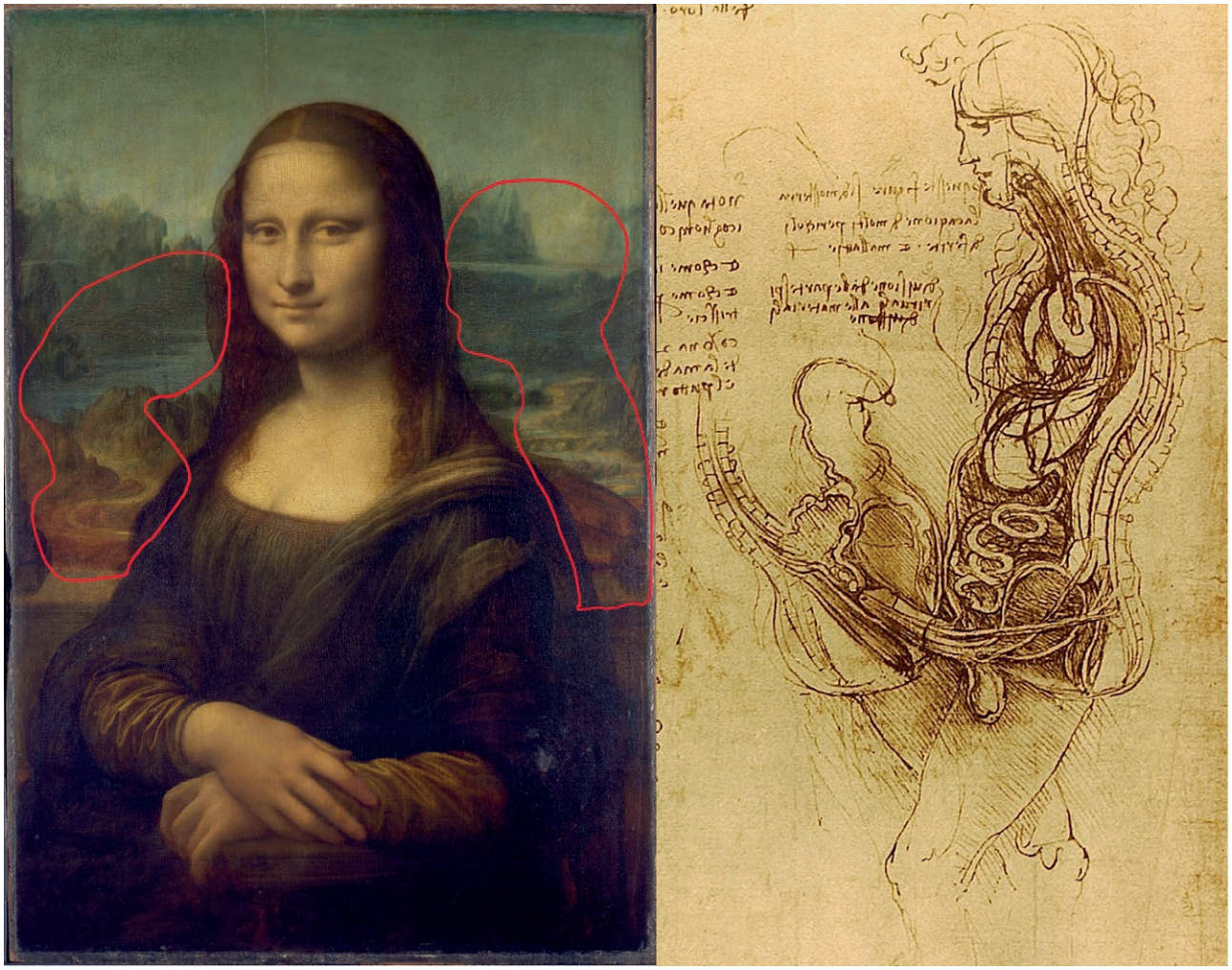

Figure 1. Left. The Monna Lisa. A landscape in two parts that does not connect. In red, the outlines of the two areas of interest of this study. Louvre Museum, Paris. Right. "Coition of a hemisected man and woman" Windsor, Royal Collection Trust. A drawing of incredible audacity which illustrates more than a mere intercourse. It is a chart of human reproduction.

head and trunk in the drawing. This theory persisted until the end of the 16th century.

METHODS

In order to demonstrate the presence of correspondences between the drawing and the painting, we compared point by point the different elements of the left part of the drawing, representing the female reproductive organs, with the left part of the landscape. We did the same with the right part of the drawing representing the male reproductive organs, comparing it with the right part of the landscape. The male reproductive organs include, according to the beliefs of the time, the base of the skull (where white matter and CSF mix together to make semen), the spine where the CSF (and the semen) flows in the thecal sac, the testicles, and the penis.

It should be remembered that Leonardo, when he painted the ML, could not have dissected women's bodies but only bovine material, gravid or not. His uterus drawings were cow uteruses and his fetus drawings were calf fetuses until 1510.

RESULTS

The anatomical drawing illustrates three key organs of the generation on the female side (1-the penis in a situation of carnal union, 2-the cervix and cervical canal and 3-the body of the uterus) and three on the male side (1-base of the skull, 2-the spine with a flow of CSF and 3-the testicles). If we carefully examine the landscape of the painting in its left and then right part, we will find these key organs (more or less camouflaged), in the same order and with the same arrangement.

First organ: the penis (Fig. 2)

There is clearly a rock looking like a penis, located to the left of the painting, halfway up. It is directed to the left as in the drawing. Its proportions and colors are accurate. One can hardly imagine another interpretation. Below is a reddish rectangular band which, in the painting, does not represent any natural element. But if we look at the anatomical drawing, we find that it is in the place occupied by the female rectum. Its representation is symbolic. These anatomical elements, arranged as in the drawing, cannot be there by chance or by a mere coincidence. Note that the sandy path that delineates this rock is very narrow and its color blends in with the surroundings. As it goes away, it widens and becomes brighter. This stratagem, against the laws of perspective, allows for camouflage because attention is drawn into the distance and not in the foreground.

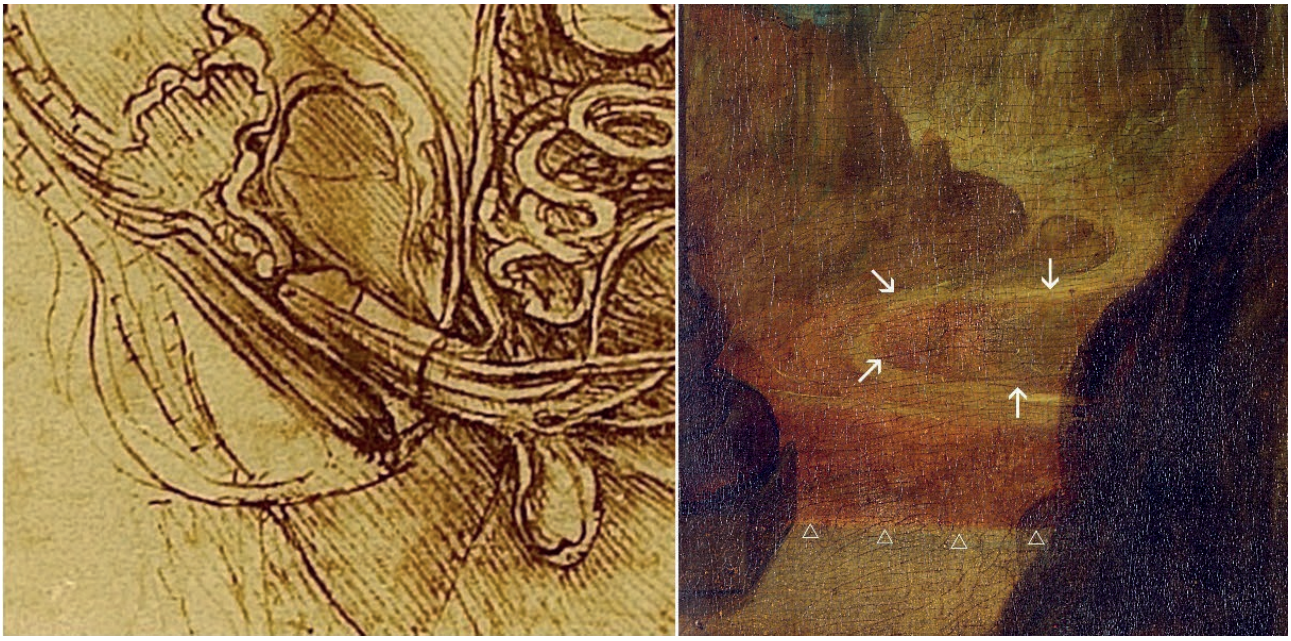

Figure 2. The rock in the center of the right image looks like a penis (white arrows). The other structure, a reddish rectangle, evokes the rectum (white triangles), with a similarity between anatomical drawing and painting.

Second organ: the cervix and cervical canal of the uterus (Fig. 3)

Above the penis, we note the presence of a perfectly spherical rock, which has not been reported by art historians. It is barely visible, which probably means that Leonardo needed it to represent what he had in mind, but that its unnatural shape required to be camouflaged. This spherical rock mirrors another rock, of a more natural rounded shape, with which it forms a pair. These two rocks seem to represent the cervix of the uterus, and the valley behind (which widens as it goes away) would represent the cervical canal. The lateral outgrowths would symbolize the circular folds he observed in the bovine uterus and which correspond to the palmate folds in humans, although bigger.

Third organ: a gravid uterus (Fig. 4)

Beyond the cervical canal, there is a lake whose longitudinal axis makes an angle of 65° with that of the valley (which represents the cervical canal); this angle is characteristic of an anteverted uterus. But a careful examination of the outline of this lake shows that it corresponds to the contours of a fetus. A fetal calf indeed, because Leonardo had never had the opportunity to dissect a human fetus, an opportunity he would have much later (circa 1510).

Fourth organ: the male's base of the skull (Fig. 5)

On the drawing, the man's head is at the top right. It is therefore by observing the upper lake that it is possible to recognize an analogy between the lake and the base of the human skull. According to the beliefs of the time, this structure was of major importance for reproduction since the CSF and white matter collected and mixed here to make semen. On the painting, the nearest shore consists of a flat part on the left and two depressions, one in the middle, the other on the right, which are in match with a profile view of the base of the skull with the anterior (which is flat), middle, and posterior fossae. The far shore draws a straight line that looks like the horizon (which means that the observer's eye is very close to the surface and in this case the lake should look horizontal), but is inclined 2.5° below the horizontal. Why? Our analysis of the drawing and the painting could explain this value (Fig. 6). Let us first look at the skulls drawn by Leonardo. He measured the obliquity of the base by drawing a line joining the junction of the vertical and the horizontal parts of the frontal bone with

Figure 3. Left. A valley which looks like the cervix and the cervical canal of the uterus. A faint spherical rock (white arrows) mirrors another rounded rock, both landmarking the cervix which extends backwards through the cervical canal. The lateral outgrowths correspond to the bovine circular folds (red arrows). Right. Image of a human cervix and cervical canal.

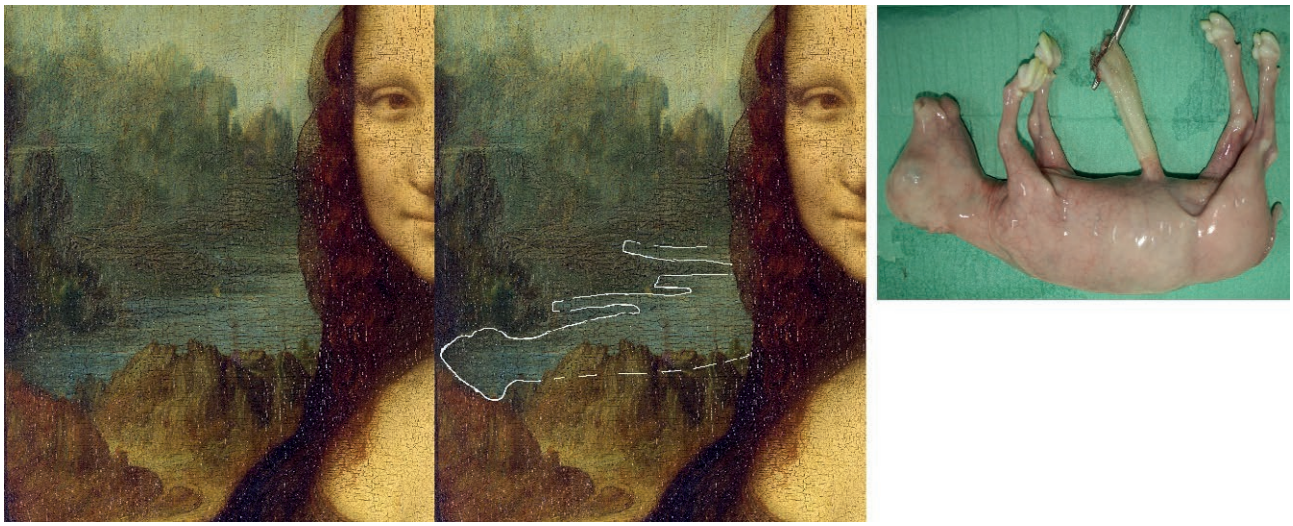

Figure 4. The outlines of the lower lake resemble to a calf fetus (seen from behind and above), which Leonardo had dissected extensively. Notice the two characteristic bumps on the skull. Courtesy Nicole Hagen, Ecole Nationale Vétérinaire de Toulouse.

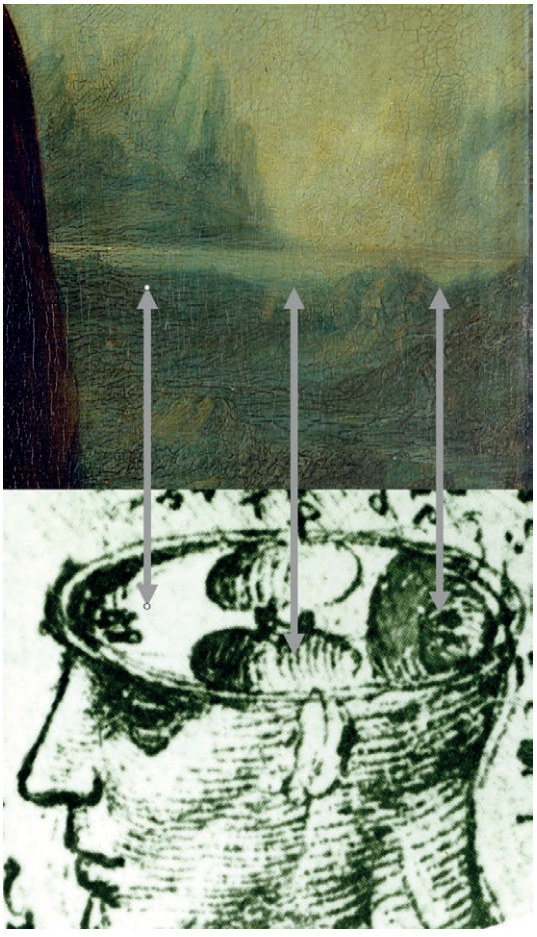

Figure 5. The superior lake can be seen as an analogy of the base of the skull with the CSF filling the temporal and occipital fossae, seen laterally. Drawing by Leonardo. Windsor, Royal Collection Trust.

the internal occipital crest, thus following the base. This line does exist on some drawings of skulls that he left us. If the gaze is horizontal, this line makes an angle of 23° with the horizontal, corresponding to the anatomical obliquity of the base of the skull. If the head flexes, this angle decreases. In the drawing, the man bends his head by 20.5°. His skull base tends to become horizontal and the angle it makes with the horizontal goes from 23° to (23°-20.5°=) 2.5°, i.e. the value of the inclination of the lake. This provides further evidence for our hypothesis.

Fifth and 6th organs: the river and the rocks (Fig. 7)

Like other elements of the landscape, the river can be read in two ways: as a river or as a symbol of the CSF flowing slowly from the base of the skull towards the bottom of the dural sac, and carrying the semen which concentrates before reaching the testicles. In favor of this interpretation, the curves of the river evoke the four curvatures of the spine as seen on the drawing.

The last element which offers a double reading is the set of two brown rocks located in the bottom right of the landscape. They are located on a line passing through the axis of the penis. This cannot be due to chance. We think that it is a scrotum that Leonardo represented. It is similar to the one in the drawing. Leonardo rotated it 70° counterclockwise, making it less identifiable than if it were in a natural position.

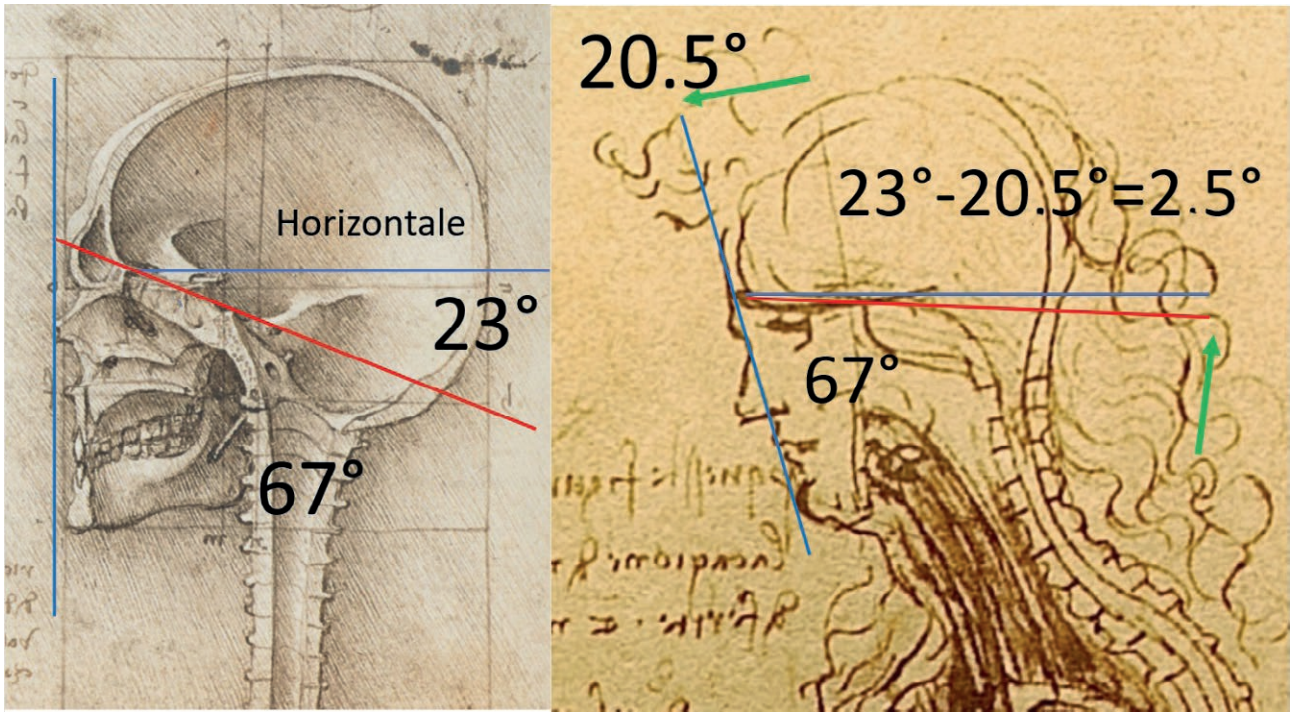

Figure 6. Left. The red line indicates the obliquity of the base of the skull, as drawn by Leonardo (Windsor, Royal Collection Trust). With a horizontal gaze, the angle is 23°. Right. Head flexed forward by 20.5°, like the young man in the drawing, the angle decreases and displays a value of 2.5°. Measurements were made by the author on high-definition reproductions.

DISCUSSION

Our results show that a famous anatomical drawing could well be the matrix of the painted landscape in the ML. If so, they could give a better understanding of the painting.

One could criticize the "subjectivity" of our description, otherwise called pareidolia. However, this word applies to forms created randomly by nature, and not by the will of a painter. Here, the realism of the penis is perfect, like that of the fetus, among others. The lake is indeed leaning by 2.5°, as predicted by our hypothesis. All this goes beyond mere subjectivity. Since there is not one but six organs represented, the probability of a resemblance due to chance becomes practically zero. Furthermore, the arrangement on the painting follows exactly that of the drawing. There is therefore a clear will from Leonardo at the origin of this composite landscape.

It is not surprising that the anatomical drawing of Coition constitutes the matrix of the landscape of the *Monna Lisa*. For Lisa Gherardini and her husband, the painting was about celebrating two motherhoods.[2] For Leonardo, it could have been also about celebrating human generation, a field that fascinated him. He was a person who disregarded conventions, as his biographers describe him.[2] Freud remarked: "The great Leonardo remained infantile all his life, in many aspects. It is said that all great men must retain something infantile. He continued to play even into adulthood, which sometimes made him strange and incomprehensible to his contemporaries."[5] The second reason could be that an anatomical drawing is destined to end up forgotten in a drawing folder. Leonardo was proud of his drawings. Paolo Giovio, an early biographer (1527), reports that he had the intention that "his work [...] would later be published in the form of engravings as an anatomy for the use of artists".[6] These engravings were not made during his lifetime. Therefore, Leonardo, choosing another way, could have wanted to discreetly incorporate his drawing into a painting, as a testimony to the mastery of his art so that it could, without the viewer knowing, be admired as long as the painting was hanging on a wall...

CONCLUSION

The results of our study shed new light on the landscape of the Monna Lisa. An anatomical drawing by Leonardo, illustrating human generation, may have

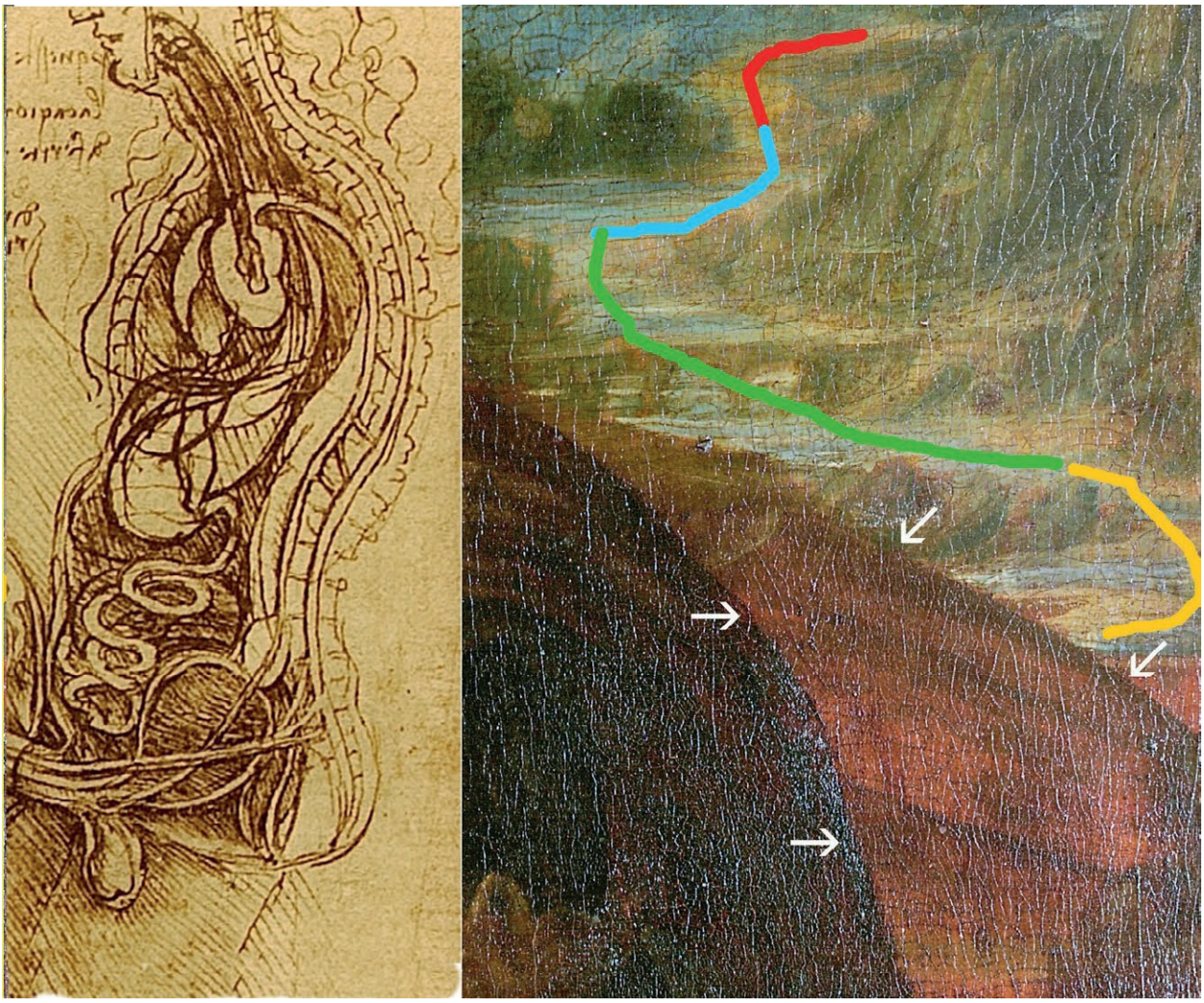

Figure 7. Left. the river and its curves, which could symbolize the flow of CSF along the cord in the spine. On the right, a spine which could correspond to the river in the painting. Windsor, Royal Collection Trust. Bottom. the two rocks are on the same horizontal line as the penis, which could indicate a connection. We interpret them as a scrotum (white arrows).

served as a matrix for the landscape, in a hidden way. We should not be surprised. Several art historians have already noted how this painting evokes the transmission of Life. In fact, our analysis extends, by deepening it, the judgments of Mohen et al: "It is the portrait of life"[7], that of Arasse[8], according to which it is one of Leonard's most personal paintings, because "he painted for him the portrait of the fertile woman" and that of Martin Kemp[9]: "Anatomy, for Leonardo, illuminated the great issues of generation, birth, life and death".

The *Monna Lisa* may not just be a portrait of a woman her husband wants to honor for the two children she gave him. It could also be a celebration of human generation. And the painter's stratagem could well explain the half smile of Lisa, like a secret between the two of them, showing complicity but also slight embarrassment.

REFERENCE

1. Arasse D. (2019) Leonard de Vinci. Hazan, Paris. p305.
2. Bramly S. (2019) Léonard de Vinci. Une biographie. Lattès, Paris. p534.
3. Carbon C., Hesslinger V. (2015) On the nature of the background behind Mona Lisa. Leonardo. 48: 182-184.

4. Clayton M., Philo R. (2012) Leonardo da Vinci anatomist. Royal Collection Enterprises Limited, Windsor. Pp. 35.
5. Freud S. (1910) Un souvenir d'enfance de Léonard de Vinci. <www.lacan-universite.fr/autour-dun-souvenir-denfance-de-leonard-de-vinci>, accessed 26 March 2024.
6. Giovio P. (1527) The life of Leonardo Da Vinci <https://nicofranz.art/en/leonardo-da-vinci/paolo-giovio-the-life-of-leonardo-da-vinci-1527>, accessed 12 December 2024.
7. Kemp M., Pallanti G. (2017) Mona Lisa. Oxford University Press, Oxford. p188.
8. Mottin B. (2006) Une lecture de l'image. In: Au cœur de la Joconde. Léonard de Vinci décodé. Gallimard, Paris. Pp. 68-70.
9. Megaloudi F., Huyghe E. (2004) L'andrologie dans la médecine hippocratique. Andrologie. 14 : 343-346.
10. Mohen J.P. et al. (2006) La Joconde, Léonard de Vinci et le visiteur : une rencontre exceptionnelle. In: Au cœur de la Joconde. Léonard de Vinci décodé. Gallimard, Paris. Pp. 119.
11. Pedretti C. (1973) Leonardo. A study in chronology and style. University of California press, Los Angeles.
12. Smith W. (1985) Observations on the Mona Lisa Landscape. The Art Bulletin. 67 (2): 183-199.
13. Vasari G. (2018) Vie des peintres, sculpteurs et architectes. Espaces&signes, Paris. Pp. 48.
14. Vinci L. (2019) Léonard de Vinci Carnets. Gallimard, Paris. Pp. 256.
15. Zöllner F. (2005) Léonard de Vinci. Taschen. Köln.

IJAE
ITALIAN JOURNAL OF ANATOMY AND EMBRYOLOGY

Firenze University Press
www.fupress.com/ijae

OPEN ACCESS

Citation: Panaccio, P. & Di Sebastiano, P. (2025). Transduodenal Surgical Ampullectomy: technical considerations. *Italian Journal of Anatomy and Embryology* 129(1): 17-20. doi: 10.36253/ijae-14856

© 2024 Author(s). This is an open access, peer-reviewed article published by Firenze University Press (https://www.fupress.com) and distributed, except where otherwise noted, under the terms of the CC BY 4.0 License for content and CC0 1.0 Universal for metadata.

Data Availability Statement: All relevant data are within the paper and its Supporting Information files.

Competing Interests: The Author(s) declare(s) no conflict of interest.

Transduodenal Surgical Ampullectomy: technical considerations

Paolo Panaccio[1,*], Pierluigi Di Sebastiano[1,2]

[1] *Department of Innovative Technologies in Medicine & Dentistry, University "G. d'Annunzio" Chieti-Pescara, Via dei Vestini, 31, 66100 Chieti, Italy*
[2] *Unit of Surgical Oncology, Casa di Cura Luigi Pierangeli, Largo Luigi Pierangeli, Pescara, Italy*
Corresponding author: E-mail: paolo.panaccio@gmail.com

Abstract. The therapeutic approaches of ampullary tumours can be both surgical and endoscopic. Surgical options include transduodenal surgical ampullectomy, first described by Halsted in 1899 and the more radical pancreaticoduodenectomy introduced by Whipple in 1935. The endoscopic ampullectomy (papillectomy) is globally recognized as the first-line procedure for benign lesions. If endoscopic resection is not feasible and safe, a surgical approach has to be considered. Surgical treatment guarantees complete removal of the lesion nevertheless, it is burdened with a mortality rate of about 3% and high morbidity (around 20–40%) even in high-volume centers. For this reason in selected cases, the local excision technique seems to be an effective and less invasive alternative to more extensive surgery (pancreaticoduodenectomy) with consequent advantages in terms of lower morbidity and mortality. A pre-operative planning in a multidisciplinary board is mandatory prior to the procedure. Given that it remains a challenging procedure that requires particular surgical experience and operative skills offering good results in terms of morbidity and mortality and should be in the armamentarium of every pancreatic surgeon. The aim of this short research article is to offer to the lecturer a comprehensive view about the transduodenal ampullectomy in the treatment of localized ampullary diseases.

Keywords: Major Duodenal Papilla, Papilla of Vater, Transduodenal Surgical Ampullectomy, local excision of Ampulla Vateri tumours.

INTRODUCTION

Knowledge of the anatomy of the Major Duodenal Papilla (MDP) or papilla of Vater and the relationship between Wirsung's duct and distal common bile duct represents an important guideline for accurate diagnostic and therapeutic approach to a variety of biliopancreatic disease (1-3). Tumours of the ampulla of Vater are relatively uncommon lesions of the digestive tract. Endoscopic papillectomy is considered as a gold standard in treatment of limited ampullary lesions. It is less extensive than transduodenal ampullectomy which involves excision of the entire ampulla together with small parts of the duodenal wall, bile duct, pancreatic duct and sometimes pancre-

atic parenchima, or pancreaticoduodenectomy (PD). The aim of this study is to report the main anatomical and embryological aspects of the ampulla of Vater and technical notes about transduodenal surgical ampullectomy (TSA) in the treatment of endoscopically non-resectable lesions of the ampulla.

MATERIAL AND METHODS

Pre-operative evaluation

The purpose of pre-operative evaluation of ampullary lesions is to determine their malignant potential, resecability, and establish stage. Preoperative work-up included computed tomography (CT-scan) and/or magnetic resonance imaging (MRI), endoscopic ultrasound (EUS) with biopsy. Endoscopic retrograde cholangiopancreatography (ERCP) and intraductal ultrasonography (IDUS) were requested in case of jaundice. EUS has been described as a critical investigation for ampullary tumours, due to its ability to determine the extent of local invasion and identify lymph-nodes metastases (4-5)

Indications for Transduodenal Surgical Ampullectomy (TSA)

Notwithstanding, many authors have described specific indications or decision making algorithms based on their own clinical series, practices or experiences (6-9). Briefly, according to our experience, suitable indications for surgical ampullectomy are: failure of endoscopic treatment (due to the presence of duodenal diverticulum or to a tumoral extension to pancreatic / duodenal /biliary wall), endoscopically unresectable bening periampullary tumors (low-grade dysplasia adenomas or high-grade/carcinoma in situ – pTis -), and selected cases of pT1 carcinoma with no lymph node involvement in patients with such comorbidities to preclude a highly complex surgical procedure such as PD. Generally accepted contraindications are T3 or T4, patients fit for PD, poorly differentiated or with nodal or distant metastases tumours. The role of TSA as a treatment for ampullary adenocarcinoma (AC) is now controversial due to the difficulty in assessment of lymph node involvement (10-12).

Surgical technique

After a right subcostal incision, a complete exploration of the cavity was carried out. The procedure started by classical cholecystectomy. After identifying the duodenum, Cattel maneuver and subsequently Kocher's maneuver was performed to allow complete exposure of the posterior duodenal wall. Bimanual palpation of the ampullary tumor complete this phase. A transverse duodenotomy of about 3–4 cm of the sec_ond duodenal portion was performed, on the antimesenteric side, facing

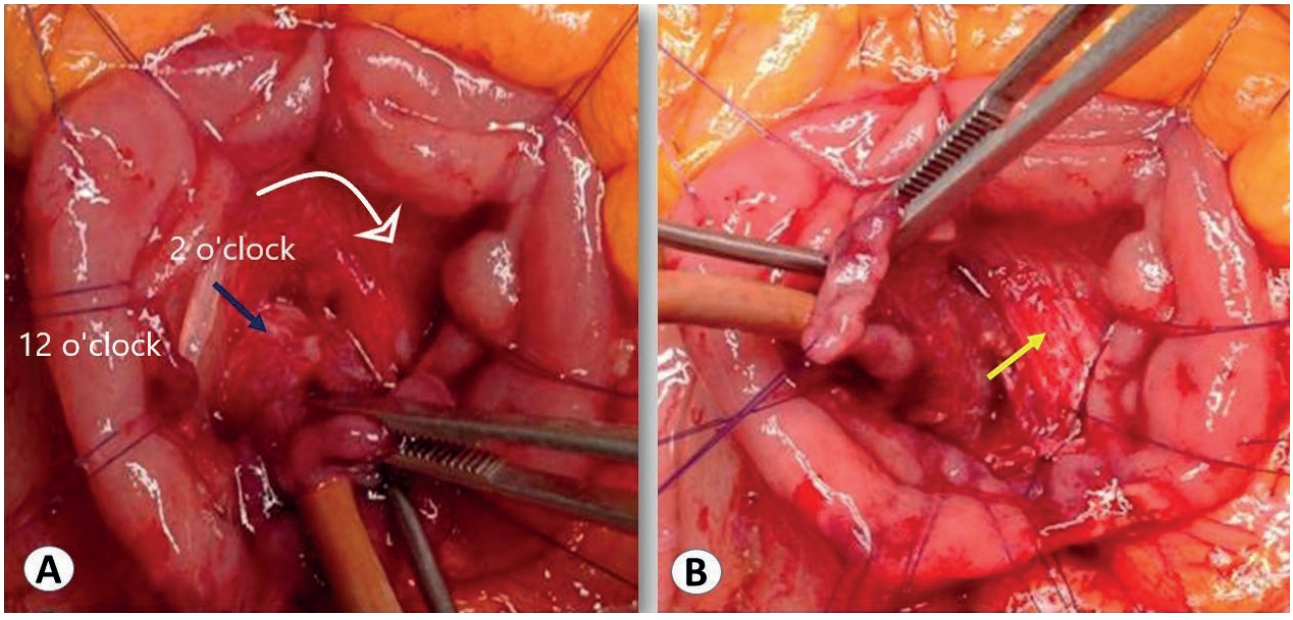

Figure 1. (a) Opening of the anterior duodenal wall and visualiza_tion of the ampulla tumor (blue arrow); (b) isolation of the ampulla from the underlying duodenal muscular layer (yel_low arrow).

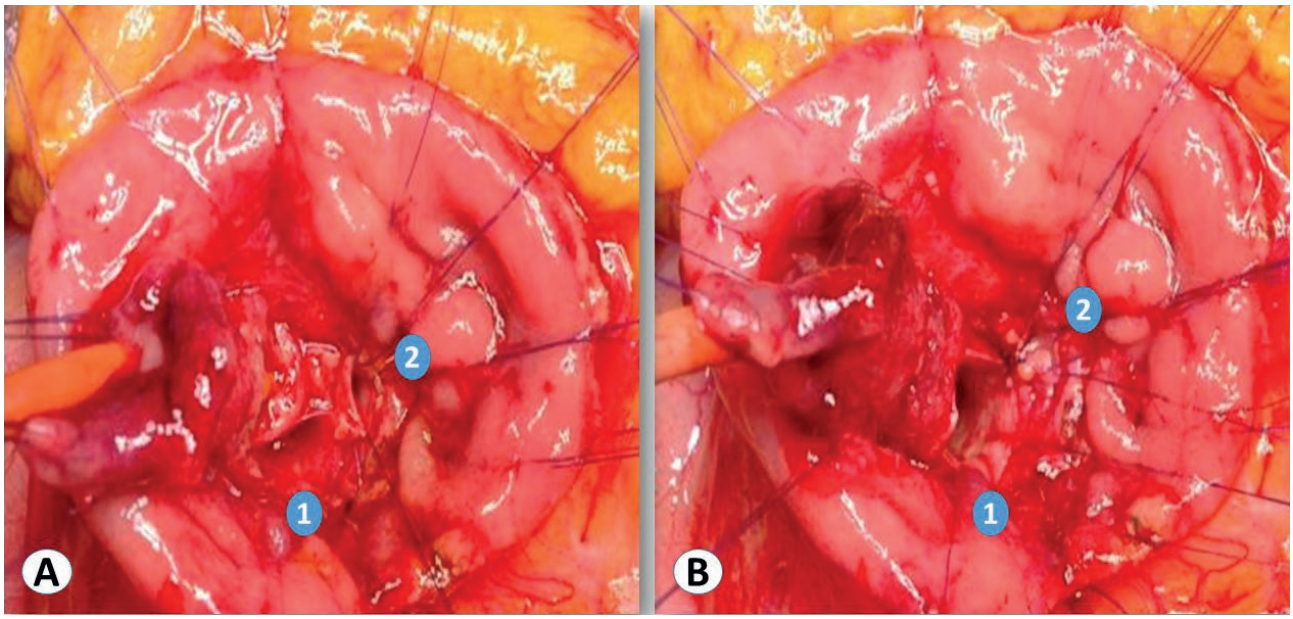

Figure 2. a Full exposure of bile duct (1) and Wirsung duct (2); b Circular clockwise dissection.

the periampullary area. To separate the wall layers, submucosal injection of adrenaline (1:1000) was performed. A "lift sign" which would exclude an infiltration by the tumor of the deeper layers. The tumor mass was then transfixed with a stitch to pull it away and better dissect the ampulla of Vater. An optimal lateral traction of the ampulla with the tumor mass during the dissection is helpful to obtain tumor-free margins. Both Wirsung and bile ducts were then separately cannulated with a Fogarty catheter as shown in Figure 1. From a frontal view and considering the major axis of the duodenum, the papilla along with Wirsung and bile duct were usually located at around 2 o'clock. The dissection of the duodenal wall, reaching the muscular layer, was made in a circular clockwise manner starting at 11 o'clock. The dissection was continued clockwise until the whole papilla was completely excised and at least 1cm free-margin was obtained as shown in Figure 2. The pancreatic and bile ducts were therefore exposed and joined together with re-absorbable stitches (5.0 PDS) so that a common ostium was created and, finally, sutured with the duodenal wall. The final appearance was shown in Figure 3. Once removed, the whole papilla was sent for intraoperative frozen section analysis. If the pathological results did not meet the criteria of a potential curative local resection through TSA (for several reasons, such as infiltration of the muscular layer of the duodenal wall, extension of the lesion beyond the biliary and/or pancreatic duct and/or histology of ampullary invasive adenocarcinoma), a pancreaticoduodenectomy was considered. A nasoduodenal tube was placed and the duodenotomy closed transversely in a double layer with interrupted monofilament reabsorbable stitches (4.0 PDS). The procedure was concluded with double laminar drainage allocation. Lastly, some authors have proposed additional components to TSA: supraduodenal lymph nodes, anterior/posterior pancreatic head lymph nodes dissection in pT1 cancers, excision of the extrahepatic bile duct providing a reduction in biliary recurrences.

RESULTS

Clinical outctome of Transduodenal Surgical Ampullectomy

No randomized clinical trial has been conducted comparing clinical outcomes in TSA, PD and endoscopic papillectomy. In recent systematic reviews and meta-analysis were reported the following results: R0 rate 96.4%, local recurrence rate 9.4%, complications rate 28.3%, mortality rate 0.9% (13-14).

DISCUSSION

While endoscopic papillectomy remains the gold standard for benign lesions, transduodenal surgical ampullectomy (TSA) can be proposed in selected cases and when endoscopy fails. With limitations of current

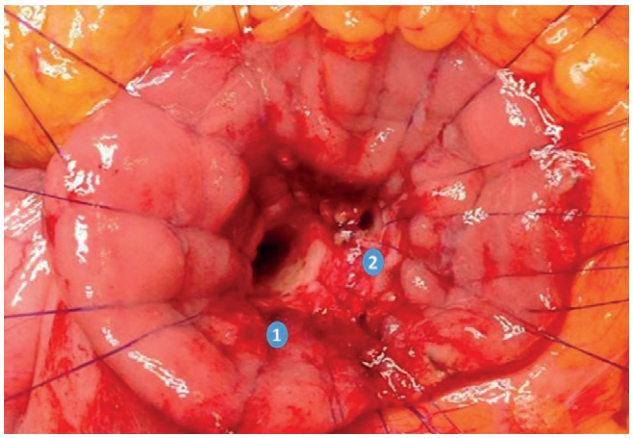

Figure 3. Bile and Wirsung ducts (1–2) are joined together with reab_sorbable stitches creating a common ostium and will be sutured with the duodenal wall in a later stage.

experience TSA is a feasible and effective. It represents and ideal therapeutic option in early ampullary lesions avoiding a demolitive procedure such as PD, with a better quality of life in a long-term follow up.

REFERENCES

1. Horiguchi SI, Kamisawa T. Major duodenal papilla and its normal anatomy. Dig Surg. 2010;27(2).
2. Taliente F, Bianco G, Moschetta G, Franco A, Giovinazzo F, Agnes S, et al. From endoscopic resection to pancreatoduodenectomy: a narrative review of treatment modalities for the tumors of the ampulla of Vater. Chinese Clin Oncol [Internet]. 2022 Jun 1 [cited 2023 Apr 30];11(3). Available from: https://pubmed.ncbi.nlm.nih.gov/35818855/
3. Dowdy GS, Waldron GW, Brown WG. Surgical Anatomy of the Pancreatobiliary Ductal System: Observations. Arch Surg. 1962;84(2).
4. Ceppa EP, Burbridge RA, Rialon KL, Omotosho PA, Emick D, Jowell PS, et al. Endoscopic versus surgical ampullectomy: An algorithm to treat disease of the ampulla of vater. Ann Surg. 2013;
5. Kandler J, Neuhaus H. How to Approach a Patient With Ampullary Lesion. Gastroenterology. 2018;155(6).
6. Kobayashi A, Konishi M, Nakagohri T, Takahashi S, Kinoshita T. Therapeutic approach to tumors of the ampulla of Vater. Am J Surg. 2006;192(2).
7. Aiura K, Shinoda M, Nishiyama R. Surgical technique for complete resection of the extrahepatic portion of the common bile duct and the ampulla of Vater for tumors of the ampulla of Vater. J Hepatobiliary Pancreat Sci. 2011;18(2).
8. Scroggie DL, Mavroeidis VK. Surgical ampullectomy: A comprehensive review. World J Gastrointest Surg. 2021;13(11).
9. Dubois M, Labgaa I, Dorta G, Halkic N. Endoscopic and surgical ampullectomy for non-invasive ampullary tumors: Short-term outcomes. Biosci Trends. 2016;10(6).
10. Song J, Liu H, Li Z, Yang C, Sun Y, Wang C. Long-term prognosis of surgical treatment for early ampullary cancers and implications for local ampullectomy Hepato-biliary-pancreatic surgery. BMC Surg. 2015;15(1).
11. Choi SB, Kim WB, Song TJ, Suh SO, Kim YC, Choi SY. Surgical outcomes and prognostic factors for ampulla of vater cancer. Scand J Surg. 2011;
12. Aiura K, Hibi T, Fujisaki H, Kitago M, Tanabe M, Kawachi S, et al. Proposed indications for limited resection of early ampulla of Vater carcinoma: Clinico-histopathological criteria to confirm cure. J Hepatobiliary Pancreat Sci. 2012;19(6).
13. Heise C, Ali EA, Hasenclever D, Auriemma F, Gulla A, Regner S, et al. Systematic review with meta-analysis: Endoscopic and surgical resection for ampullary lesions. J Clin Med. 2020;9(11).
14. Garg R, Thind K, Bhalla J, Simonson MT, Simons-Linares CR, Singh A, et al. Long-term recurrence after endoscopic versus surgical ampullectomy of sporadic ampullary adenomas: a systematic review and meta-analysis. Vol. 37, Surgical Endoscopy. 2023.

IJAE
ITALIAN JOURNAL OF ANATOMY AND EMBRYOLOGY

Firenze University Press
www.fupress.com/ijae

OPEN ACCESS

Citation: Sedeeq, B., Abdullah, A. G. & Azzubaidi, M. S. (2025). Radiographic detection of anatomical variations in the mental foramen position in a sample of Salahuddin province population. *Italian Journal of Anatomy and Embryology* 129(1): 21-27. doi: 10.36253/ijae-15656

© 2024 Author(s). This is an open access, peer-reviewed article published by Firenze University Press (https://www.fupress.com) and distributed, except where otherwise noted, under the terms of the CC BY 4.0 License for content and CC0 1.0 Universal for metadata.

Data Availability Statement: All relevant data are within the paper and its Supporting Information files.

Competing Interests: The Author(s) declare(s) no conflict of interest.

Radiographic detection of anatomical variations in the mental foramen position in a sample of Salahuddin province population

Ban Sedeeq[1], Ali G. Abdullah[1], Marwan Saad Azzubaidi[2]*

[1] *Department of Dental Anatomy, College of Dentistry, Tikrit University, Salahuddin Province, Iraq*
[2] *Pharmacology Department, Faculty of Medicine, Universiti Sultan Zainal Abidin, 20400Kuala Terengganu, Malaysia*
*Corresponding author. E-mail: mazzubaidi@unisza.edu.my

Abstract. The mental foramen (MF) is an important anatomical structure represented as a bilateral opening located on the buccal surface of the mandible, most often situated between the lower first and second premolars. This study was conducted to evaluate the size& position of mental foramen in the Iraqi population of Salahuddin province. A total of 146 OPG radiographs were included according to criteria of: Position 1: Situated anterior (medial) to the first premolar; Position 2: In line with the first premolar; Position 3: Between the first and second premolars; Position 4: In line with the second premolar; Position 5: Posterior (lateral) to the second premolar. The results revealed that the mental foramen was found most frequently at Position 4, in line with the second premolar (43.2%). Position 3, located between the first and second premolars, accounted for 31.5% of the cases. Positions 1 (anterior to the first premolar), 2 (in line with the first premolar), and 5 (posterior to the second premolar) were less common at 8.2%, 6.2%, and 11.0%, respectively. The average size of the mental foramen in the study population was 3.52 ± 0.56 mm. There was no statistically significant difference between males and females in the mental foramen size. Both groups demonstrated a similar mean size of 3.5 mm. This variation in the position of mental foramen may be due to several causes: developmental disturbances of the mandible during the fetal period, or position can be change as a consequence of dental loss and aging, as age advances and teeth are lost, the resorption of the alveolar ridges result in an apparent change in position of the mental foramen when measured from the superior border.

Keywords: mental foramen, Salahuddin, anatomical variation, radiography.

INTRODUCTION

The mental foramen (MF) is an important anatomical structure represented as a bilateral opening located on the buccal surface of the mandible, most often situated between the lower first and second premolars [1].

The mental nerve – a branch of the inferior alveolar nerve from the mandibular division of the trigeminal nerve- together with corresponding arteries and veins, exit through the mental foramen (MF) [2].

The mental nerve supplies sensation to the lower lip, the labial mucosa, lower canines, and premolars, whereas blood vessels supply soft tissues of the lower jaw [3]. To anesthetize the anterior teeth, including the premolars and canines, it is possible to avoid using an inferior alveolar nerve block by injecting an anesthetic solution adjacent to the mental foramen [4].

Anatomy of mental nerve and foramen

The mandibular canal runs anteriorly along the internal surface of the mandible; it splits into the mental and incisive canals; the incisive canal continues anteriorly to the incisors & lower canine teeth, and the mental canal runs superior-laterally to the mental foramen [5].

The mandibular nerve (V3) originates from the trigeminal nerve (CN V). It enters the mandibular foramen at the medial aspect of the ramus and horizontally forward in the body as an inferior alveolar nerve (IAN) along with the inferior alveolar artery and vein [5].

The mental foramen is situated on the buccal cortex of the mandibular bone, just below the corner of the lip on either side and in close relation to the root of the 2nd mandibular premolar tooth. It moves in a posterior direction during the development of the mandible [6][7].

A very small percentage of the population (1%) has bifurcated mandibular canals. Therefore, the bifurcated mandibular canal will exit in two separate mental foramina. In this case, clinicians must be cautious since a panoramic or periapical film may not show it. However, there are some rare reports of anatomical variations, including accessory mental foramina [8,9].

The significance of mental foramen

A mental nerve block, performed in the mental foramen region, is a very useful method of achieving local anesthesia for carrying out painful procedures in its field of supply. Mental nerve blocks are frequently carried out by dentists, oral maxillofacial surgeons, emergency physicians, and plastic and reconstructive surgeons [10]. It is an important landmark to consider during surgical endodontic procedures [11]

Dentists carry out mental nerve blocks to facilitate the management of periodontal pathologies such as tooth extractions, root canal treatments, scaling, polishing, and the treatment of gingival disease. Oral maxillofacial surgeons need to accurately locate the mental foramen and nerve during complex intra-oral procedures such as implant surgery, periapical surgery, orthognathic procedures, and trauma to avoid injury to the nerve [12].

Plastic and reconstructive surgeons perform mental nerve blocks for the repair of lower lip and chin lacerations and reconstructive procedures involving the area of supply of the mental nerve [13].

Complications related to procedures involving the mental nerve include local anesthetic toxicity due to inadvertent intravascular administration or from using large toxic doses of local anesthetic agent, inadequate anesthesia, hematoma formation, and nerve injury [14].

The mental nerve may be injured by direct trauma from the injection needle, nerve compression as a result of inadvertent infiltration into the mental foramen, nerve compression secondary to hematoma formation, and neurotoxicity from the local anesthetic itself [15].

Mental foramen in radiograph

A precise size and location of mental foramen (MF) is important for different clinical dental procedures [16]. Lack of knowledge about the correct position of the mental foramen leads to repeated failure during injections and operative procedures [17]. Before dental surgery, high safety measures must be taken to avoid harming these vital structures using appropriate imaging techniques [18, 19].

Injuries of the mental nerve via dental procedures such as curettage, root canal treatment, periapical surgery, orthognathic surgery, or local anesthetics injection in implant will lead to defects in the lower lip sensation, in addition, the surrounding skin and soft tissues [20, 21].

The exact identification of the mental foramen area is still, even now, the most common challenge for many dentists arranging to operate on or close the mental foramen.

Panoramic radiograph allows us to get a clear image of layers where the maxilla and mandible are in, called focal trough, while other parts are blurred. In panoramic radiographs, the entire body of the mandible can be viewed, which allows a more accurate location of the mental foramen in buccolingual measurement and both the horizontal and vertical dimensions. Hence, there are no absolute anatomical landmarks for reference, and the foramen cannot be clinically visualized or palpated [15].

This study aims to evaluate the radiographical size and location of the mental foramen in the Iraqi population of Salah-Uddin province.

MATERIALS AND METHODS

Radiographic determination of the position and size of mental foramen was done. Of 255 recruited OPG

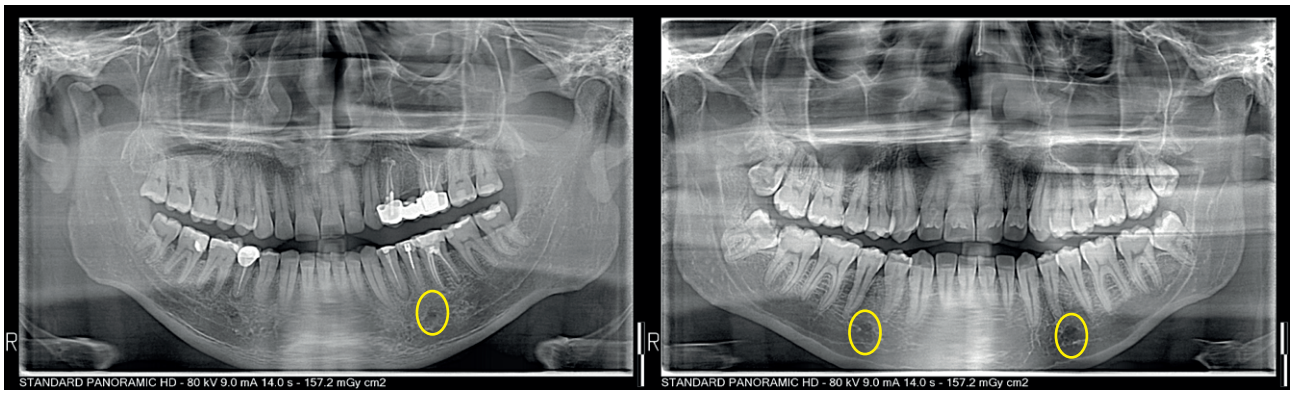

Figure 1. Different OPG images demarcating mental foramen. Yellow circles indicate the mental foramen position.

radiographs, 146 (96 males and 50 females) were deemed suitable and examined. The remaining 104 patients did not tally with the inclusion and exclusion criteria. OPG radiographs were initially decided for patients in Salahuddin province, Iraq, for various diagnostic reasons such as treatment planning before implant placement, assessment of relationships of teeth location with clinically important anatomical structures, dental surgery, and diagnosis of radiolucent lesions, as revealed in Fig. 1.

Inclusion criteria	Exclusion criteria
High quality with respect to angulations and contrast	Inadequate Radiograph quality.
Presence of mandibular teeth from the right first molar to the left first molar	Previous orthodontic treatment.
Visibility of mental foramen	There is no visualization of the mental foramen unilaterally and bilaterally on OPG.
No lesion in the apical area of premolars and MF,	Presence of pathological lesions in the mandible
No bone resorption.	Bone resorption or fractures in regions of examination.
	Extraction of lower 1st molars, 1st or 2nd premolars unilaterally and bilaterally

The OPG Radiographs were selected according to the following criteria:

The position (P) of the MF was recorded according to the following:

P 1: MF situated anterior (medial) to the first premolar; P 2: MF is in line with the first premolar; P 3: MF is between the first and second premolars; P 4: MF is in line with the second premolar; P 5: Posterior (lateral) to the second premolar, as shown in Fig. 2 [22].

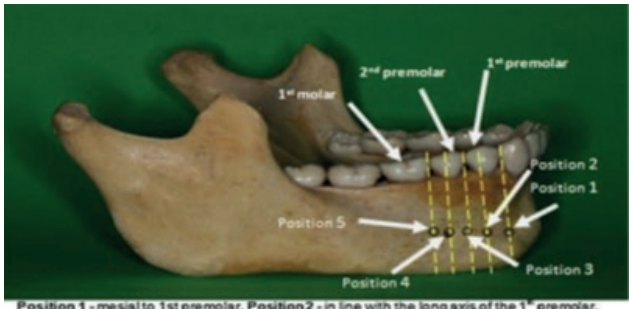

Figure 2. Different estimated locations of mental foramen.

RESULTS AND DISCUSSION

Position of the Mental Foramen (see Table 1).

Mental Foramen Size according to Side and patient's sex

A significant difference in the mental foramen size between the left and right sides was observed, with the mean foramen size being larger on the left (3.73 ± 0.4 mm) than the right (3.3 ± 0.6 mm), as per the Independent Samples Test ($p < 0.01$) (Table 2). There was no statistically significant difference between males and females in the mental foramen size. Both groups demonstrated a similar mean size of 3.5 mm. The Independent Samples Test yielded a p-value of 0.51, indicating that the difference was not statistically significant (Table 2).

Mental Foramen Size according to Position

Notably, the size of the mental foramen varied significantly based on its position, as demonstrated by the

Table 1. Study population data

Index	Frequency (n=146)	Percentage
Sex		
Female	50	34.2 %
Male	96	65.8 %
Position of mental foramen		
P1	12	8.2 %
P2	9	6.2 %
P3	46	31.5 %
P4	63	43.2 %
P5	16	11.0 %
Mental Foramen Size (Mean ± SD) (mm)	3.52±0.56	

Table 2. Mental foramen size according to side and sex

	Mean ± SD (mm)	P value
Side		
Left	3.73±0.4	<0.01**
Right	3.3±0.6	
Sex		
Female	3.5±0.7	0.51 NS
Male	3.5±0.4	

P value calculated by Independent Samples T Test*

Table 3. Mental foramen size according to position

Position of mental foramen	Mean ± SD (mm)
P1	3.4±0.43
P2	4±0.63
P3	3.1±0.64
P4	3.6±0.25
P5	3.9±0.55
P value	<0.01**

P value calculated by One-way ANOVA Test*

One-way ANOVA Test ($p < 0.01$). The largest average size was recorded for P 2 (4 ± 0.63 mm), followed by P 5 (3.9 ± 0.55 mm), P 4 (3.6 ± 0.25 mm), P 1 (3.4 ± 0.43 mm), and P 3 (3.1 ± 0.64 mm) (Table 3).

Mental Foramen Size according to Position, sex, and side

In summary, the results indicate a broad variation in the size and position of the mental foramen in the examined population. Additionally, a significant difference in the foramen size was found between the left and right sides of the mandible. However, no significant differences were observed between males and females. These findings underscore the importance of carefully evaluating the mental foramen during dental surgical procedures and implant planning.

Table 4. Mental Foramen Size sorted by Position, Sex, and Side.

Position	Gender	Side	Number	Percentage (by Group)	Size (mm)
P1	Male (n=96)	Right	3	6%	2.77
		Left	3	6%	3.23
	Female (n=50)	Right	3	12%	3.87
		Left	3	12%	3.6
P2	Male	Right	3	6%	4
		Left	2	4%	3.4
	Female	Right	1	4%	3
		Left	3	12%	4.7
P3	Male	Right	16	33%	2.68
		Left	17	35%	3.61
	Female	Right	7	28%	2.23
		Left	6	24%	4.12
P4	Male	Right	21	44%	3.74
		Left	21	44%	3.89
	Female	Right	9	36%	3.47
		Left	12	48%	3.2
P5	Male	Right	5	11%	3.88
		Left	5	11%	3.85
	Female	Right	5	20%	3.68
		Left	1	4%	6

There is considerable debate regarding the normal position of mental foramen in different populations [23]. According to the available research findings, the mental foramen is usually located between the lower premolars [24, 25]. However, some studies reported that the mental foramen most commonly lies near the apex of the second premolar [26].

The current study results for mental foramen position demonstrate that the commonest position for the right side in both male and female patients was P4 (n=30, 41%), followed by P3 (n=23, 31.5%), then P5 (n=10, 13.6%), then P1 (n=7, 8.3%), and then P2 (n=4, 5.6%).

For the commonest position of the mental foramen on the left side in male and female patients, the results were P4 (n=33, 45.2 %) followed by P3 (n=23, 31.5%), then P1 (n=6, 8.2%) and P5 and (n=6, 8.2%) respectively, then P2 (n=5, 6.9%).

These findings showed that the most common position for the mental foramen was in line with the second premolar in the given population, which comes in agree-

ment with findings reported by Sankar *et al.* [21], *Ukoha et al.* [22], *Gangotri et al.* [27]. Contrastingly, a study on a Chinese population sample showed that the MF was most commonly located between the first and second premolars and its position was related to the height of the mandibular ramus. [28] In another study on a sample of the Korean population, the MF was below the second premolar. [29]

Regarding mental foramen size according to side, the current study findings revealed a significant difference between the left and right sides, with the left side having a larger mean size (3.73±0.4 mm) than the right side (3.3±0.6 mm). This finding is contrary to a study by Bello *et al.* [30], which found no significant difference in the size of mental foramen with respect to side; this is an interesting finding that could warrant further investigation.

In terms of mental foramen size according to position, the present study found that there was a significant difference between positions, with position 2 (in line with the first premolar) having the largest mean size (4±0.63 mm) and position 3 (between the first and second premolars) having the smallest mean size (3.1±0.64 mm). This is also an interesting finding that could be compared to other studies; for instance, a study by Shalash et al. on an Egyptian population found that the most common location of the mental foramen was below the apex of the second premolar, with a mean size of 3.32 mm in females and 3.60 mm in males [31]

In terms of differences in mental foramen size with regards to sex, the current study found no statistically significant difference between the males and females, in contrast to a study by Pelé et al. [32], which demonstrated that the mean diameter of the mental foramen was found to be larger in males than in females, with a difference that could reach up to 0.62 mm.

Another survey by Ngeow et al. [33] on the Malay population reported that the mental foramen was located under the second premolar in most cases and between the two premolars in 19.6%.

Although the outcomes of this study did not coincide with research on the Nigerian population by Olasoji et al. reported that the mental foramen was located between the first and second premolars in 34% of the cases and below the apex of the second molar in 24.5% of the cases [23].

This variation in the position of mental foramen may be due to several causes: developmental disturbances of the mandible during the fetal period, or position can be change as a consequence of dental loss and aging, as age advances and teeth are lost, the resorption of the alveolar ridges result in an apparent change in position of the mental foramen when measured from the superior border. The distance of the foramen from the alveolar margin is significantly reduced when edentulous [34].

Gender also influences the position of the mental foramen. Moreover, genetics, ethnics or race affect the position of the mental foramen, where it was in line & below the apex of lower second premolars but with a higher rate of 58.9% in Chinese population [25], of 52.9% in British mandibles [26], of 45.3% in Saudi population [35], and of 47.2% in Iranian population [18].

In addition, the food & feeding behaviors are important factors in the morphologic characteristics of dental structures; variability in mental foramen position may be related to different feeding habits, subsequently affecting mandibular development [34].

CONCLUSIONS

- The mental foramen is an important anatomical landmark in the orofacial region, especially when administering dental anesthetics.
- The position of the mental foramen varies among ethnic groups.
- The present study found that the most common mental foramen position in a selected sample from the population of Salahuddin province in Iraq was below the second premolar, followed by between the two premolars.

ACKNOWLEDGMENTS

The authors would like to thank Prof. Dr. Syed Hatim for contributing to the statistical evaluation of the results.

REFERENCES

[1] S. Boopathi, S Chakravarthy Marx, S Dhalapathy, and S Anupa, "Anthropometric analysis of the infraorbital foramen in a south Indian population," *Singapore Medical Journal* 2010; 51(9), 730–735.

[2] M. Concepcion and H. J. Rankow, "Accessory branch of the mental nerve," *Journal of Endodontics*, 26(10), 619-620, 2000.

[3] J. Iwanaga, K. Watanabe, T. Saga et al., "Accessory mental foramina and nerves: Application to periodontal, periapical, and implant surgery," *Clinical Anatomy* 2016, 29(4), 493– 501.

[4] M. Lipski, I. M. Tomaszewska, W. Lipska, G. J. Lis, and K. A. Tomaszewski, "The mandible and its fora-

men: Anatomy, anthropology, embryology, and resulting clinical implications," *Folia Morphologica (Poland)*, 2013; vol. 72, no. 4, pp. 285–292.

[5] I. Roa Henr´ı?quez and O. Arriagada, "Anatomical variations of Mandibular canal with clinical significance. Case Report," *International Journal of Morphology*, vol. 33, no. 3, pp. 971–974, 2015.

[6] Chu RA, Nahas FX, Di Martino M, Soares FA, Novo NF, Smith RL, Ferreira LM (2014) The enigma of the mental foramen as it relates to plastic surgery. J Craniofac Surg 25:238–242. https://doi.org/10.1097/SCS.0000000000000445

[7] Wadu SG, Penhall B, Townsend GC (1997) Morphological variability of the human inferior alveolar nerve. Clin Anat 10: 82-87.

[8] Neves FS, Torres MGG, Oliveira C, Campos PSF, Crusoe´-RebelloI (2010) Lingual accessory mental foramen: a report of an extremely rare anatomical variation. J Oral Sci 52:501–503

[9] Al-Khateeb T, Al-Hadi Hamasha A, Ababneh KT (2007) Position of the mental foramen in a northern regional Jordanian population. Surg Radiol Anat 29:231–237. doi:10.1007/s00276-007-0199-z

[10] F. M. Fabian, "Position, shape and direction of opening of the mental foramen in dry mandibles of Tanzanian adult black males," *Italian Journal of Anatomy and Embryology*, vol. 112, no. 3, pp. 169–177, 2007.

[11] Moiseiwitsch JR (1998) Position of the mental foramen in a North American, white population. Oral Surg Oral Med Oral Pathol Oral Radiol Endod 85: 457- 460.

[12] Aminoshariae, A., Su, A., Kulild, J.C., 2014. Determination of the location of the mental foramen: a critical review. J. Endodontics 40 (4), 471–475.

[13] Loudon J (2011) Beware the mental foramen. Br Dent J 210:293. doi:10.1038/sj.bdj.2011.249

[14] Smith MH, Lung KE (2006) Nerve injuries after dental injection: a review of the literature. *J Can Dent Assoc* 72, 559–564.

[15] Meechan JG (2011) The use of the mandibular infiltration anesthetic technique in adults. *J Am Dent Assoc* 142(Suppl):19S–24S

[16] Bou Serhal C, Jacobs R, Flygare L, Quirynen M, van Steenberghe D. Perioperative validation of localisation of the mental foramen. *Dentomaxillofac Radiol* 2002;31(1): 39–43.

[17] Haghanifar S, Rokouei M. Radiographic evaluation of the mental foramen in a selected Iranian population. *Indian J Dent Res* 2009; 20:1502.

[18] Seema S, Bhavana D, Kamlesh T. Morphometric analysis of mental foramen in human mandibles of Gujarat region. *Int J Sci Res* 2014; 1:367.

[19] Kquiku L, Weiglein A, Kamberi B, Hoxha V, Meqa K, Stadtler P. Position of the mental foramen in Kosovarian population. *Coll Antropol* 2013; 37:545-549.

[20] Sankar DK, Bhanu SP, Susan PJ. Morphometric and morphological study of mental foramen in dry dentulous mandibles of South Andhra population of India. *Indian J Dent Res* 2011; 22, 5426.

[21] Ukoha UU, Umeasalugo KE, Ofoego UC, Ejimofor OC, Nzeako HC, Edokwe CG. Position, shape and direction of the mental foramen in mandibles in South Eastern Nigeria. *Int J Biomed Res* 2013; 4: 499503.

[22] Abdullah Ebrahim Laher, Mike Wells, Feroza Motara, Efraim Kramer, Muhammed Moolla, Zeyn Mahomed. Finding the mental foramen. *Surg Radiol Anat* 2016; 38:469–476.

[23] Olasoji HO, Tahir A, Ekanem AU, Ab-ubakar AA. Radiographic and anatomic locations of mental foramen in northern Nigerian adults. *Niger Postgrad Med J.* 2004 Sep;11(3):230-3

[24] Akhilandeswari. B Priya Ranganath. A morphologic and morphometric study of incidence & position of mental foramen in south Indian dry mandibles. International Journal of Anatomy and Research, *Int J Anat Res* 2017, Vol 5(1):3470-73.

[25] Wang TM, Shih C, Liu JC, Kuo KJ. A clinical and anatomical study of the location of the mental foramen in adult Chinese mandible. *Acta Anat* 1986; 126:29-33.

[26] Santini A, Land M. A comparison of the position of the mental foramen in Chinese and British mandibles. *Acta Anat* 1990; 137:208-212.

[27] Gangotri S, Patni VM, Sathwane RS. Radiographic determination of position and symmetry of mental foramen in Central Indian population. *J Indian Acad Oral Med Radiol* 2011;23:1013.

[28] Guo JL, Su L, Zhao JL, Yang L, Lv DL, Li YQ, Cheng FB (2009) Location of mental foramen based on soft- and hard-tissue landmarks in a Chinese population. *J Craniofac Surg* 20:2235–2237. https://doi.org/10.1097/SCS.0b013e3181bf85f4

[29] Kim IS, Kim SG, Kim YK, Kim JD. Position of the mental foramen in a Korean population: a clinical and radiographic study. *Implant Dent.* 2006 Dec;15(4):404-11.

[30] Bello SA, Adeoye JA, Ighile N, Ikimi NU. Mental Foramen Size, Position and Symmetry in a Multi-Ethnic, Urban Black Population: Radiographic Evidence. *Journal of Oral and Maxillofacial Research* 2018;9.

[31] Shalash M, Khallaf ME, Ali AR. Position and dimensions of the mental foramen and presence of the

anterior loop in the Egyptian population: a retrospective CBCT study. *Bulletin of the National Research Centre* 2020; 44.
[32] Pelé A, Berry P-A, Evanno C, Jordana F. Evaluation of Mental Foramen with Cone Beam Computed Tomography: A Systematic Review of Literature. *Radiology Research and Practice* 2021;2021:1–10.
[33] Ngeow WC, Yuzawati Y. The location of the mental foramen in a selected Malay population. *J Oral Sci* 2003; 45:171-5.
[34] Greenstein, G., Tarnow, D., 2006. The mental foramen and nerve: clinical and anatomical factors related to dental implant placement: a literature review. *J. Periodontol.* 77 (12), 1933–1943.
[35] Al Jasser NM, Nwoku AL. Radiographic study of the mental foramen in a selected Saudi population. *Dento-maxillofacial Radiol* 1998; 27, 341-3

IJAE
ITALIAN JOURNAL OF ANATOMY AND EMBRYOLOGY

Firenze University Press
www.fupress.com/ijae

OPEN ACCESS

Citation: Mbelengwa, P. A., Mpholwane, M. L. & Xhakaza, N. K. (2025). Effect of streptozocin-induced diabetes on the histomorphometry of the liver and kidneys of male sprague dawley rats. *Italian Journal of Anatomy and Embryology* 129(1): 29-39. doi: 10.36253/ijae-15806

© 2024 Author(s). This is an open access, peer-reviewed article published by Firenze University Press (https://www.fupress.com) and distributed, except where otherwise noted, under the terms of the CC BY 4.0 License for content and CC0 1.0 Universal for metadata.

Data Availability Statement: All relevant data are within the paper and its Supporting Information files.

Competing Interests: The Author(s) declare(s) no conflict of interest.

Effect of streptozocin-induced diabetes on the histomorphometry of the liver and kidneys of male sprague dawley rats

Pfarelo A. Mbelengwa[1]*, Matome L. Mpholwane[2], Nkosi Xhakaza[1]

[1] *Department of Anatomy, School of Medicine, Sefako Makgatho Health Sciences University, Ga-Rankuwa, Pretoria, South Africa*
[2] *Department of Physiology and Environmental Health, University of Limpopo, Sovenga, 0727, South Africa*
*Corresponding author. E-mail: mbelengwapfarelo@gmail.com

Abstract. The liver and kidneys are among primary organs affected by Diabetes mellitus (DM), whereas chronic antidiabetic medication has side effects on these organs. Due to the said side effects, there is an increase in research for new natural based antidiabetic medication making use of streptozocin (STZ) induced diabetic rodent model. However, dosage and duration of STZ in diabetes induction vary with potential inconsistencies in interpretation of the results by different authors. We investigated the effects of a single dose, (50mg/kg) of STZ on the histomorphometry of liver and kidneys of male Sprague Dawley rats after 21 days of diabetes induction. Hepatocyte (HA), nuclear and cytoplasmic (CA) areas were measured in zones 1 and 3 of the liver tissues from 16 [8 Normal C, 8 STZ diabetic DM] male Sprague Dawley rats. Corpuscular, renal, glomerular tuft, tubular, epithelial, luminal areas and connective tissue were also measured in kidney tubules from the same animals using a hand tool of ImageJ software. Means were compared using a student's t-test in SPSS software. HA in zone1 of DM was significantly higher than that of the C (p=0.009), while HA in zone 3 of DM were significantly lower than in C (p=0.032). The CA in zone1 of DM was significantly higher than that of C (p=0.006). A significant change was only fibrosis of the glomerular tuft in kidneys. 50mg/kg STZ induced diabetes caused some changes in the liver and kidney tissues but not a full pathologic profile as seen in studies with a longer duration.

Keywords: diabetes mellitus, diabetic nephropathy, kidneys, liver, steatohepatitis.

INTRODUCTION

Diabetes mellitus (DM) is a metabolic condition defined by hyperglycemia resultant from lack of insulin secretion and activity. Hyperglycemia is related to organ damage and dysfunction specifically affecting the liver and kidneys, resulting in steatosis, steatohepatitis and glucosuria among other things (Guilnerme et al., 2019). As per the report by the World Health Organization (WHO), a person dies from diabetes every seven seconds, with over 4 million of these fatalities occurring in adults under 60 years (WHO, 2022). In the year

2021, diabetes statistics estimated that DM affected 536.6 million people among individuals ranging from 20 to 79 years old in 215 countries with an estimation of 783.2 million for the year 2045. It has been predicted that the total number of diabetic patients would increase by 46% in the year 2045 due to population growth in the middle income countries (Sun et al., 2022).

The liver is one of the main organs that are vulnerable to oxidative stress caused by high blood glucose levels, causing harm such as steatosis in the liver tissue (Mohamed et al., 2016). Diabetes can also cause non-alcoholic fatty liver disease (NAFLD) (Calzadilla, Bertot and Adams, 2016). Besides liver injury, DM complications include diabetic nephropathy characterised by glomerular basement membrane thickness, mesangial cell growth, and nephron ischemia in addition to liver injury (Tang, 2018).

The commonly used antidiabetic medication includes metformin and insulin injection (Hossain and Pervin, 2018). However, due to side effects and cost of the currently available antidiabetic medication, some populations resort to herbal medication believed to have antidiabetic properties (Abd Rashed and Rathi, 2021). Streptozocin (STZ)-induced diabetic rodent experimental model is commonly used in antidiabetic drug testing, however, experimental design such as the dosage of STZ and the length of time animals are observed after induction of diabetes are highly variable amongst different authors (Norgaard et al., 2020). The dosage of STZ used to induce diabetes in rats ranges from 20 mg/kg to 80 mg/kg with differing durations animals are kept after induction of diabetes in across different studies (Naseri et al., 2022). Whether the varying dosages and differences in time the diabetic animals are kept after induction of diabetes possess the same effects on organs, particularly liver and kidneys, has not been fully investigated. The dosage of 50mg/kg STS and duration of 21 days of observation of animals is common in studies looking at physiological parameters. Whether this dosage and duration induces histological changes is of scientific importance for the studies that might be interested in organ or tissue changes. The current study investigated the effects of a 50 mg/kg STZ induced diabetes over a period of 21 days in the kidneys and livers of the male Sprague Dawley rats.

MATERIALS AND METHODS

Animals

Sixteen adult male Sprague Dawley rats (three months old) weighing 220–350 g, purchased from Northwest University in South Africa were used in this study. Live animals were housed in the animal unit of Sefako Makgatho Health Sciences University's Department of Physiology. Each animal was housed in a cage in a temperature-controlled room on a 12-hour light/12-hour dark cycle, with unlimited supply of water and rat chow in accordance with the animal ethics prescriptions. Ethics approval with the ethics number (SMUREC/M/127/2022) was obtained from the animal ethics committee of Sefako Makgatho Health Sciences University which complies with the National Institute of Health (NIH) for Care and Use of Laboratory Animals in scientific experimentation.

Induction of diabetes

After a week of acclimation, the animals were fasted for 18 hours before receiving an intraperitoneal injection of freshly prepared pancreatic-cell toxin streptozocin (STZ) 1ml/kg dissolved in 0.1M sodium citrate buffer (pH 4.5) at a dose of 50 mg/kg bodyweight. Animals were then given a 5% glucose solution in their drinking water over night to prevent hypoglycemia. Blood from the tail vein was used to measure blood glucose levels after 72 hours. Fasting blood glucose levels of above 10.0 mM confirmed hyperglycemia. Bodyweights were measured daily, and blood glucose levels were measured on day 3, 7, 14 and 21 post induction of diabetes.

Experimental design

Animals were randomly assigned to one of two experimental groups: Group 1 (n=8) were normal (Control) rats, Group 2 (n=8) were STZ (50mg/kg) induced diabetic rats, all with unlimited supply of food and water. After induction of diabetes, the animals were kept for 21 days with no intervention. At the end of the 21-day period (day 22), the animals were anesthetized with an intraperitoneal injection of a mixture (1.4 ml/kg.bw) of Anaket V (Ketamine) 40-80mg/kg and Rompun 2% (Xylazine) 5-10mg/kg, after which the liver and kidney tissues were collected and preserved in 10% buffered formalin prior to processing for histological sectioning and staining.

Histological procedure

The automatic tissue processor was utilized to process liver and kidney tissues, followed by paraffin embedding. Processed and paraffin embedded liver and kidney tissues were sectioned at 5 μm thickness using

the rotary microtome and then mounted on glass slides before staining. Slide mounted liver and kidney tissues were stained with Hematoxylin and Eosin (H&E) stain for tissue architecture and Masson Trichrome (MT) stain for collagen fibre content of connective tissue using the staining protocol by Bancroft and Gamble, 2008.

Histomorphometric measurements

The photomicrographs of the H&E and MT-stained sections were taken with an Image Focus Alpha version 2.4 software connected to Image Focus light microscope (Euromex, Netherlands at 10X, 40X, and 100X). The ImageJ area tool (Schneider et al. 2012) was used to measure the hepatocyte area (HA) and nuclear area (NA) of hepatocytes (H&E at 40X magnification) in the periportal (Zone 1) and centrilobar (Zone 3) zones from slide mounted liver sections. The cytoplasmic area (CA) of each hepatocyte was calculated by subtracting the nuclear area from the total hepatocyte area, as stated by Fazelipour et al. (2008). The transitional zone, sometimes known as Zone 2, was not considered since its limits were difficult to define. A minimum of 50 hepatocytes with a nucleus and a distinct nucleolus were measured in the liver of each animal.

The ImageJ area tool was also used to measure the following parameters on kidney sections Nakayama et al. (2010): renal corpuscular area (RCA) and glomerular tuft area (GTA), proximal convoluted tubular outer area (PCT OA), proximal convoluted tubular luminal area (PCT LA), distal convoluted tubular outer area (DCT OA), and distal convoluted tubular luminal area (DCT LA). The urinary space area (USA) of each renal corpuscle was calculated by subtracting the glomerular tuft area from the renal corpuscular area. The epithelial areas of the proximal and distal convoluted tubules (PCT EA and DCT EA) were calculated by subtracting the luminal areas from the outer regions. At least 50 renal corpuscles, proximal and distal convoluted tubules were examined in each kidney, with a total of 400 measurements per treatment group.

To determine the area and area percentage of the liver occupied by collagen fibres, 50 photomicrographs per animal in each group (n = 8, i.e. 400 per group) were evaluated using the point counting method and ImageJ's cell counter plugin, as described by Ibrahim et al. (2019). The area fraction ($A_{fraction}$) occupied by connective tissue in each liver section (40X magnification) was determined using equations (a) and (b) below.

$$A_{fraction} = A \div A_{camera} \quad (a)$$

Where A = is the area occupied by collagen fibres, calculated using equation (b), and A_{camera} = area of the camera field at 40X.

$$A = App \times \Sigma p. \ (\Sigma p = \text{sum of points of the grid intersecting at connective tissue}) \quad (b)$$

Data analysis

A students t-test statistical analyses was used to compare the means of measurements done in the liver and kidney sections in SPSS version 27. Measurements for each variable were expressed as mean± standard error. A P value of ≤ 0.05 was considered as significant difference. Shapiro Wilk test was used to test for normality. P>0.05 was considered normal distribution.

RESULTS

Induction of diabetes, weights and glucose level changes

Before the induction of diabetes with STZ injection, all animals had normal blood glucose levels ranging from 4.8 to 5.8 mmol/L. After 72 hours of STZ injection, the STZ diabetic induced animals (DM) had a drastic increase of blood glucose levels to an average of 30.38 mmol/L which continued to increase over a period of 21 days to the average of 32.35 mmol/L by day 21. On the other hand, the C group maintained the normal blood glucose levels ranging from 4.8-5.8 mmol/L (Figure1A). In this experiment, animals with approximately the same body weights were used with an average weight of 316g for the DM group, and an average weight of 342g for control. The terminal weights of DM group showed a significant weight loss when compared to the initial average body weight of this group, while the control group showed a significant weight gain when compared to the initial average body weight of this group (Figure 1B). There were no statistically significant differences in the weights of liver and kidney tissues of the control and DM animals. (Table 1).

Morphological changes in the liver and kidney tissues

In the control group, no significant changes were seen on the structure of the hepatocytes in zones 1 and 3 of the H&E-stained liver tissues (Figure 2A-B). In zone 3 of the DM group, a number of hepatocytes with double nuclei, hepatotrophy and inflammatory infiltrates were observed (Figure 2C). Zone 1 showed widened sinusoi-

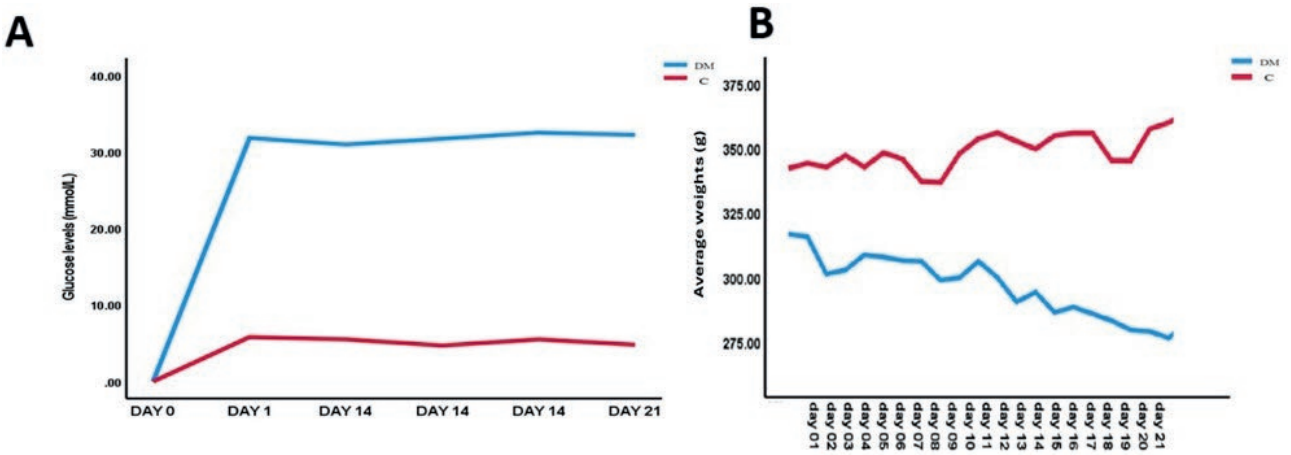

Figure 1. A: changes in the glucose levels of STZ diabetic induced and control animals from day 0 to day 21. B: graphic representation of the weight changes of the animals through the 21 days of experimental period.

Table 1. Body weight, liver, kidney and glucose level

		Control	Diabetic	P value
Weights(g)	Initial BW	343 ± 1.41	316 ± 0.78	0.005
	Terminal BW	363.75 ± 0.88	282.22 ± 0.3	0.002
	Liver	10.98 ± 0.85	10.24 ± 1.33	0.18
	Kidney	3.08 ± 0.34	3.27 ± 0.35	0.24
Glucose levels (mmol/L)	Initial	5.1 ± 0.57	30.38 ± 0.81	0.009
	Terminal	5.7±0.21	32.35±0.21	0.006

Data of all variables expressed as mean ± standard deviation.

dal spaces in some tissues of DM group (Figure 3D). In MT-stained liver sections, both control and DM groups showed moderate to no accumulation of connective tissue collagen fibers (Figure 3A-B). However, excessive accumulation of connective tissue collagen fibers was observed around the central veins (Figure 3C) and periportal areas with a few adipocyte patches.

Hepatocyte area in zone 1 of the liver was significantly higher in DM animals when compared to control animals (Figure 4; Table 2). On the contrary, hepatocyte area in zone 3 was significantly lower in DM animals compared to Control animals (Figure 4; Table 2). Nuclear area in zone 3 was significantly lower in DM animals when compared to control animals (Figure 4; Table 2). The cytoplasmic area in zone 1 was significantly higher in DM than in control animals (Figure 4; Table 2). When comparing zone 1 and zone 3 of the same animal in the DM group, hepatocyte area was significantly higher in zone 1 compared to zone 3 of control group (Figure 4; Table 2). The nuclear area was significantly lower in zone 3 compared to zone 1 in the same animal in the DM group (Figure 4; Table 2). The cytoplasmic area of zone 3 showed no significant differences when comparing the DM and control groups, even though it was slightly higher in the DM group (Figure 4; Table 2). Similarly, the student t-test detected no statistically significant differences in the nuclear area of zone 1 in the DM group compared to the C group, with the DM group showing a slightly high nuclear area of this zone (Figure 5; Table 2).

The connective tissue area fraction in the liver tissue of the DM group was significantly higher than that of the C group (Table 2). In H&E-stained sections of kidney tissues, the C group had normal renal corpuscular, glomerular, and tubular structures (Figure 5A). Kidney tissues from DM group showed glomerular basement membrane thickening, enlarged distal and proximal convoluted tubules (Figure 5B).

There were no statistically significant differences between glomerular tuft area of the control when compared to DM animals in a student t-test (Figure 4D; Table 3). The glomerular tuft area of DM animals was

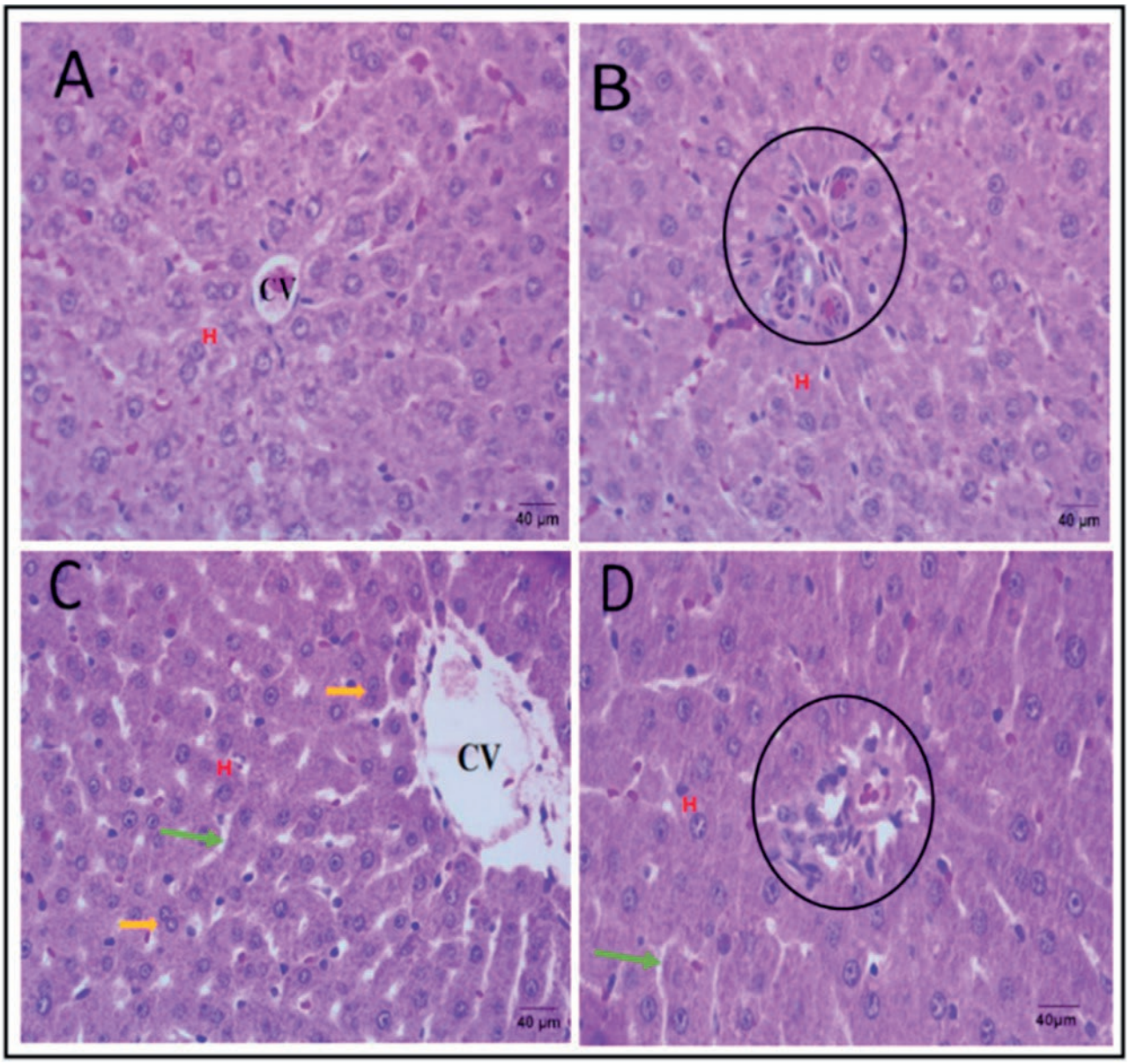

Figure 2. Photomicrographs showing the liver sections (H&E, 40X) of the control group and STZ induced diabetic animals. A) Normal liver tissue in zone 3 with intact hepatocytes and un-dilated sinusoids. B) Normal liver tissues in zone 1 as described for zone 3. C) Liver tissue of DM group showing dilated sinusoids (green arrow), a lot of cells with double nuclei (yellow arrow) and small sized hepatocytes. D) Liver tissues in the periportal area showing inflammatory cell infiltration (black circle), a few adipocytes, dilated sinusoids (green arrow), and enlarged hepatocytes with basally located nuclei. **H**= hepatocytes, **CV**=Central Vein, **Green Arrow**= Sinusoids, **Black Circle**= portal triad. **Yellow arrow**= double nuclei

slightly lower than that of control animals (Figure 4D; Table 3). Similarly, the student t-test detected no statistically significant difference between renal corpuscular area of control and DM animals, even though a slight reduction was observed in the DM animals compared to control animals (Figure 4D; Table 3). The student t-test also detected no significant differences in the urinary space area between control and DM animals, with a slight increase in the urinary space area of DM animals (Figure 4D; Table 3).

The corpuscular area also showed a slight nonsignificant reduction in DM animals in a student t-test (Table 3). There were no statistically significant differences between urinary space area of control and DM animals.

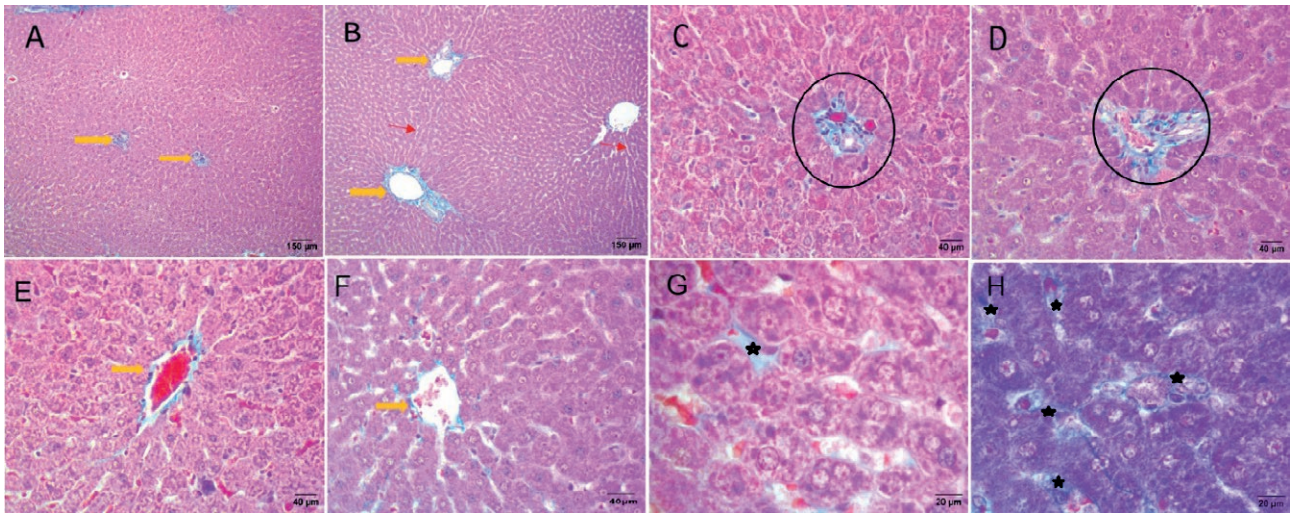

Figure 3. Photomicrographs showing MT-stained liver tissues of control and STZ induced diabetic (DM) animals. **A)** Normal distribution of collagen fibers in the liver tissue of the C group (yellow arrows) (10X). **B)** large bundles of collagen fibers around the central veins and the periportal areas (yellow arrows) of the livers of the DM group and dilated sinusoids (red arrows) (10X). **C)** Moderate bundles of collagen fibers around d the structures of the portal area in the liver tissue of the C group (black circles) (40X). **D)** Large bundles of collagen fibers around the structures of the portal area in DM group (black circles) (40X). **E)** Pericentral area of the liver tissue of the C group showing moderate amount of collagen fiber bundles around the central vein and interstitial tissue (yellow arrows) (40X). **F)** Pericentral area of the liver tissue of the DM group showing moderate amount of collagen fiber bundles around the central vein and interstitial tissue (yellow arrows). **G)** Moderate collagen fiber bundles in the interstitial space of liver tissue of the C group (black stars) (100X). **H)** Excess accumulation of collagen fiber bundles in the interstitial area of the liver tissue of the DM group (black stars) (100X). Scale bars: 10X=150μm; 40X=40μm; 100X=20μm.

Table 2. Hepatocellular, nuclear, cytoplasmic areas and connective area fraction

		C	DM	P value
Zone 1	HA	1177.41 ± 69.07	1365.48 ± 84.88	0.009
	NA	218.15 ± 21.66	234.83 ± 13.68	0.098
	CA	959.64 ± 55.57	1129.79 ± 79.63	0.006
Zone 3	HA	1009.42 ± 94.88	925.80 ± 60.93	0.032
	NA	210.10 ± 24.41	184.20 ± 24.27	0.028
	CA	799.69 ± 75.00	741.60 ± 40.91	0.061
LIVER	CT Area fraction	0.23 ± 0.84	0.38 ± 0.54	0.004

Data of all variables expressed as mean ± standard deviation.

The urinary space area of DM animals was slightly higher than that of control animals (Table 3).

The student t-test detected no significant differences in the outer area of the proximal convoluted tubule of control and DM animals, even though the proximal convoluted tubular area of the DM animals was slightly higher (Figure 4B; Table 4). Similarly, a non-significant increase in the proximal convoluted tubular luminal area was observed in DM animals compared to the control animals (Figure 4B; Table 4). The proximal convoluted tubular epithelial area also had no statistically significant differences, with slight increase in the epithelial area in DM compared to control animals (Figure 4B; Table 4). The student t-test detected no significant differences in the distal convoluted tubular outer area, luminal area and the epithelial area when comparing the DM to control animals. However, all three of the above parameters, showed a slight increase in DM animals (Figure 4C; Table 4).

In MT-stained kidney tissues, moderate accumulation of glomerular connective tissue was observed in control animals (Figure 6A), whereas kidney tissues of DM animals showed excess accumulation of collagen fibers in the glomerular tuft (Figure 6B). The connec-

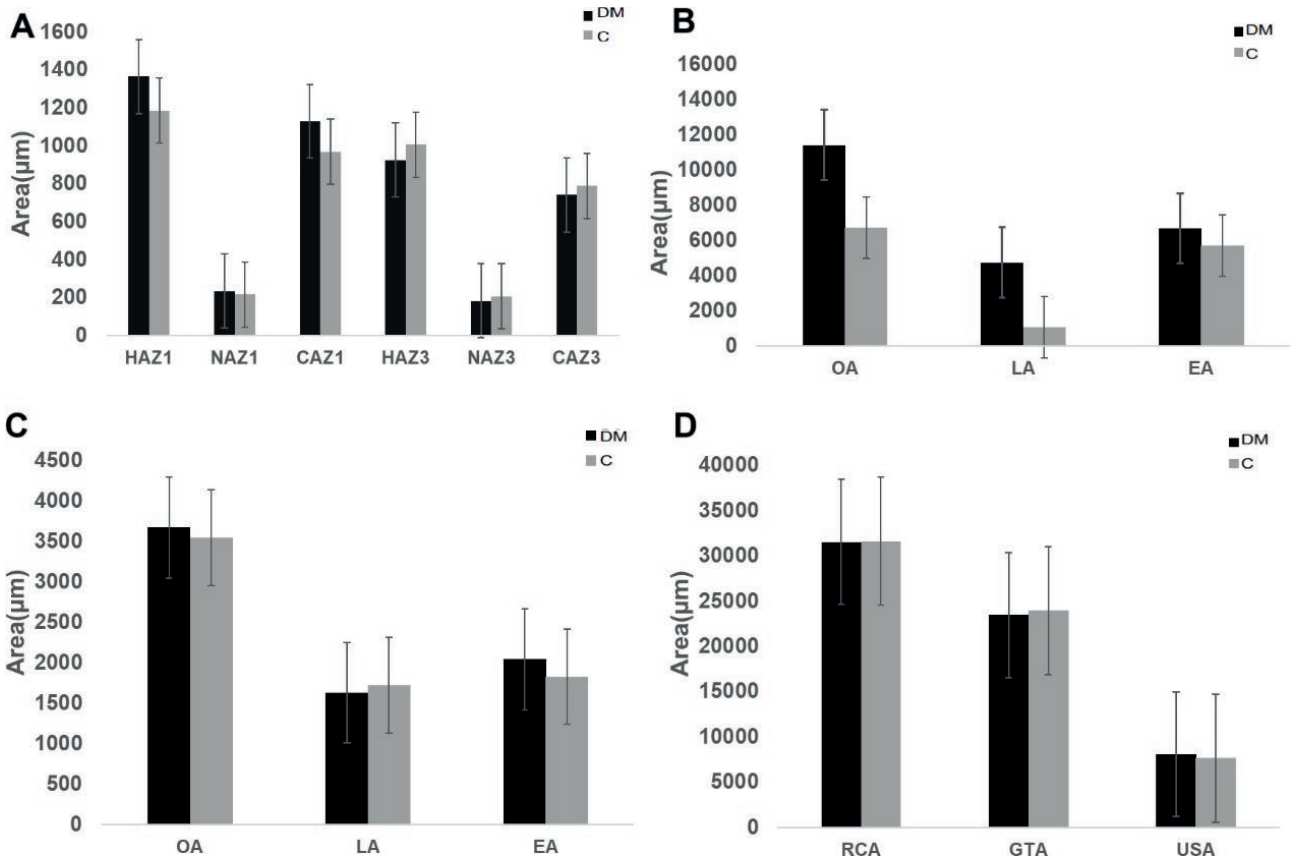

Figure 4. Graphic representation of the **A**: hepatocyte, nuclear and cytoplasmic areas in zone 1 and zone 3 of the liver tissues of control and DM, **B**: changes in tubular outer, luminal and epithelial areas of the proximal convoluted tubule in control and DM animals, **C**: changes in tubular outer, luminal and epithelial areas of the distal convoluted tubule in control and DM animals, **D**: renal corpuscular, glomerular tuft and urinary areas of control and DM animals.

Table 3. Renal corpuscular, glomerular tuft, urinary space areas and connective tissue area fraction.

	C	DM	P value
RCA	32177.98 ± 4067.97	31531.95 ± 1614.26	0.383
GTA	24408.61 ± 3757.01	23448.74 ± 1503.30	0.294
USA	7769.37 ± 1541.50	8083.22 ± 1205.63	0.379
GT CT Area fraction	0.72 ± 0.29	1.39 ± 0.33	0.009

Data of all variables expressed as mean ±standard deviation.

tive tissue area fraction in the glomerular tuft of DM animals was significantly higher than that of the control animals (Table 4).

DISCUSSION

The study aimed to investigate the effects of a single dose of 50mg/kg Streptozocin (STZ) induced diabetes on the histomorphometry of the liver and kidneys of male Sprague Dawley rats over 21 days. Hyperglycemia caused by STZ resulted in a decrease in body weight over 21 days. This decrease could be attributed to the induction of ketoacidosis, wherein the body, lacking insulin in Type 1 Diabetes Mellitus (T1DM), turns to fat oxidation, leading to the production of ketones and subsequent weight loss (Dhillon and Gupta, 2018).

Liver weights decreased in STZ-induced diabetic rats compared to controls, in agreement with Salahshoor et al. 2019 who found the same weight differences

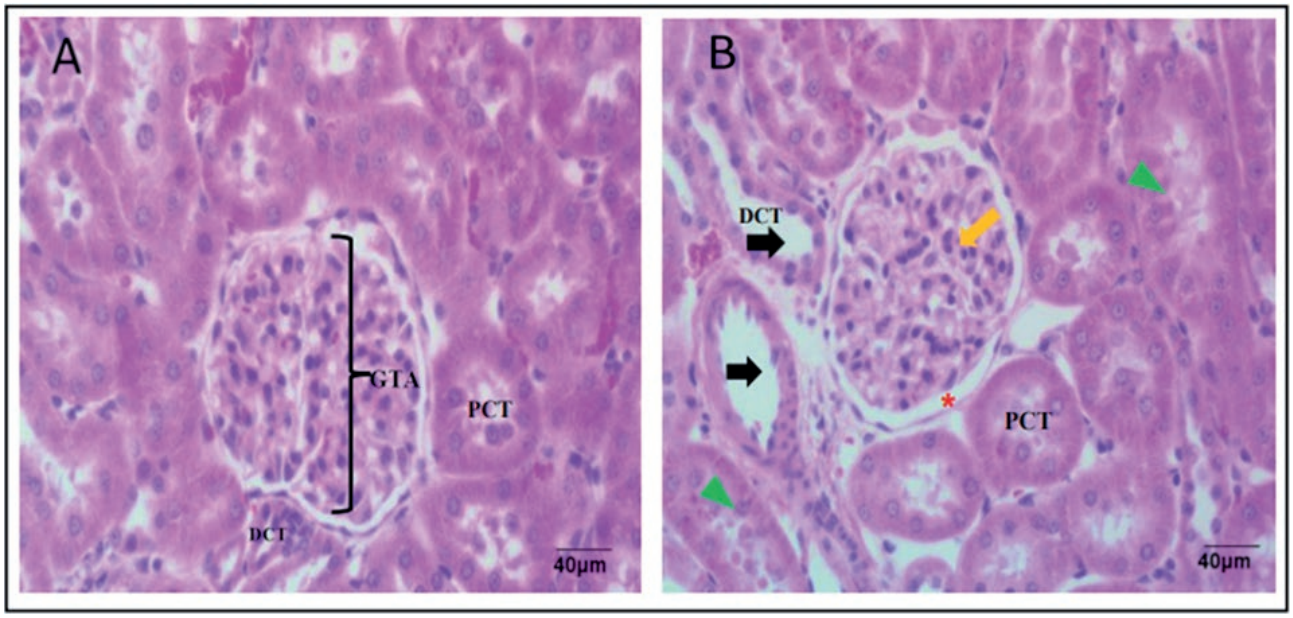

Figure 5. Photomicrographs showing kidney tissues of control and DM animals (H&E 40X). **A**: Control group, showing normal renal corpuscular, glomerular, and tubular structures. **B**: DM group showing slightly enlarged renal corpuscular area (orange arrow), distorted renal corpuscle (red star), enlarged luminal area of PCT (green arrowhead) and DCT (black arrow). **PCT**= Proximal convoluted tubule, **DCT**= Distal convoluted tubule, **GTA**= Glomerular tuft area.

Table 4. Proximal and distal convoluted tubular areas.

	C	DM	P value
PCT OA	6859.81 ± 753.91	11432.19 ± 10169.98	0.167
PCT LA	1016.14 ± 149.55	4739.05 ± 8531.91	0.171
PCT EA	5843.67 ± 728.26	6693.14 ± 1667.22	0.172
DCT OA	3512.40 ± 485.27	3676.71 ± 583.97	0.33
DCT LA	1703.13 ± 329.16	34808.05 ± 81450.65	0.183
DCT EA	1809.26 ± 223.19	2044.88 ± 384.15	0.107

Data of all variables expressed as mean ±standard deviation.

even though they used a higher dose (60mg/kg) and a longer duration (28 days). The observed weight reduction is likely due to high blood glucose levels causing cell damage and liver cell shrinkage (Michalopoulos and Bhushan, 2021). Conversely, kidney weights exhibited a slight increase, possibly indicating fibrosis due to renal inflammation. Histomorphometric analysis revealed significant changes in hepatocellular and renal structures. In the liver, an increase in hepatocyte area in zone 1 was observed in diabetic induced animals, potentially indicating steatohepatitis, characterized by liver inflammation and fat accumulation (Scorletti and Carr, 2022). There was a decrease in the zone 3 hepatocellular area, nuclear area and cytoplasmic area of diabetic induced animals compared to control animals. The observed decrease in hepatocytes of zone 3 could be due to steatosis associated with NAFLD. Non-alcoholic fatty liver disease can cause a decrease of hepatocytes through NASH which is characterized by inflammation and damage to liver cells that can lead to shrinkage and death of hepatocytes (Brunt et al., 2015). Steatosis is one of the prominent effects of diabetes in the liver. However, in the current study, steatosis was not observed in the liver tissues of diabetic animals. A previous study that observed the animals for a period of six weeks recorded severe steatosis in the liver tissues of the animals suggesting that steatosis is related to prolonged periods of diabetes (Yao et al., 2021).

Connective tissue area fraction around hepatocytes increased slightly, suggesting inflammation-induced liver fibrosis. Such increases are attributed to chronic inflammation, activating hepatic stellate cells and promoting connective tissue fiber production, leading to liver fibrosis (Faddladdeen and Ojaimi, 2019). Inflammatory markers like TNF-α, IL-6, and IL-1β, along with TGF-β, are implicated in the above process (Akbari and Hassan-Zadeh, 2018). Additionally, chemokines like MCP-1 and normal T cell expressed may contribute to immune cell recruitment to the liver in diabetic liver disease (Mohammadi et al., 2019). Similarly, in the kidneys, reduced renal corpuscular and glomerular tuft areas indicated inflammation-related shrinkage, while

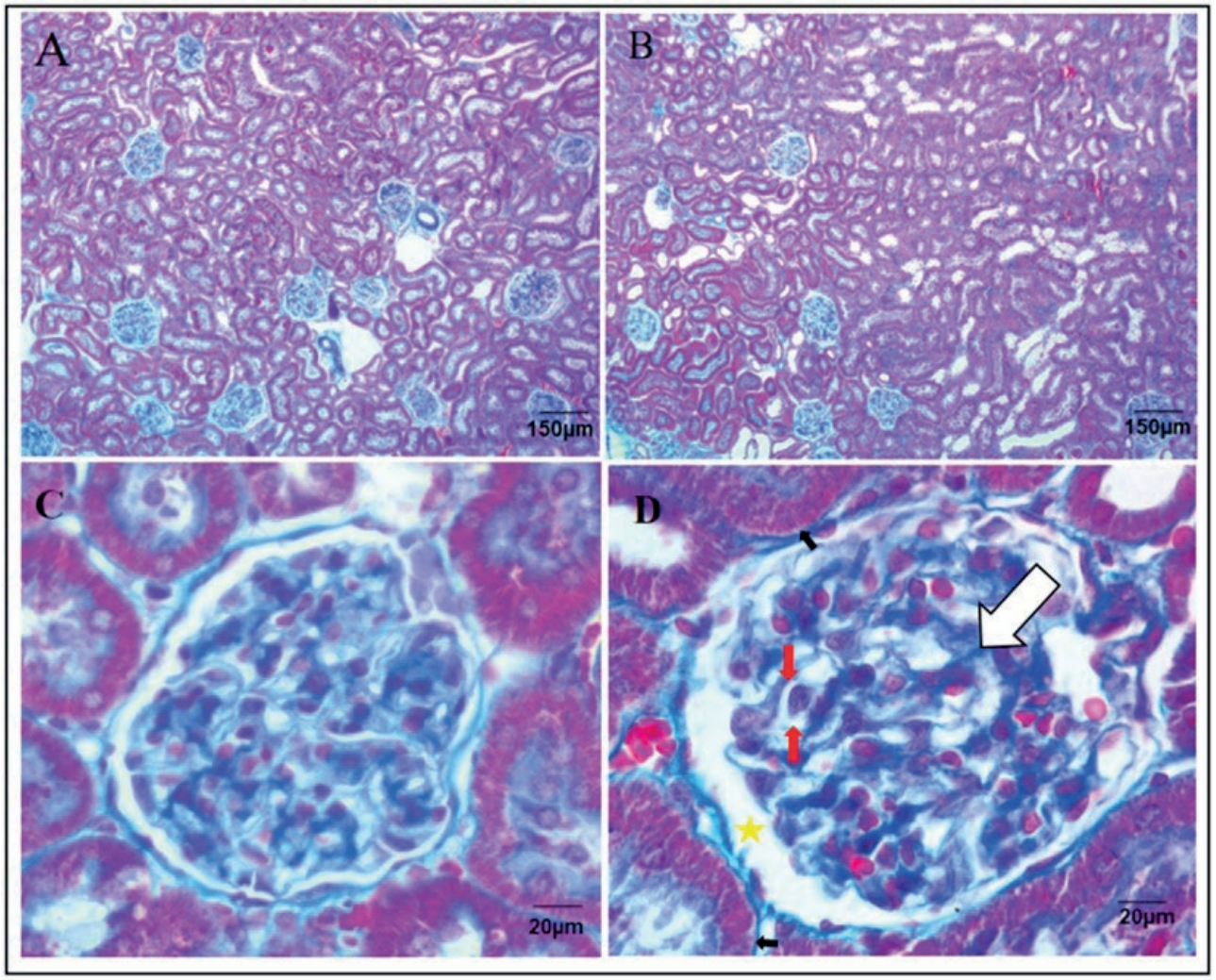

Figure 6. Masson's Trichrome Photomicrographs showing the collagen fiber bundles in the glomerular tuft of the kidneys of control and STZ induced diabetic animals. A: Control group (10X) with moderate collagen fibers in the glomerular tufts across the kidney tissue, B: DM group (10X) showing excess accumulation of collagen fibers in the glomerular tuft. C: Control group (100X), showing more details of moderate amount of collagen fiber bundles in the glomerular tuft area and in the basement membrane of kidney tubules. D: STZ induced diabetic group (100X), showing details of abundant collagen fiber bundles in the glomerular tuft (white arrow), vacuolization (red arrow), enlarged renal corpuscular space (yellow star), and thickening of basement membrane (black arrow) around the kidney tubules.

increased urinary space area suggested glomerular damage (Hu and Layton, 2021). Proximal and distal convoluted tubules exhibited hypertrophy, possibly due to prolonged exposure to elevated glucose levels, leading to epithelial cell degeneration (Hu and Layton, 2021).

Connective tissue area fraction was measured in glomerular tuft of kidney tissues. Our findings showed a significant increase in the connective tissue area fraction in the glomerular tuft of DM animals compared to control animals. These results are in agreement with that of Jia et al. 2018 (55mg/kg observed for 8 weeks) who recorded similar results, stating that an increase of connective tissue is involved in the pathophysiology of diabetic nephropathy such as fibrosis in the glomeruli.

CONCLUSION

The current study successfully induced hyperglycemia in rats using a single dose of 50mg/kg Streptozocin (STZ), resulting in significant histomorphometric changes in the liver that manifested as increased hepatocyte area in zone 1 and reduced size in zone 3 over 21 days. However, no significant changes were observed in the

kidneys. The findings suggest that while 50mg/kg STZ-induced diabetes affects some aspects of the histomorphometry of the liver and kidneys within 21 days, it does not produce full pathologic profile as recorded in other studies. Future studies should consider extending observation periods for comprehensive analysis of liver and kidney tissue changes.

AUTHOR CONTRIBUTIONS

Conceptualization: MK Mpholwane, PA Mbelengwa and NK Xhakaza. Manuscript drafting: PA Mbelengwa. Critical review of the manuscript: ML Mpholwane and NK Xhakaza. Final manuscript approval: Both authors.

REFERENCES

Abd Rashed, A., & Rathi, D.N.G. 2021. Bioactive components of Salvia and their potential antidiabetic properties: A review. *Molecules*, 26(10): 3042.

Akbari, M., & Hassan-Zadeh, V. 2018. IL-6 signalling pathways and the development of type 2 diabetes. *Inflammopharmacology*, 26: 685-698.

Brunt, E.M., Wong, V.W.S., Nobili, V., Day, C.P., Sookoian, S., Maher, J.J., Bugianesi, E., Sirlin, C.B., Neuschwander-Tetri, B.A. & Rinella, M.E. 2015. Nonalcoholic fatty liver disease. Nature reviews Disease primers, 1(1): 1-22.

Calzadilla Bertot, L. & Adams, L.A. 2016. The natural course of non-alcoholic fatty liver disease. *International journal of molecular sciences*, 17(5): 774.

Dhillon, K.K. & Gupta, S. 2018. Biochemistry, Ketogenesis. *National Library of Medicine*.

Faddladdeen, K.A. & Ojaimi, A.A. 2019 .Protective effect of pomegranate (Punica granatum) extract against diabetic changes in adult male rat liver: histological study. *Journal of microscopy and ultrastructure*, 7(4): 165.

Fazelipour, S., Kiaei, S.B., Tootian, Z. & Dashtnavard, H. 2008. Histomorphometric study of hepatocytes of mice after using heroin. *International Journal of Pharmacology*, 4(6): 496-9.

Guilherme, A., Henriques, F., Bedard, A.H. & Czech, M.P. 2019. Molecular pathways linking adipose innervation to insulin action in obesity and diabetes mellitus. *Nature Reviews Endocrinology*, 15(4): 207-225.

Hossain, M.A. & Pervin, R. 2018. Current antidiabetic drugs: review of their efficacy and safety. *Nutritional and therapeutic interventions for diabetes and metabolic syndrome*, 455-473.

Hu, R. & Layton, A. 2021. A computational model of kidney function in a patient with diabetes. *International journal of molecular sciences*, 22(11): 5819.

Michalopoulos, G.K. & Bhushan, B. 2021. Liver regeneration: biological and pathological mechanisms and implications. *Nature reviews Gastroenterology & hepatology*, 18(1): 40-55.

Jia, Q., Yang, R., Liu, X.F., Ma, S.F. & Wang, L. 2019. Genistein attenuates renal fibrosis in streptozocin induced diabetic rats. *Molecular medicine reports*, 19(1): 423-431.

Mohamed, J., Nafizah, A.N., Zariyantey, A.H. & Budin, S. 2016. Mechanisms of diabetes-induced liver damage: the role of oxidative stress and inflammation. *Sultan Qaboos University Medical Journal*, 16(2): 132.

Mohammadi, A., Blesso, C.N., Barreto, G.E., Banach, M., Majeed, M. & Sahebkar, A. 2019. Macrophage plasticity, polarization and function in response to curcumin, a diet-derived polyphenol, as an immunomodulatory agent. *The Journal of nutritional biochemistry*, 66: 1-16.

Nakayama, T., Kosugi, T., Gersch, M., Connor, T., Sanchez-Lozada, L.G., Lanaspa, M.A., Roncal, C., Perez-Pozo, S.E., Johnson, R.J. & Nakagawa, T. 2010. Dietary fructose causes tubulointerstitial injury in the normal rat kidney. *American journal of physiology-renal physiology*, 298(3): 712-720.

Naseri, M., Sereshki, Z.K., Ghavami, B., Zangii, B.M., Kamalinejad, M., Moghaddam, P.M., Asghari, M., Hasheminejad, S.A., Emadi, F. & Ghaffari, F. 2022. Preliminary results of effect of barley (Hordeum vulgare L.) extract on liver, pancreas, kidneys and cardiac tissues in streptozocin induced diabetic rats. *European Journal of Translational Myology*, 32(1).

Norgaard, S.A., Sondergaard, H., Sorensen, D.B., Galsgaard, E.D., Hess, C. & Sand, F.W. 2020. Optimising streptozocin dosing to minimise renal toxicity and impairment of stomach emptying in male 129/Sv mice. *Laboratory Animals*, 54(4): 341-352.

Salahshoor, M.R., Mohammadi, M.M., Roshankhah, S., Najari, N. & Jalili, C. 2019. Effect of Falcaria vulgaris on oxidative damage of liver in diabetic rats. *Journal of Diabetes & Metabolic Disorders*, 18: 15-23.

Schneider, C.A., RASBAND, W.S. & Elicieri K.W. 2012. NIH Image to ImageJ: 25 years of image analysis. *Nature Methods*, 9(7): 671.

Scorletti, E. & Carr, R.M. 2022. A new perspective on NAFLD: Focusing on lipid droplets. *Journal of hepatology*, 76(4): 934-945.

Sellamuthu, P.S., Arulselvan, P., Kamalraj, S., Fakurazi, S. & Kandasamy, M. 2013. Protective nature of mangiferin on oxidative stress and antioxidant status in

tissues of streptozocin-induced diabetic rats. *International Scholarly Research Notices*, 2013(1): 750109.

Sun, H., Saeedi, P., Karuranga, S., Pinkepank, M., Ogurtsova, K., Duncan, B.B., Stein, C., Basit, A., Chan, J.C., Mbanya, J.C. & Pavkov, M.E. 2022. IDF Diabetes Atlas: Global, regional and country-level diabetes prevalence estimates for 2021 and projections for 2045. *Diabetes research and clinical practice*, 183: 109119.

Tang, S.C. 2018. September. An overview of IgA nephropathy: 50 years on. *Seminars in nephrology*, 38(5): 433-434.

World Health Organization. 2022. Diabetes. Diabetes (who.int)

Yao, M., Teng, H., Lv, Q., Gao, H., Guo, T., Lin, Y., Gao, S., Ma, M. & Chen, L. 2021. Anti-hyperglycemic effects of dihydromyricetin in streptozocin-induced diabetic rats. *Food Science and Human Wellness*, 10(2): 155-162.

IJAE
ITALIAN JOURNAL OF ANATOMY AND EMBRYOLOGY

Firenze University Press
www.fupress.com/ijae

OPEN ACCESS

Citation: Melovitz-Vasan, C., Huff, S. & Vasan, N. (2025). A case report of the right vertebral artery's origin as a unique 'trifurcation' involving the brachiocephalic trunk, right common carotid artery, and the right vertebral artery. *Italian Journal of Anatomy and Embryology* 129(1): 41-45. doi: 10.36253/ijae-15808

© 2024 Author(s). This is an open access, peer-reviewed article published by Firenze University Press (https://www.fupress.com) and distributed, except where otherwise noted, under the terms of the CC BY 4.0 License for content and CC0 1.0 Universal for metadata.

Data Availability Statement: All relevant data are within the paper and its Supporting Information files.

Competing Interests: The Author(s) declare(s) no conflict of interest.

A case report of the right vertebral artery's origin as a unique 'trifurcation' involving the brachiocephalic trunk, right common carotid artery, and the right vertebral artery

Cheryl Melovitz-Vasan[1]*, Susan Huff[2], Nagaswami Vasan[1]

[1] *Department of Biomedical Sciences, Cooper Medical School of Rowan University, Camden, New Jersey, 08103 USA*
[2] *Medical Education Research Collaborator, Winston-Salem, NC, USA*
[3] *Department of Biomedical Sciences, Cooper Medical School of Rowan University, 401 South Broadway, Camden, New Jersey 08103, USA*
*Corresponding author. E-mail: melovitz-vasan@rowan.edu

Abstract. While the anomalous origin of the left vertebral artery is more often reported, the atypical right vertebral artery arising from the aortic arch is sparsely recognized. During the dissection of a donor's body, we recognized that the right vertebral artery arose as a 'trifurcation' from the aortic arch distal to the right subclavian artery. Intrigued, we explored the arterial branching further to realize a unique pattern not seen in earlier reports. The trifurcation involved the brachiocephalic trunk, right common carotid, and right vertebral artery. It is essential to recognize the possibility of people living normally without symptoms due to some anomalous arterial pattern.

Keywords: anomalous origin of right vertebral artery, right vertebral artery origin as a 'trifurcation', dilatation at the proximal and distal end of the right vertebral artery.

INTRODUCTION

Any observations related to anatomical structures identified during the dissection of a donor body or in patients following various radiographic modalities are to further our knowledge and or provide better treatment. However, minor vascular anomalies may or may not often cause clinical symptoms, and people could live normal asymptomatic lives. Prior articles about the vertebral arteries have been published since the beginning of the last century (Poynter, 1916; Congdon, 1922; Iyer, 1927; Adachi, 1928; Windle et al., 1928). These include how the vertebral arteries originate and from which part of the aortic origin, the number of vertebral arteries (up to six), and other details. Most importantly, knowledge of vascular anomalies is invaluable when surgical modalities are contemplated. In the case of the vertebral artery, prior knowledge of the region is vital because of its location,

which is close to several other critical neurovasculatures. As presented in this report, the unique trifurcation of the right vertebral artery involving the brachiocephalic trunk, right common carotid artery, and right vertebral artery could significantly impact surgical planning and patient outcomes. To our knowledge, there are no reported cases in the literature where the right vertebral artery arises as a trifurcation from the brachiocephalic trunk, right common carotid artery, and right vertebral artery.

In 1999, Lemke et al. reviewed the literature on the anomalous origin of the right vertebral artery and sketched images of different variants of anomalous right vertebral artery origins, rate of occurrence, and their potential embryological development. This report describes an anomalous right vertebral artery origin as a 'trifurcation' with the brachiocephalic trunk, right common carotid artery, and right vertebral artery (Fig. 1).

MATERIALS AND METHODS

The cadaveric specimen in this study was obtained from the willed body program for medical student dissection. The donor was a 94-year-old Caucasian female who died of right femur fracture sequelae. During routine cadaveric dissection of the thorax, we observed that the right vertebral artery originated as a 'trifurcation' with the brachiocephalic trunk, right common carotid artery, and right vertebral artery (Fig. 1). Proximally and distally, before entering the foramen transversarium, the right vertebral artery also exhibited recognizable distension (Fig. 1). A plausible explanation for this feature will be further explained and discussed in the later section.

RESULTS AND OBSERVATION

During the dissection of the donor thoracic structures, we observed that the right vertebral artery originated as a 'trifurcation' with the brachiocephalic trunk, right common carotid artery, and right vertebral artery (Fig. 1). Proximally at its origin and distally before entering the foramen transversarium, the right vertebral artery also exhibited recognizable distension (Fig. 1). A plausible explanation for this physical feature will be further explained and discussed in the subsequent section. The right vertebral artery displayed some natural tortuosity during its course through the cervical region before entering the foramen transversarium (Fig. 1).

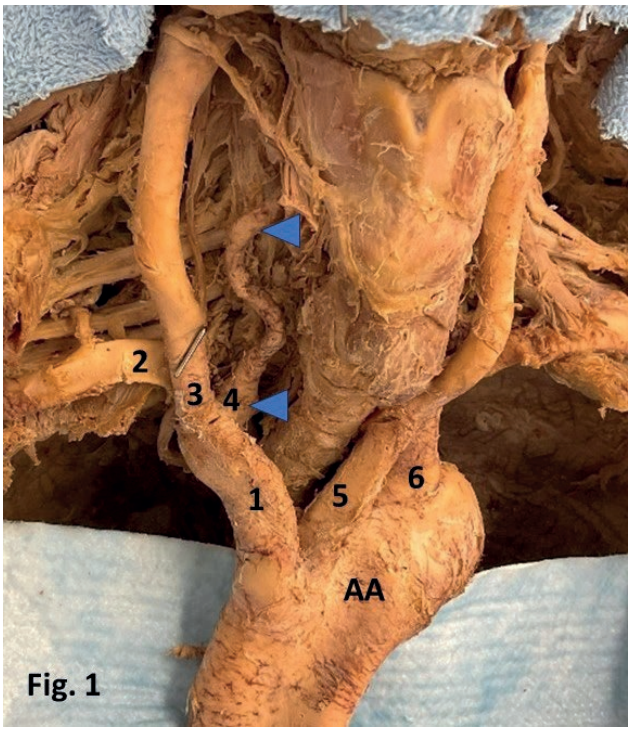

Figure 1. AA: Aortic Arch; 1: Right brachiocephalic trunk. 2: Right Subclavian Artery; 3: Right Common Carotid Artery; 4: Right Vertebral Artery; 5: Left Common Carotid Artery 6: Left Subclavian Artery. Blue arrowheads show the dilatations in the vertebral artery. It shows the origin of the right vertebral artery (RVR) as a 'trifurcation' between the brachiocephalic trunk (BrT) and the right common carotid artery (RCC). The blue arrowhead underscores the crucial aspect of comprehending the proximal and distal dilatation of the RVR in vascular physiology. This figure is obtained from the author's earlier work *accepted/in press* for publication in the Italian Journal of Anatomy and Embryology (2024).

DISCUSSION

Since Poynter's 1916 report that there were 4-6 vertebral artery branches from the aortic arch, there have been other similar studies (Matula et al., 1997; Lemke et al., 1999). To our knowledge, no case has been reported in the literature in which the right vertebral artery originates as a 'trifurcation' between the brachiocephalic trunk, right common carotid artery, and right vertebral artery (Fig. 1). Is there a clinical significance to our findings? Yes, in surgical reconstructions of the aortic arch and its branches, one must be aware of this 'trifurcation' anomaly.

It has been noted that the vertebral artery's preforaminal (V1 segment) tends to have a tortuous path in about 39% of cases Matula et al. (1997) studied, which is consistent with our observation in this study (Fig. 1) and an earlier report (Freilich et al., 1986). Additionally, there is a difference in the twistiness of the right and left

vertebral arteries, with 32% of the right vertebral artery being twisted compared to 68% of the left vertebral arteries. The V1 segment of both the right and left preforaminal vertebral arteries showed some natural tortuosity, with the left artery more tortuous than the right. The prevalence of transverse tortuosity was the highest compared to coronal and sagittal tortuosity (Matula et al., 1997; Russo et al., 2011; Uchino et al., 2013). While the twists in the proximal or preforaminal segment of the vertebral artery do not have any hemodynamic consequences (Wuttke et al., 1990), the loops of the proximal segments have been known to cause nerve root compressions, leading to radicular symptoms. Some experts believe that abnormalities in the origins and distribution of the large aortic arch vessels can cause changes in cerebral hemodynamics, which can result in cerebral abnormalities (Wuttke et al., 1990). According to Wuttke et al. (1990), the anomalous origins and distribution of the large vessels of the aortic arch can alter cerebral hemodynamics, which might result in cerebral abnormalities and pathology (Lemke et al., 1999). The diagnostic advantage prior to surgery of supraaortic arteries is the actual value of detecting anomalous origins (Flynn, 1968; Tardieu, 2017).

Furthermore, the right vertebral artery showed noticeable distension both proximally at its origin and distally before entering the foramen transversarium (see Fig. 1). A potential reason for the observed bulge in the vertebral artery is that, at its beginning, the flow of blood from the aorta (a larger vessel with high pressure) into the narrower vertebral artery most likely could have caused the distension observed. Similarly, the vertebral artery entering the narrower foramen transversarium might cause a distention because of the resistance encountered. Thus, the vascular pressure gradient is a natural physiological phenomenon likely to cause a bulge or distension.

Besides embryological, physical, and physiological studies, vertebral artery anomalies have clinical significance in birth defects such as Down syndrome. Research has shown a 40% occurrence rate of vertebral artery anomalies and a 36% occurrence rate of aberrant Right Subclavian Carotid Artery (RSCA) in individuals with Down syndrome (Roofthooft et al., 2008; Chen et al., 2023). Other case studies (Rathore et al., 1989; Mishra et al., 2012) also demonstrated both an aberrant RSCA and an anomalous origin of the right vertebral artery from the right common carotid artery in a patient with Down syndrome. The deletion of Chromosome 22q11, also known as CATCH 22, is commonly associated with DiGeorge syndrome, conotruncal anomaly face syndrome, and velocardiofacial syndrome. Patients with this deletion are more likely to have anomalies of the aortic arch, aortic branches, ductus arteriosus, and pulmonary arteries than those without the deletion (Momma et al., 1999).

ANALYSIS

The following analysis, related to the case presented here, is based on our observations, findings, and published research studies on vertebral artery origin, malformations, and their effect on anatomy and physiology. In the analysis, we have considered the donor's age and gender and the cause of death. Any conclusion drawn in the discussion is the authors' assumption or based on available published materials. During routine cadaveric dissection of the thorax, we observed that the right vertebral artery originated as a 'trifurcation' with the brachiocephalic trunk, right common carotid artery, and right vertebral artery (Fig. 1).

In general, vertebral artery anomalies are due to how they begin during embryonic development, how they course through the cervical region of the neck, and the morphology of each of the four segments. The vertebral artery starts to form during weeks four to eight of embryonic development. At this stage, the horizontal part of the 1-6 intersegmental arteries (ISA) begins to recede. By developing longitudinal anastomoses that link the cervical ISA, the seventh ISA becomes the proximal subclavian artery. This artery is the starting point of the adult vertebral artery.

The anomalous origins of the right vertebral artery were divided into three categories: those originating directly from the aorta, carotid arteries, or the brachiocephalic artery. The variant of the right vertebral artery originating from the brachiocephalic trunk, right subclavian artery, and the right vertebral artery itself as a 'trifurcation' is unique and hitherto unreported.

In an earlier article, Lemke et al. (1999) used 11 drawings to schematically represent the anomalous origin of the right vertebral artery based on publications dating from 1927 to 1992. In the case currently presented, the origin of the right vertebral artery as a 'trifurcation' appears unique. As a result, this warrants that clinicians in cardiothoracic surgery are aware of this and other rare and atypical variations.

CONCLUSION

In the above paragraphs, this study provides an embryological explanation for how and why the right vertebral artery originates as a 'trifurcation' involving

the brachiocephalic trunk, the right subclavian artery, and the right vertebral artery. In the analysis, we have provided some historical relevance and schematic diagrams showing earlier views of the origin of the right vertebral arteries. The study also captures how this anomalous origin of vertebral arteries is clinically relevant in surgeries that involve the cervical region and supraaortic arch. The study also explores how the tortuosity of the proximal vertebral artery, the aortic origin of the left vertebral artery, and their impact on the hemodynamics of cerebral circulation are related.

Our research goes beyond simply reporting the 'trifurcation' as a unique vertebral artery anomaly and delves into their clinical significance in relation to other birth defects, such as Down syndrome.

ACKNOWLEDGEMENTS:

The authors sincerely thank the donor and her family for their generosity, which made this study possible and facilitated scientific and medical innovations in patient care. We are indebted to the families of our donors.

For research using human subjects, the American Association for Anatomy endorses the protections embodied in the Basic Principles of the Declaration of Helsinki and their expansion in the regulations governing research supported by the U.S. Government (45 CFR Part 46; 56 FR 28003). The authors state that every effort was made to follow all local and international ethical guidelines and laws regarding the use of human donors in anatomical research.

DECLARATION

The authors state that every effort was made to comply with all the local and international ethical guidelines and laws that pertain to the use of human cadaveric donors in anatomical research.

FUNDING

This study was supported by the Faculty Development for Research and Innovation grant administered by the Cooper Medical School of Rowan University.

AUTHOR CONTRIBUTIONS

All the authors were involved in the research, preparation, and final approval of the manuscript. Dr. Melovitz-Vasan was responsible for conceiving the project idea, creating the initial draft with Dr. Vasan, and revising the manuscript until the final version. Dr. Melovitz-Vasan and Dr. Vasan were responsible for dissection and collecting images. Ms. Huff and Dr. Vasan conducted the literature search, which was used to draft the manuscript and prepare the final format.

ABBREVIATIONS USED

AA: Aortic Arch; RVA: Right vertebral artery; BrT: brachiocephalic trunk; RCC: Right common carotid artery.

REFERENCES

1. Adachi, B. (1928) Das Arteriensystem der Japaner. Verlag der Kaiserl. Jap. Univ., Kyoto, Vol. 1.
2. Chen J., Liu L, Kou X., Wang C. (2023) Case report: Right vertebral and carotid artery anomalies with an aberrant right subclavian artery in two patients. Front Neurol. 14. https://doi.org/10.3389/fneur.2023.1282127.
3. Congdon B.D. (1922). Transformation of the aortic-arch system during the development of the human embryo. Cont Embryol. 14: 47–110.
4. Flynn R.E. (1968) External carotid origin of the dominant vertebral artery. Case report. J Neurosurg. 29: 300–301. PMID: 5684411 https://doi.org/10.3171/jns.1968.29.3.0300
5. Freilich M., Virapongse C., Kier E.L., Sarwar M., Bhimani S. (1986) Foramen transversarium enlargement due to tortuosity of the vertebral artery. Computed tomographic appearance. Spine. 11: 95–98. https://doi.org/10.1097/00007632-198601000-00030.
6. Iyer A.A. (1927) Some anomalies of origin of the vertebral artery. J Anat. 62 (Pt 1): 121–122.
7. Lemke A.J., Benndorf G., Liebig T., Felix R. (1999). Anomalous origin of the right vertebral artery: review of the literature and case report of right vertebral artery origin distal to the left subclavian artery. Am J Neuroradiol. 20: 1318–1321. PMID: 10472992; PMCID: PMC7055987.
8. Matula C., Trattni S., Tschabitscher M., Day J.D., Koos W.T. (1997) The course of the prevertebral segment of the vertebral artery: anatomy and clinical significance. Surg Neurol. 48: 125–131. PMID: 9242236 https://doi.org/10.1016/s0090-3019(97)90105-1
9. Mishra A., Pendharkar H., Jayadaevan E.R., Bodhey N. (2012) Anomalous origins of bilateral vertebral arteries in a child with Down syndrome and Moy-

amoya disease: A case report. Interv Neuroradiol. 18: 259-263. https://doi.org/10.1177/159101991201800303
10. Momma K., Matsuoka R., Takao A. (1999) Aortic arch anomalies associated with Chromosome 22q11 Deletion (CATCH 22). Pediatr Cardiol. 20: 97–102. PMID:9986884: https://doi.org/10.1007/s002469900414
11. Poynter, C.W.M. (1916) Arterial anomalies pertaining to the aortic arches and the branches arising from them. Nebr. Univ. Stud. 16: 229-345.
12. Rathore M.H., Sreenivasan V.V. (1989) Vertebral and right subclavian artery abnormalities in the Down syndrome. Am J Cardiol. 63: 1528– 1529. PMID: 252496 https://doi.org/10.1016/0002-9149(89)90023-4
13. Roofthooft M.T., van Meer H., Rietman W.G., Ebels T., Berger R.M. (2008) Down syndrome and aberrant right subclavian artery. Eur J Pediatr. 167(9): 1033-6. https://doi.org/10.1007/s00431-007-0637-2. Epub 2008 Jan 3. PMID: 18172685; PMCID: PMC2491432.
14. Russo V.M., Graziano F., Peris-Celda M., Russo A., Ulm A.J. (2011) The V(2) segment of the vertebral artery: Anatomical considerations and surgical implications. J. Neurosurg Spine. 15: 610–619. https://doi.org/10.3171/2011.7.spine1132
15. Tardieu G.G., Edwards B., Alonso F., Watanabe K., Saga T., Nakamura M., Motomura M., Sampath R., Iwanaga J., Goren O., Monteith S., Oskouian R.J., Loukas M., Tubbs R.S. (2017) Aortic arch origin of the left vertebral artery: An anatomical and radiological study with significance for avoiding complications with anterior approaches to the cervical spine. Clin Anat. 30: 811–816. https://doi.org/10.1002/ca.22923. Epub 2017. PMID: 28547783
16. Uchino A., Saito N., Takahashi M., Okada Y., Kozawa E., Nishi N., Mizukoshi W., Nakajima R., Watanabe Y. (2013) Variations in the origin of the vertebral artery and its level of entry into the transverse foramen diagnosed by CT angiography. Neuroradiology. 55: 585–594. PMID: 23344682. https://doi.org/10.1007/s00234-013-1142-0
17. Windle W.F., Zeiss F.R., Adamski M.S. (1928) Note on a case of anomalous right vertebral and subclavian arteries. J Anat. 62(Pt 4): 512-514. PMID: 17104207; PMCID: PMC1249992.
18. Wuttke V., Schmitt R., Pogan J., Clar H.E. (1990) Zervikales Wurzelkompressionssyndrom durch die Arteria vertebralis [Cervical nerve root compression syndrome caused by the vertebral artery]. Rofo. 152: 473-4. German. https://doi.org/10.1055/s-2008-1046908. PMID: 2160113.

IJAE
ITALIAN JOURNAL OF ANATOMY AND EMBRYOLOGY

Firenze University Press
www.fupress.com/ijae

OPEN ACCESS

Citation: Pires de Aguiar, P. H., Martini, C. S., Bassalo Canals Silva, G., Zambo Galafassi, G., Maciel da Cunha, J., Figueira Rodrigues Vieira Pessano, G. & Silva Centeno, R. (2025). Corpus callosum motor fibers dissection using Klingler's method and methylene blue. *Italian Journal of Anatomy and Embryology* 129(1): 47-53. doi: 10.36253/ijae-15941

© 2024 Author(s). This is an open access, peer-reviewed article published by Firenze University Press (https://www.fupress.com) and distributed, except where otherwise noted, under the terms of the CC BY 4.0 License for content and CC0 1.0 Universal for metadata.

Data Availability Statement: All relevant data are within the paper and its Supporting Information files.

Competing Interests: The Author(s) declare(s) no conflict of interest.

Corpus callosum motor fibers dissection using Klingler's method and methylene blue

Paulo Henrique Pires de Aguiar[1,2], Carolina Simão Martini[3,*], Giulia Bassalo Canals Silva[4], Giovanna Zambo Galafassi[5], Jemaila Maciel da Cunha[6], Giovana Figueira Rodrigues Vieira Pessano[6], Ricardo Silva Centeno[7]

[1] *Federal University of São Paulo, (UNIFESP) São Paulo, Brasil*
[2] *Anatomy Department of ABC Medical School, Santo André, Brazil*
[3] *Neurosurgery resident at Santa Paula Hospital, São Paulo, Brazil*
[4] *Medical Student at Pontifical Catholic University of São Paulo (PUC/SP), São Paulo, Brazil*
[5] *Neurosurgery resident at ABC medical school, Santo André, Brazil*
[6] *Neurosurgery resident at Heliopólis Hospital, São Paulo, Brazil*
[7] *Chief of Epilepsy Department at Federal University of São Paulo (UNIFESP), São Paulo, Brasil*
*Corresponding author. E-mail: carolina.smartini@gmail.com

Abstract. *Background:* The corpus callosum (CC) is the largest white matter bundle in the brain, connecting the left and right cerebral hemispheres. It plays a crucial role in integrating information and facilitating somatosensory, motor, and cognitive function. This study examined the anatomy of the CC using white matter dissection and explored a posterior callosotomy approach for treating drop attacks in Lennox-Gastaut syndrome (LGS). LGS is a rare form of childhood-onset epilepsy, characterized by multiple seizure types, abnormal electroencephalograms, and progressive mental retardation. The authors proposed that fibers from the medial and posterior CC regions converge on the precentral gyrus, and dissection was performed to investigate this theory. *Methods:* This study employed the Klingler method to examine white matter fibers in four adult brains. Dissection involved removing the cortex from the superior frontal, precentral, and postcentral gyri, followed by the cingulate gyrus. *Results*: The CC is divided into five parts: the rostrum, genu, body, isthmus, and splenium. Each part has distinct anatomical relationships with the lateral ventricles and connects to different cortical regions *Conclusions*: Our findings are consistent with the evidence that the motor fibers of the brain traverse the posterior region of the corpus callosum, suggesting that selective posterior callosotomy may be a more effective treatment for refractory drop attacks in Lennox-Gastaut Syndrome.

Keywords: Lennox Gastaut Syndrome, corpus callosum, white matter.

INTRODUCTION

The corpus callosum (CC), the largest commissural white matter bundle, is a crucial structure of the brain. It connects the left and right cerebral hem-

ispheres and plays a vital role in integrating the information between the.[1,2]. The corpus callosum comprises myelinated nerve fibers that extend across the midline of the developing brain and connect the two hemispheres. This structure facilitates the transmission of sensory, motor, and cognitive functions between the homologous regions of the brain.[3,4]

It is divided into regions, from anterior to posterior, the rostrum, genu, body isthmus, splenium, and tapetum, each with fibers in different cerebral regions[2].The CC is intimately related to the fornix and lateral ventricles and represents the anterior, superior, and posterior border of the septum pellucidum, which together with the fornix separates the lateral ventricles from each other[1].

Lennox-Gastaut syndrome (LGS) is a severe form of epilepsy that affects children. It was first identified by Henri Gastaut in 1966. In 1950, Dr. William G. Lennox characterized the electroencephalogram features of this condition. LGS represents approximately 2-5% of all childhood epilepsies. [5]. It is one of the most intractable epilepsies and is characterized by multiple types of seizures, electroencephalographic (EEG) characteristics such as generalized slow sharp and wave discharges (GSW), generalized paroxysmal fast activities, and progressive mental retardation. GSW with bilateral synchronization in secondary generalized epileptic encephalopathy, such as LGS, can originate from the primary epileptogenic zone through the transcallosal pathway[6]. Due to the difficulty of identifying and localizing single epileptogenic lesions and the presence of multifocal characteristics, most patients with LGS are ineligible for resective surgery[5]. Palliative surgical procedures, including corpus callosotomy, for refractory epilepsy were first introduced in the 1940s by Van Wagenen and Herren, and have since become an established treatment option for patients with intractable epilepsy who are not suitable candidates for resective surgery.[5,7]. The most common indication for corpus callosotomy is a drop attack. Patients who undergo total corpus callosotomy show a higher reduction in seizures than patients who undergo partial corpus callosotomy[7]. Epileptic drop attacks are usually refractory to medication, and their association with the sudden bilateral synchronization of ictal discharges provides a rationale for callosotomy. The procedure is indicated when focal resection is not feasible and specifically targets sudden falls irrespective of the underlying etiology. Thus, the clinical heterogeneity of the candidates is the norm[8]. Although a 1-stage total corpus callosotomy can be performed in patients younger than 16 years, a 2-stage corpus callosotomy is preferred for patients older than 16 years, given its lower risk for disconnection syndrome[9].

This article delves into the physiopathology of LGS-related drop attacks and posterior callosotomy employed as a treatment, with a foundation in the anatomy of the corpus callosum and its constituent fibers. The authors proposed that fibers from the medial and posterior regions of the corpus callosum converge on the precentral gyrus. To investigate this theory, dissection of the corpus callosum and a study of its fibers were conducted.

MATERIALS AND METHODS

This study employed the Klingler method to examine white matter fibers. It comprises of four (4) phases: fixation, freezing, thawing, and dissection.

Four normal adult brains (eight hemispheres) were fixed in a 10% formalin solution for at least three months. The superficial veins and arachnoid membranes were carefully removed before the brains were frozen at 0–5°C for three weeks. This step allowed formalin to crystallize between the fibers, causing them to swell and separate for further preservation and observation. Samples were thawed and stored in diluted formalin. A ZEISS EyeMag with 2-2,5x amplification, a medical loupe, was used to better visualize the fibers during dissection, and a wooden spatula was used to remove the cortex and other regions during the procedure.

Following dissection of the zone of interest (forceps major and minor), the brains were stained with methylene blue 5% aqueous solution using a painting brush. After one hour, the hemispheres were rinsed, and the fibers emerging from the forceps major were traced to determine their endings. In addition, fibers from the medial and posterior regions of the CC that were not stained were studied.

RESULTS

The dissection involved the removal of the cortex from the superior frontal gyrus, precentral gyrus, and postcentral gyrus. Subsequently, the white fibers were extracted to access the cingulate gyrus, which was also removed. The anterior fibers of the corpus callosum were traced into the forceps minor, situated under the frontal lobe, whereas the posterior fibers were located to lead to the forceps major, situated under the occipital lobe (Figure 1 and 2).

Subsequently, the major and minor forceps were exposed and stained with methylene blue to make their paths more visible (Figure 3).

The use of methylene blue 5% to staining the major and minor forceps (as shown in Figure 3) enabled

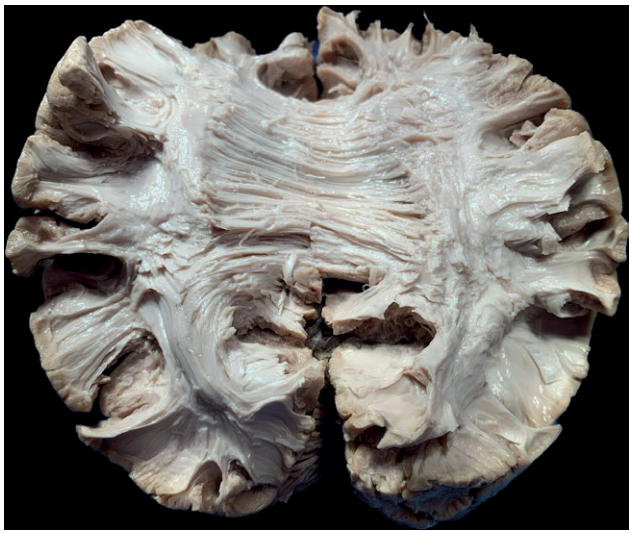

Figure 1. Corpus Callosum white matter fibers.

Figure 2. Corpus Callosum white matter fibers. Legend: A: Forceps Minor, B: Medial Fibers, C: Posterior Fibers, D: Forceps Major.

researchers to more clearly observe the path of the fibers emanating from these areas.

Regarding the medial portion of the CC, in all eight hemispheres examined, the fibers were traced from this region to the precentral gyrus as well as connecting the two occipital hemispheres. In the posterior region of the CC, the fibers were traced to the precentral and postcentral gyri in all eight hemispheres (Table 1).

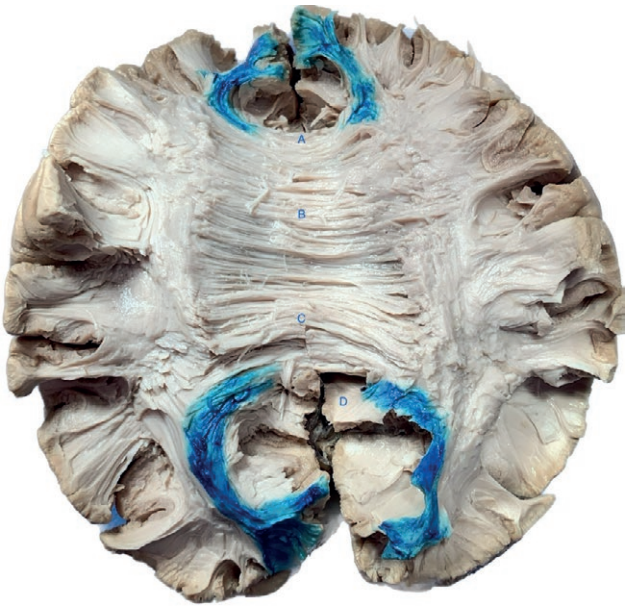

Figure 3. Forceps Major and Minor after the use of methylene blue. Legend: A: Forceps Minor, B: Medial Fibers, C: Posterior Fibers, D: Forceps Major.

Table 1. Forceps Major and Minor dissection findings.

Structure	Number of hemispheres	White Fibers ending point
Medial region	8 (100%)	Precentral gyrus
Posterior region	8 (100%)	Precentral and postcentral gyrus

The percentage in parentheses indicates the proportion of findings found compared to the total number of cases (n=8).

DISCUSSION

Anatomy and physiology

The corpus callosum is the largest bundle of white fibers in the human brain, with over 200 million axons communicating with the two cerebral hemispheres. It participates in connections in motor, sensory pathways, and cognitive functions [10,11]. The corpus callosum appears to be a "C" shape structure, viewed from above the interhemispheric fissure [12], and lies contouring almost all walls of the lateral ventricles [13,14].

The corpus callosum has two different embryogenic origins, dividing it into an anterior portion, which comprises the genu, rostrum, and body, and a posterior portion, represented by the splenium. The anterior portion, originating from the glial sling, merges with fibers from the hippocampal commissure and parieto-temporo-occipital cortex [15].

Histologically, the corpus callosum has a higher density of larger-diameter fibers in the isthmus and posterior splenium, while finer fibers are more abundant in the genu and anterior splenium. The splenium is the thickest part of the corpus callosum [15,16].

It is divided in five parts: rostrum, genu, body, isthmus, splenium – anterior to posterior extent, respectively[14]. The rostrum forms the floor of the frontal horn, the genu forms its anteromedial portion, the body forms the roof of the body of the lateral ventricle, the isthmus forms the medial wall of the atrium of the lateral ventricle, and the splenium forms the medial wall of the atrial and occipital horn of the lateral ventricle [14,17].

The rostrum begins at the anterior commissure and extends to the genu, which is the anterior limb of the septum pellucidum, and has fibers that connect the prefrontal cortex and anterior cingulate area, forming the forceps minor. The callosal body begins in the genu and extends to the fornix. The isthmus ends at the point where the fornix meets the inferior callosal surface, the splenium forms the forceps major, and the callosal body, together with the splenium, forms the tapetum, arising in the posterior part of those structures [14,18].

Above the corpus callosum, acting as a thick layer, the indusium griseum covers its surface, and on each side, there is a fine line of myelinated fibers and the medial and lateral longitudinal striae of Lancisi [18].

The internal carotid artery system and pericallosal artery provide arterial supply to the cingulate cortex (CC), with the exception of the splenium, which is vascularized by the terminal and choroidal branches of the posterior cerebral artery. Additionally, the anterior communicating artery, a part of the carotid system, contributes to the arterial supply of the CC by removing its median artery. The callosal and callosal cingular veins are responsible for facilitating venous drainage of the CC towards the internal cerebral veins.[1].

Superior/dorsal callosal radiation arises from the corpus callosum and runs medially into brain hemispheres. It courses below the cingulate gyrus and medial superior longitudinal fasciculus (SLF), and laterally to the SLF. It ascends and forms the corona radiata, which connects the motor and supplementary motor areas of both hemispheres [17]. Dorsal callosal radiation is divided into anterior and posterior components, which originate from the genu and anterior body of the CC and form the roof of the frontal horn of the lateral ventricle; the posterior component, also known as the tapetum, originates from the posterior region of the CC and forms the roof and lateral wall of the atrium as well as the lateral wall of the temporal horn of the lateral ventricle [17]. The anterior callosal radiations originate from the genu and rostrum, with the majority of fibers bending anteriorly to reach the medial frontal-orbital region, also known as the forceps minor (Figure 2), forming the lateral ventricle frontal horn. Additionally, other fibers emerge from the rostrum and curve laterally on the basal surface of the frontal lobe, running along the medial surface of the uncinate fasciculus, ultimately reaching the temporal stem in close association with the external capsule, and connecting the insular regions of both hemispheres [17]. Posterior callosal radiations originating from the CC splenium extend posteriorly to the medial occipital region. This structure is known as forceps major, as it connects the occipital lobes of both hemispheres. It creates a protuberance in the medial wall of the atrium of the lateral ventricle known as the atrium bulb[17].

With human cadaveric dissection and a study of primate brains, Witelson in 1989 proposed that the human corpus callosum should be divided into seven segments, according to geometric landmarks, associated with a cortical region: rostrum, genu, rostral body, anterior midbody, posterior midbody, isthmus and splenium [19]. Each of these subregions sends and receives fibers from the cortical regions, basal ganglia, thalamus, and the brainstem [20].

The genu and anterior third of the body of the corpus callosum are associated with the prefrontal cortex; the central part is linked to the premotor and supplementary motor cortex; the posterior third is associated with the primary motor area (precentral gyrus); the posterior third and splenium are associated with the primary sensory cortex (postcentral gyrus); and the splenium is associated with the parieto-temporo-occipital cortex [2,11,21]. Moreover, the posterior part of the corpus callosum (posterior midbody, isthmus, and splenium) contains fibers projecting from the posterior parietal cortex to the hippocampus through the para-hippocampal and entorhinal areas [22].

With the development of tractography and functional magnetic resonance imaging studies, it is known that the organization of the white matter of the corpus callosum is more complex, showing a spatial distribution pattern of its fibers. There is also an overlap between the communicated regions, and the fibers are not only related to cortical regions, but can also connect with other white fiber bundles (Wang et al., 2021).

An investigation conducted by Küçükyürük et al. in 2020 revealed that motor fibers originating from the motor cortex traverse the posterior section of the corpus callosum, primarily in the posterior body and isthmus, a conclusion that aligns with the research conducted by Shah et al. in 2021. This finding was also documented in a study led by Hofer and Frahm in 2006, who utilized DTI to

highlight the corpus callosum white matter tracts[17,23,24]. The results of our dissection are consistent with literature findings, which indicate that motor fibers from the brain connect to the posterior area of the corpus callosum.

Due to the complex connections of the corpus callosum with various areas of the brain, it is the main interhemispheric pathway for the spread of epileptic activity, and therefore, is of interest in Epilepsy Surgery [20].

Callosotomy x Epilepsy

Lennox-Gastaut Syndrome (LGS) is one of the most difficult epileptic syndromes to control and accounting for 1-10% of childhood epilepsies. It consists of a triad of different types of seizures, a characteristic interictal electroencephalogram with a slow spike-wave pattern or generalized paroxysms of fast activity, and cognitive deficits. It can be caused by various factors, such as traumatic or hypoxic brain injuries, tuberous sclerosis complex, congenital infections, brain malformations, and hereditary metabolic diseases. There is no common epileptogenic zone (EZ) for all patients, and in most cases, the EZ is multiple or diffuse. Hence, in addition to being drug-resistant, there is a wide range of responsiveness to different surgical modalities. Furthermore, the maintenance of seizures is related to a worse cognitive prognosis, in addition to the risk of direct injury during seizures like generalized tonic-clonic and drop attacks, so delaying surgical treatment in an attempt to control the disease with medication is not advisable [5,6,21,25].

EZ resection surgery with curative potential is the treatment of choice when the syndrome is caused by a focal and well-defined epileptogenic zone. However, not all patients achieve seizure freedom, as LGS is considered a disease of intercortical connections and white fiber pathways [6,20]. Studies have shown that animal models with epileptogenic lesions in the neonatal period exhibit a decrease in the corpus callosum surface area, indicating alterations in its microstructure, and hence, its connections [22]. Furthermore, Andrade et al. demonstrated diffusion alterations in the corpus callosum of patients with cortical developmental anomalies, which is probably a combined entity with defects in white matter development [21].

Therefore, when the EZ is diffuse, multiple or poorly defined palliative procedures, such as callosotomy, are employed. Callosotomy was introduced in 1940 and aims to interrupt the propagation of the epileptic pathway. It mainly affects tonic seizures, atonic seizures, such as drop attacks, and tonic-clonic seizures. There are different modalities of callosotomy: resection of the anterior third, anterior half, anterior two-thirds, preservation only of the splenium, total callosotomy, and selective posterior callosotomy [6,8,25].

Total callosotomy and anterior callosotomy were similar in technique. Disconnection in anterior callosotomy starts at the genu/rostrum of the corpus callosum and ends at the transition between the body and the isthmus. In total callosotomy, disconnection ends at the splenium of the corpus callosum. In posterior callosotomy, disconnection starts at the posterior end of the splenium and ends at the isthmus.

Disconnection syndrome, severity of cognitive deficit, and developmental delay should be considered when deciding the volume of resection of the corpus callosum. Total callosotomy tends to be more effective in seizure control. However, they have a higher risk of developing disconnection syndrome, especially in elderly patients. In cases where anterior callosotomy did not effectively reduce the number of seizures, complementary posterior callosotomy might be considered [26].

The most common complication of callosotomy is the disconnection syndrome. They can be classified as either acute or chronic. Acute syndrome comprises severe decreases in spontaneous speech, paresis of the non-dominant leg, and incontinence. Several patients may require tube feeding during the postoperative period. These symptoms tended to disappear after a few months. On the other hand, the chronic syndrome is characterized by alien hand syndrome, dichotic listening suppression, tactile dysnomia, hemispatial neglect, non-dominant hand agraphia, and tachistoscopic visual suppression [26]. Other possible complications include temporary postoperative disturbance of consciousness and chemical meningitis [27].

Selective posterior callosotomy (SPC) is mainly performed for cases of drop attacks, such as fibers from the premotor cortex, primary motor cortex, and sensorimotor area responsible for axial and lower limb control crossing from the midbody to the posterior half of the corpus callosum. Therefore, SPC interrupts the pathway that leads to atonic seizures without disconnecting the frontal pathways responsible for aspects of cognition, volition, and sphincter control. In a study by Paglioli et al., 83% of patients experienced complete reduction or >90% reduction in drop attacks after SPC, along with improved functionality scores, and none experienced mutism, ataxia, or sphincter incontinence. SPC has a higher incidence of disconnection syndromes than selective anterior callosotomies, but in patients with LGS, who already have significant cognitive impairment, these changes do not result in noticeable deficits [8,9].

Our work demonstrates, using the white matter dissection technique combined with methylene blue stain-

ing, the path of motor and sensitive fibers via the posterior portions of the corpus callosum. This corroborates with the statement made by Pagliogli et al. that selective posterior callosotomy is sufficient to treat refractory epilepsy cases that lead to falls, especially drop attacks; therefore, we can provide the patient with a better treatment, with less risk of disconnection syndrome and greater control of the disease. To the best of our knowledge, this is the first anatomical study to show these connections enhanced by methylene blue staining.

CONCLUSIONS

Our research aimed to provide further evidence that the motor fibers of the brain traverse the posterior region of the corpus callosum, suggesting that selective posterior callosotomy may be a more effective treatment for refractory drop attacks in Lennox-Gastaut Syndrome. Our findings are consistent with those of the latest studies. The novel aspect of our work was the utilization of methylene blue to examine CC fibers.

REFERENCES

1. Fitsiori A, Nguyen D, Karentzos A, Delavelle J, Vargas MI. The corpus callosum: white matter or terra incognita. Br J Radiol. 2011 Jan;84(997):5–18.
2. Radwan AM, Sunaert S, Schilling K, Descoteaux M, Landman BA, Vandenbulcke M, et al. An atlas of white matter anatomy, its variability, and reproducibility based on constrained spherical deconvolution of diffusion MRI. NeuroImage. 2022 Jul 1;254:119029.
3. Pearce JMS. Corpus Callosum. Eur Neurol. 2007;57(4):249–50.
4. Fabri M, Polonara G, Mascioli G, Salvolini U, Manzoni T. Topographical organization of human corpus callosum: An fMRI mapping study. Brain Res. 2011 Jan;1370:99–111.
5. Alanazi GM, ALOsaimi TF, Alwadei AH, Al-Otaibi AD, Jad LA, Al-Attas AA. Efficacy and safety of corpus callosotomy versus vagus nerve stimulation as long-term adjunctive therapies in children with Lennox–Gastaut syndrome: Experience of a tertiary care center. Neurosciences. 2022 Apr;27(2):59–64.
6. Hur YJ, Kim HD. The causal epileptic network identifies the primary epileptogenic zone in Lennox–Gastaut syndrome. Seizure – Eur J Epilepsy. 2015 Dec 1;33:1–7.
7. Ueda R, Matsuda H, Sato N, Iwasaki M, Sone D, Takeshita E, et al. Alteration of the anatomical covariance network after corpus callosotomy in pediatric intractable epilepsy. Biagini G, editor. PLOS ONE. 2019 Dec 5;14(12):e0222876.
8. Paglioli E, Martins WA, Azambuja N, Portuguez M, Frigeri TM, Pinos L, et al. Selective posterior callosotomy for drop attacks: A new approach sparing prefrontal connectivity. Neurology. 2016 Nov 8;87(19):1968–74.
9. Ito H, Morino M, Niimura M, Takamizawa S, Shimizu Y. Posterior callosotomy using a parietooccipital interhemispheric approach in the semi-prone park-bench position. Abstract.
10. Ruddy KL, Leemans A, Carson RG. Transcallosal connectivity of the human cortical motor network. Brain Struct Funct. 2017 Apr;222(3):1243–52.
11. Wang P, Wang J, Tang Q, Alvarez TL, Wang Z, Kung YC, et al. Structural and functional connectivity mapping of the human corpus callosum organization with white-matter functional networks. NeuroImage. 2021 Feb 15;227:117642.
12. Shah A, Goel A, Jhawar SS, Patil A, Rangnekar R, Goel A. Neural Circuitry: Architecture and Function—A Fiber Dissection Study. World Neurosurg. 2019 May;125:e620–38.
13. Cumming WJK. An Anatomical Review of the Corpus Callosum. Cortex. 1970 Mar;6(1):1–18.
14. Rhoton AL. THE CEREBRUM. Neurosurgery [Internet]. 2007 Jul;61(1). Available from: https://journals.lww.com/00006123-200707001-00004
15. Fabri M, Pierpaoli C, Barbaresi P, Polonara G. Functional topography of the corpus callosum investigated by DTI and fMRI. World J Radiol. 2014;6(12):895.
16. Ribas EC, Yağmurlu K, De Oliveira E, Ribas GC, Rhoton A. Microsurgical anatomy of the central core of the brain. J Neurosurg. 2018 Sep;129(3):752–69.
17. Shah A, Jhawar S, Goel A, Goel A. Corpus Callosum and Its Connections: A Fiber Dissection Study. World Neurosurg. 2021 Jul;151:e1024–35.
18. Raybaud C. The corpus callosum, the other great forebrain commissures, and the septum pellucidum: anatomy, development, and malformation. Neuroradiology. 2010 Jun;52(6):447–77.
19. Witelson SF. Hand and sex differences in the isthmus and genu of the human corpus callosum. Brain. 1989;112(3):799–835.
20. Asadi-Pooya AA. Lennox-Gastaut syndrome: a comprehensive review. Neurol Sci. 2018 Mar;39(3):403–14.
21. Andrade CS, Leite CC, Otaduy MCG, Lyra KP, Valente KDR, Yasuda CL, et al. Diffusion abnormalities of the corpus callosum in patients with malformations of cortical development and epilepsy. Epilepsy Res. 2014 Nov;108(9):1533–42.

22. Meng Y, Hu X, Zhang X, Bachevalier J. Diffusion tensor imaging reveals microstructural alterations in corpus callosum and associated transcallosal fiber tracts in adult macaques with neonatal hippocampal lesions. Hippocampus. 2018 Nov;28(11):838–45.
23. Hofer S, Frahm J. Topography of the human corpus callosum revisited—Comprehensive fiber tractography using diffusion tensor magnetic resonance imaging. NeuroImage. 2006 Sep;32(3):989–94.
24. Küçükyürük B, Uzan M, Avyasov R, Tahmazoğlu B, İşler C, Sanus GZ, et al. Evaluation of Ideal Extent of Corpus Callosotomy Based on the Location of Intracallosal Motor Fibers. World Neurosurg. 2020 Dec;144:e568–75.
25. Thirunavu V, Du R, Wu JY, Berg AT, Lam SK. The role of surgery in the management of Lennox–Gastaut syndrome: A systematic review and meta-analysis of the clinical evidence. Epilepsia. 2021 Apr;62(4):888–907.
26. Uda T, Kunihiro N, Umaba R, Koh S, Kawashima T, Ikeda S, et al. Surgical Aspects of Corpus Callosotomy. Brain Sci. 2021 Dec 5;11(12):1608.
27. Fujimoto A, Okanishi T. Corpus Callosotomy: Editorial. Brain Sci. 2022 Jul 29;12(8):1006.

IJAE
ITALIAN JOURNAL OF ANATOMY AND EMBRYOLOGY

Firenze University Press
www.fupress.com/ijae

OPEN ACCESS

Citation: Queiroz, D. T., Trentini, J. L. A., Centeno, R. S. & Aguiar, P. H. P. (2025). Technical update of Delalande's hemispherectomy. *Italian Journal of Anatomy and Embryology* 129(1): 55-65. doi: 10.36253/ijae-16011

© 2024 Author(s). This is an open access, peer-reviewed article published by Firenze University Press (https://www.fupress.com) and distributed, except where otherwise noted, under the terms of the CC BY 4.0 License for content and CC0 1.0 Universal for metadata.

Data Availability Statement: All relevant data are within the paper and its Supporting Information files.

Competing Interests: The Author(s) declare(s) no conflict of interest.

Technical update of Delalande's hemispherectomy

Danilo T. Queiroz[1]*, João Luís A. Trentini[1], Ricardo S. Centeno[2], Paulo Henrique Pires de Aguiar[3,4]

[1] *School of Medicine of Pontifical Catholic University of São Paulo (PUC-SP), Brazil*
[2] *School of Medicine, Federal University of São Paulo (UNIFESP), Brazil*
[3,] *Faculty of Medical Sciences, ABC Medical School (FMABC), Brazil*
[4] *Department of Neurosurgery, Hospital Santa Paula, São Paulo, Brazil*
*Corresponding author. E-mail:danilotdequeiroz@gmail.com

Abstract. *Introduction*: Epilepsy is a common neurological disorder characterized by unprovoked seizures, affecting patients socially, psychologically, economically, and cognitively. When pharmacological treatment is insufficient, surgical intervention becomes necessary. Among hemispherectomy procedures, the most notable are anatomical (classic) and functional approaches, including Rasmussen, Delalande, Villemure, and Schramm. Other techniques described in the literature include cerebral hemicorticectomy, hemispherical deafferentation, transcortical subinsular hemispherectomy, and transopercular hemispherectomy. This study aims to analyze surgical methods and their effects while introducing a modified Delalande procedure and evaluating its efficacy through experiments on postmortem brains. *Material and methods*: The study used magnifying lenses (4.5x and 2.5x) and microsurgical instruments, funded by a PIBIC-CNPq scholarship. The proposed modification maintains the original disconnections but starts in the pericallosal area, offering a direct view of the corpus callosum. The procedure was tested on two formalin-fixed brains, divided into two groups of six coronal sections. Results were analyzed using the Student's t-test. *Results*: The number of pericallosal artery lesions was statistically similar in both procedures. However, the modified technique resulted in a smaller neurosurgical incision. *Conclusion*: While the risk of pericallosal artery injury remains unchanged, a smaller incision may lead to shorter procedure time, better prognosis, and increased safety for both physician and patient. Further studies with larger samples and additional variables are necessary to fully assess its effectiveness.

Keywords: hemispherectomy, epilepsy, seizure, neurosurgery.

1. INTRODUCTION

Epilepsy is a disease defined by excessive or synchronous abnormal activity of neurons, even in the absence of external and reversible causative factors, such as toxins, metabolic substances, or fevers. It involves neuronal cells predisposed to generating recurrent seizures; with cognitive, neurobiological, psychological, and social consequences resulting from these episodes.

Epilepsy itself cannot be understood as a single disease; it is, in fact, a multifaceted pathology with various etiological elements, including structural, genetic, infectious, metabolic, autoimmune, or even unknown factors.

Worldwide, it presents as one of the most common neurological diseases, alongside with chronic diseases such as migraine, stroke, and Alzheimer's disease. According to the World Health Organization, an estimated 68 million people worldwide have epilepsy, with an active prevalence of 6.38 per 1,000 people and an incidence of almost 61.44 new cases per 100,000 population, a mortality rate 2 to 3 times higher than the general population (mostly when related to refractory crises and symptomatic etiology) and also high morbidity contributing to 0.7% of disability-adjusted life years, either through direct actions such as the risk of injuries and traumas or through indirect actions, such as the use of medications and negative impact on the quality and life experience of individuals with the condition.

Although anticonvulsant medications have the potential to suppress and even control seizures in up to two-thirds of all individuals with the disease, it does not alter its long-term prognosis. Therefore, epilepsy surgery is the most effective way to achieve long-term seizure freedom in selected individuals with drug-resistant focal epilepsy (also known as refractory epilepsy); however, it is currently underutilized. Thus, a better understanding of the gradual development of epilepsy, along with its epigenetic and pharmacogenomic determinants, gives hope for better pharmacological and non-pharmacological treatment strategies in the future, modifying the course of this disease or even, in the best cases, curing it.

Patients indicated for hemispherectomy are those who have:

- Resistance to pharmacological treatment of seizure crises.
- A remaining hemisphere suitable for good outcomes after seizures, noting that the spread of epileptiform discharges to the normal hemisphere, as seen on electroencephalogram, or even rare independent discharges on the normal side, do not indicate a poor response to surgery.
- A contralateral hemisphere to the hemisphere with possible hemiplegia that can be identified with radiological and functional imaging as having diffuse abnormality.

Other indications for hemispherectomy are described in the literature, but with certain criteria sometimes controversial or relative, including patients with the following characteristics:

- Contralateral hemiplegia, because if the procedure is done before total hemiplegia, the quality of distal lower limb movements (foot and digits) may be lost, even though the patient can walk and use the proximal muscles of the upper limb.
- Delayed neurodevelopment is generally present due to the interference of seizures in the normal hemisphere's development. Therefore, this would actually be a kind of relative prerequisite for hemispherectomy.

In pediatric patients, the use of hemyspherectomy presents itself as a favorable prognosis treatment, thanks to the high potential for neural plasticity present in this age range, offering many benefits for these young patients diagnosed with epilepsy:

- Not having to deal with the harmful effects of frequent episodes of uncontrolled seizures, neither the use of high doses of antiepileptic medications during this period of neurological development.
- Avoiding the debilitating social implications of the disease and the time lost/wasted in learning due to the disease and its symptoms must be considered.
- Patients under 9 years of age, in a study, have shown better cognitive and motor postoperative outcomes, except for those who develop post-infarction sequelae.

On the other hand, it is also necessary to consider the morbidity of major surgeries in young patients and the possibility of increased neurological deficits in some cases, thus requiring careful and balanced consideration of hemispherectomy guidance against the substantial gains offered by the procedure for long-term seizure relief and functional outcomes; so that each family can weight out the potential benefits and risks in order to decide what is best for their child.

Nevertheless, there is also a discussion in the neurosurgery field about whether the presence of bilateral abnormalities in preoperative epileptogenic evaluation is actually associated with a worse postoperative outcome in hemispherectomy. It should also be noted that there are studies suggesting that hemispherectomy surgery can sometimes be used as a palliative exclusive focus procedure for severe cases with the onset of bilateral seizures predominating in one cerebral hemisphere. Additionally, surgery may be performed in cases of bilateral epilepsy with the attempt that, after its procedure, the use of antiepileptic medications may control seizures in the contralateral hemisphere.

Regarding the types of hemispherectomy, we will review:

Anatomical hemispherectomy

In this approach, the procedure begins by cautiously opening the Sylvian fissure, with great caution, as errors

at this stage can cause severe damage to contralateral vessels. After ensuring access through the fissure, it is necessary to identify, dissect, clip, and divide the lateral branches of the lenticulostriate arteries of the ipsilateral basal ganglia. Similarly, it is also necessary to divide the proximal portion of the origin of the callosomarginal artery from the ipsilateral anterior cerebral artery.

In the second step, a cottonoid is placed in the foramen of Monro to protect the underlying choroid plexus and prevent blood and debris from entering the ventricular system through which the interhemispheric callostomy is performed.

Thus, for the implementation of callosotomy, microdissection, coagulation, and aspiration of the knee, the anterior portion, up to the splenium, which defines the posterior limit, can be used

Lastly, the frontobasal white matter is divided through the anterior part of the lateral ventricle. Then, the temporal stem is dissected, while the posterior communicating arteries are clipped and divided at segment P3 (34).

It is worth noting that the amygdala and hippocampus are removed by applying subpial dissection with special care to preserve the oculomotor nerve (34, 35, 36, 38).

Regarding the choroid plexus, it is worth mentioning that it may be coagulated or left intact according to the surgeon's preference, while the ipsilateral basal nuclei and the thalamus are left in situ for better motor outcomes (34, 35, 36, 38).

Functional Hemispherectomy (Rasmussen Variation)

In this modification, the temporal lobe is removed with two cortical incisions, one in the superior temporal gyrus, running parallel to the Sylvian fissure, and the second located in the dorsal part of the temporal lobe, below the temporal lobe, perpendicular to the first and located 8cm from the pole of the temporal lobe (34). The hippocampus, parahippocampal gyrus, medial part of the uncus, and lateral part of the amygdala are removed with an ultrasonic aspirator after opening the temporal pole, emphasizing that the ipsilateral third cranial nerve must be protected.

The next step involves providing access to the ipsilateral lateral ventricle through the resection of the suprasylvian cortex via two incisions parallel and perpendicular to the Sylvian fissure (34, 35, 39, 40, 41). Finally, this stage ends with the transection of the corona radiata (34).

The following step is the completion/conclusion of the parasagittal transventricular callosotomy, followed by the removal of this cortical portion (34). The pericallosal artery constitutes the medial border of the resection, given that it vascularized the knee of the corpus callosum. The fibers of the remaining posterior and anterior callosal tracts are disconnected by the ependymal surface towards the cingulate gyrus (34, 35, 39, 41).

Lastly, the resection of the anterior and posterior connections of the frontal lobe with the parietal and occipital lobes is necessary (34, 39). Thus, the anterior cerebral artery, the superior circular sulcus, and the M1 segment of the medial cerebral artery are the borders of the transection of the corona radiata. The posterior disconnection occurs upon the full opening of the Sylvian fissure and the immediate elevation of the parietal operculum (35, 41).

Highlighting the final part of this procedure, the disconnection line extends from the posterior part of the opening of the lateral ventricle to the trigone of the temporal pole cavity (34, 35, 41).

Functional Transsylvian Hemispherectomy (Schramm Variation)

Regarding the skin incision, it is characterized as curved from the anterior portion of the tragus to the incision in the upper frontal area. The temporal fascia is opened in the same manner (10, 34, 38).

A bone flap, measuring 4x5 cm, is used over the Sylvian fissure with the use of neuronavigation. The inferior and anterior edges are formed by the temporal operculum and the limen of the insula, respectively. The anterior edge is located 5cm anterior to the posterior edge, represented by the pulvinar projection (10, 34, 42).

After this step, the Sylvian fissure is extensively opened to expose the circular sulcus and the insula, as well as to identify and properly expose and skeletonize all branches of the middle cerebral artery. For the purpose of performing uncus-amygdalo-hippocampectomy, the temporal horn is opened through the inferior circular sulcus (10, 42).

Thus, the next step involves the transection of the long fibers of the corona radiata, as a consequence of opening the ipsilateral lateral ventricle along its entire length. With this, the insular cortex becomes visible and can be safely resected (34).

Finally, the mesial disconnection is performed, which involves the frontobasal disconnection of the white matter fibers followed by the disconnection of the corpus callosum, along with the disconnection of the white matter fibers of the occipital and parietal lobes (10, 34, 42).

Lateral Perinsular Hemispherectomy (Villemure Variation)

The Villemure variation is a lateral disconnection procedure of the fronto-parieto-temporal opercular cortices. The skin incision is made centered topographically on the insula, with a bony window from the coronal suture, about 3-4 cm posterior to the external auditory canal. The lower part should be just above the middle fossa and ideally should extend upward to the mid convexity to provide access to the suprasylvian circular sulcus. Adequate exposure should allow access to the brain 2-2.5 cm below and above the Sylvian fissure. The dura mater is reflected either caudally or rostrally.

This technique is divided into three stages: the supra-insular, infra-insular, and insular phases. Subpial resection technique is employed during all phases of this procedure.

First, in the supra-insular phase, the resection of the frontal and parietal operculum is performed, leaving the adjacent insular cortex completely exposed.

The transection of the corona radiata is achieved by opening the lateral ventricle from the frontal horn to the trigone. All tissue entering the corpus callosum from the medial wall is sectioned, aiming to perform a transventricular parasagittal callosotomy. Orientation and location are confirmed by the cerebral falx, pericallosal vessels, and cingulate gyrus. At the level of the splenium, extending the anterior medial incision to reach the choroidal fissure will interrupt the fimbria-fornix and disconnect the hippocampus. The final step of this stage involves disconnecting the frontal lobe just anterior to the basal ganglia, from the rostrum toward the direction of the sphenoidal wing, while maintaining the frontal horn.

During the infra-insular phase, a temporal lobectomy is performed, including resection of the temporal operculum, transection of the temporal stalk, uncus, and removal of the amygdala and the anterior portion of the hippocampus. At this stage, with maximal resection, the optic tract becomes visible.

Finally, during the insular phase, the insula can be resected by subpial aspiration or undermined with an incision at the level of the claustrum/external capsule.

Vertical Parasagittal Hemispherectomy (Delalande Variation)

The first step of this approach is to make a linear transverse incision, which will allow for a small frontoparietal parasagittal craniotomy measuring 3x5 cm located 1-2 cm from the midline and 1/3 anterior and 2/3 posterior to the coronal suture (10, 34, 46).

After the skin incision, it is necessary to reach the ependyma of the lateral ventricle through cortical resection in the frontal cortex, measuring 3x2 cm (10, 34, 46). After opening the lateral ventricle, the foramen of Monro and the posterior aspect of the thalamus must be identified, while the corpus callosum is found following the roof of the lateral ventricle medially(10, 34, 46).

With this, the body and the splenium are resected up to the roof of the third ventricle, and the arachnoid cisterns are exposed (10). Subsequently, disconnection of the hippocampus is achieved by cutting the posterior column of the fornix at the level of the ventricular trigone (10, 56). A vertical incision is made laterally to the thalamus, guided by the choroid plexus of the temporal horn, and then follows the temporal horn of the trigone to the most anterior portion of the ventricle, keeping the incision in the white matter (10, 34, 46).

The callosotomy is then completed with the resection of the knee and rostrum of the corpus callosum up to the anterior commissure (34, 46). The next step is the resection of the posterior part of the straight gyrus, which allows visualization of the anterior cerebral artery and the optic nerve, as well as providing enough space for the final step of disconnection – a narrow anterolateral incision through the caudate nucleus of the straight gyrus to the anterior temporal horn (10, 34).

The objectives of this work are to describe a new technique, within the variation of the functional hemispherectomy surgery described by Delalande, to open up more possibilities for performing the surgical intervention for epilepsy and seizure conditions. This variation aims to minimize the risk of involvement of the pericallosal artery, which can be damaged during Delalande's hemispherectomy.

We also aim to review the main hemispherectomy techniques known and discussed in scientific articles, as well as their indications and risks, and to create a new possibility for surgical intervention for epilepsy and seizure disorders from an already used and documented technique, but with modifications to reduce the possibility of risk and harmful consequences to the patient and procedure.

Therefore, the objectives of this work are to approach the technical details, types of surgical methods and their effects (including benefits and harms to the patient), as well as point out, describe and test (in formalinized brains) a deepened technique variation of the Delalande procedure

2. MATERIAL AND METHODS

The work was carried out under the auspices of the Institute of Medical Assistance of the Public Service of

the State of São Paulo (IAMSPE-SP), with the co-participation of the Faculty of Medical and Health Sciences of the Pontifical Catholic University of São Paulo – Sorocaba Campus (FCMS-PUC-SP), where the practical work was performed. The project received a PIBIC-CNPq scholarship for the duration it was conducted, without specifications regarding the destination of the funds.

The materials used were: a 4.5x Loupe (Designs for Vision, Inc. – USA), 2.5x Loupe (Univet – Italy), and microsurgery materials (Aesculap). These materials were already available at the location where the practical part of the procedure was conducted (the autopsy lab of the Faculty of Medical and Health Sciences of the Pontifical Catholic University of São Paulo (PUC-SP) – Sorocaba Campus).

The modification proposed here to Delalande's hemispherectomy variation is based on a different order and means of performing callosotomy, given that, due to the sequence of manipulations and physical processes of the procedure, rupture and/or injury to the pericallosal artery may occur.

In the planned technique, the process of craniotomy will be the same, with modifications starting from the identification of the corpus callosum. Instead of the resection process proceeding laterally to the thalamus and then ascending for callosotomy, the process begins with an incision made directly on the corpus callosum, and only then are the structures of the basal ganglia disconnected. This choice is made because, through this sequence, the pericallosal artery is less at risk of being injured, as previously mentioned.

The procedure was performed on 14 formalin-fixed brains for illustration of the technique, and their results are present at the end of the article. The used brains were collected through the Death Verification Service (SVO), which performs the procedure in the autopsy room of the Faculty of Medical and Health Sciences of the Pontifical Catholic University of São Paulo – Sorocaba Campus, located on the ground floor of the building. All the brains undergo cranial structure removal in a procedure performed by the responsible service technicians. It is important to note that there is absolutely no transportation and/or removal of this material from the premises of the Faculty of Medical and Health Sciences of the Pontifical Catholic University of São Paulo – Sorocaba Campus.

It should also be noted that, as needed, the brains were collected after filling out a free and informed consent form, ensuring the awareness of close family members and/or responsible parties who claim full knowledge of the destination of the material for research; guaranteeing social, physical, and other integrity for the family and for the deceased. No brain was obtained from prisoners and/or prisoners of conscience. All personal information present will be duly protected and kept in total confidentiality in compliance with the General Data Protection Law (LGPD) – Brazilian Law No. 13.709, of August 14, 2018.

Of the 14 brains used in this project, one was subjected to the original procedure and another to the procedure suggested by this work without being subjected to a coronal sectioning beforehand. The other 12 were subjected to a coronal cut, to enable observation, measurement, and assessment of the differences obtained between the two surgical cuts, with this sample of 12 pieces being therefore those submitted to statistical analysis and discussed in the "Results" and "Discussion" sections.

By performing the procedures on these brains that were not subjected to coronal cuts (whole brains), it was possible to obtain a clear visualization of the anatomical structures involved during the surgical procedure, as well as an important qualitative assessment of the operation itself. Through these experiments, it was really perceived how vulnerable the pericallosal artery is to being injured/perforated by the scalpel during the procedure (during the partial resection stage of the corpus callosum).

Even so, the majority of experiments were performed on brains subjected to a coronal cut due to the possibility to collect much more measurement data from the procedures, a greater and better anatomical assessment over the traditional technique and the proposal, as well as a better understanding, through the photos, of what this work aims to achieve.

For the evaluation of both methods, 5 items were proposed to be assessed after the completion of all the procedures on all the selected pieces (12):

- Thickness of the corpus callosum
- Distance from the initial incision to the pericallosal artery
- In a straight line
- Continuously
- Distance from the initial incision to the insula
- In a straight line
- Continuously
- Total distance traveled by the procedure
- Presence or absence of lesion in the pericallosal artery

In the following figures, authored by us but based on the illustration by Peter A. Winkler (54), on the left (Fig. 1), it is possible to identify the locations covered by the hemispheric disconnection proposed by Delalande in its traditional form. Immediately to the right (Fig. 2) is the method proposed by our work to modify the technique.

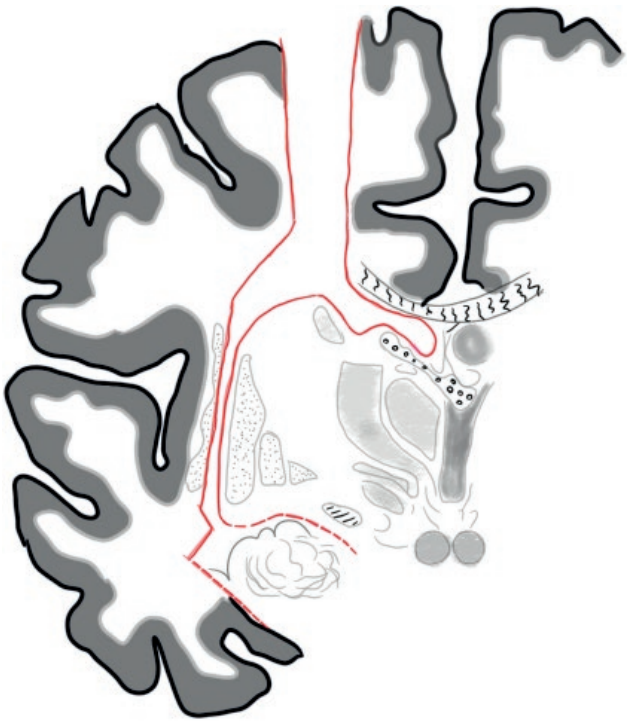

Figura 1. Colored illustration of the original variation proposed by Delalande.

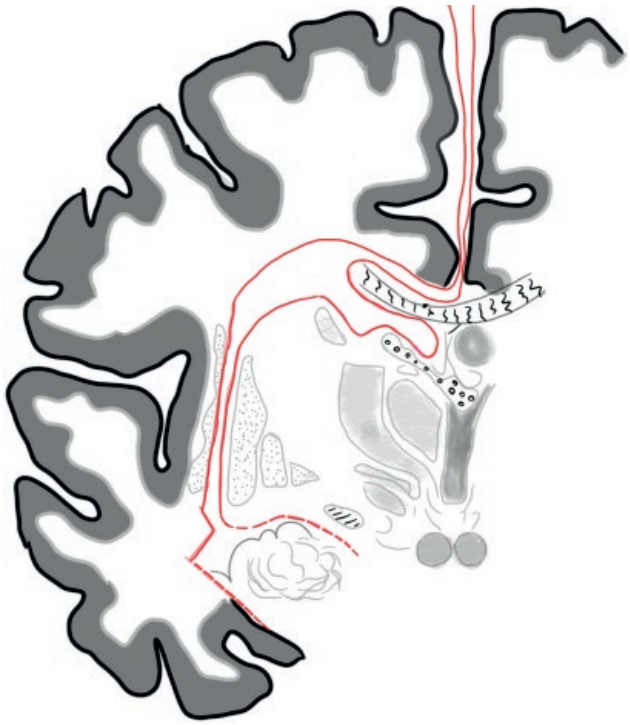

Figure 2. Colored illustration of the variation proposed by this work.

2.1. Exclusion criteria

For the use of formalin-fixed brains, some exclusion criteria were defined and adopted, including brains with the following characteristics:

- Hemorrhages
- Cause of death from serious infectious diseases
- Tumors
- Malformations
- Obtained from cadavers who died under the age of 18 or over the age of 60.

2.2. Statistical evaluation

Finally, for the purpose of better statistical understanding and the impact of the work, a comparative analysis between two groups was conducted. One group consisted of 6 formalin-fixed brains using the traditional technique and another group, also composed of 6 formalin-fixed brains, using the alteration proposed in this work, making a total of 12 brains for the analytical power of this study. The results will be presented and evaluated using the Student's t-test method, which will allow for a clearer and more reliable assessment of the effect and consequence of the work on the addressed procedure.

Regarding the literature review, articles were selected from a bibliographical search of databases such as PUBMED, using terms such as "hemispherectomy," "epilepsy," and "convulsion" to construct this systematic review.

This work was approved by the research ethics committee of both IAMSPE-SP and FCMS-PUC-SP.

3. RESULTS

In total, fourteen procedures were performed; two of them were conducted on whole brains, and twelve were performed on coronal sections of brains (which allowed clear visualization of the structures involved – also enabling more anatomically and surgically accurate procedures). Simultaneously, conducting procedures on whole brains allowed for significant learning regarding the procedures themselves (through both the traditional Delalande technique and the variation proposed in this work). In both scenarios – with whole brains and those with coronal sections – the procedures were conducted using both the Delalande method and the one proposed by this work.

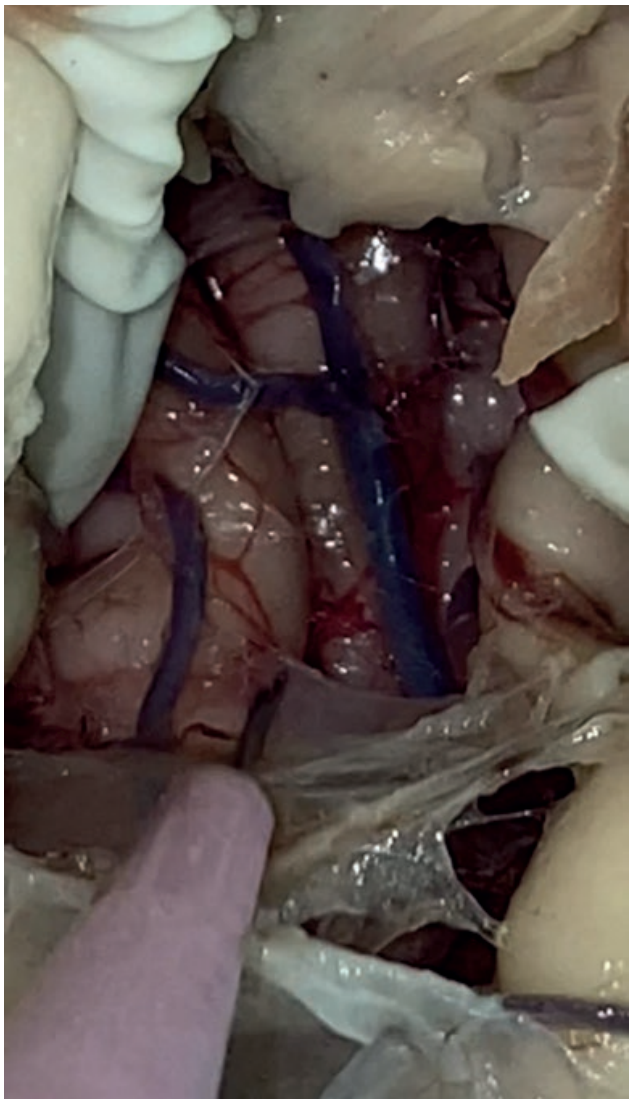

Figure 3. Visualization of the pericallosal artery through the traditional Delalande procedure performed on a whole brain.

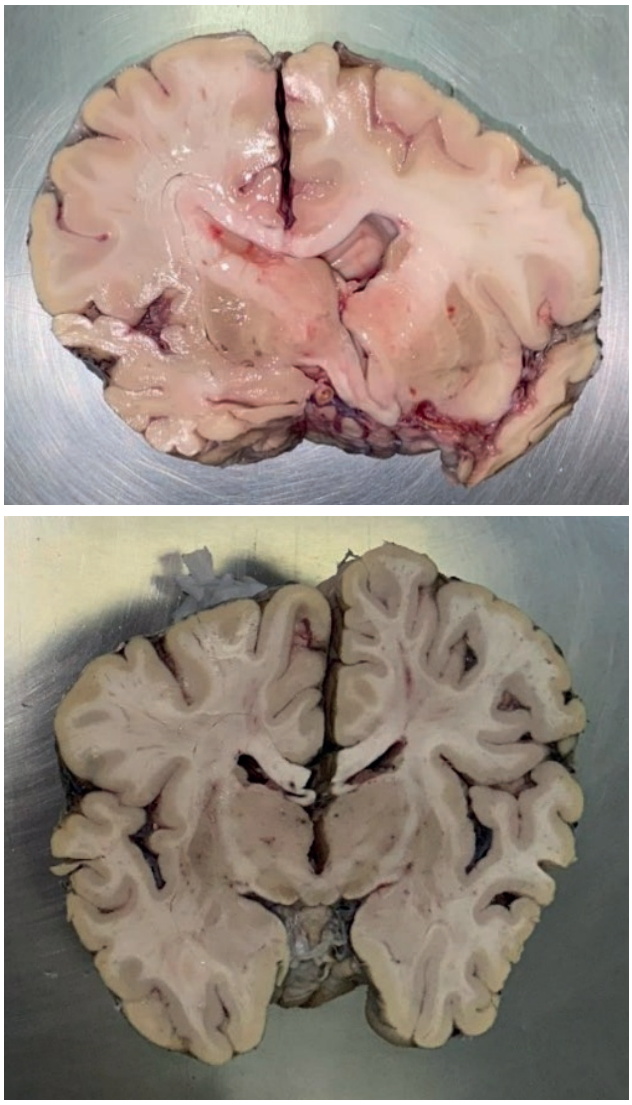

Figure 4. Outline of the hemispherectomy using the technique proposed in the study.

3.1. Whole brains

Above, Fig. 3 shows the pericallosal artery via Delalande's original procedure on a brain without a coronal cut, which was not used in the statistical analysis.

3.2. Brains in coronal section

Above it's possible to see, in Figs 4 and 5, some brains used for data collection that we will present. Below, it is possible to analyze the table with the results of both methods comparing the 5 items addressed (Table 1), with measurements in millimeters.

As the number of lesions to the pericallosal artery was equal in both procedures (Table 2), it is impossible to associate lesser or greater safety with either procedure, which precludes evaluating this data to conclude our initial hypothesis. Therefore, we delved into the analysis of the distance traveled, in millimeters, in each procedure, using the statistical methodology of the Student's t-test, promoting reliability and applicability to the collected results (Table 3).

Below is the table showing the application of the Student's t-test, which reinforces and reveals the good association of the values with the conclusion, as the p-value is below 0.05 (Table 4).

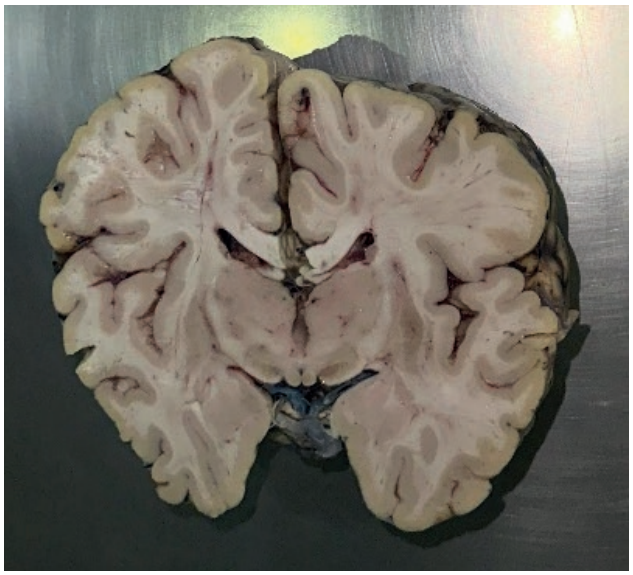

Figure 5. Outline of the hemispherectomy using the traditional Delalande technique.

Finally, we have the normality test revealing that the analysis meets the assumption of normality (since the p-value is above 0.05), a fact that, together with the data from the study, which are quantitative results, suggests a better indication for the use of the Student's t-test (Table 5).

4. DISCUSSION

As observed, there was not a decreased likelihood of injury to the pericallosal artery when six procedures of each version (traditional/Delande and the one proposed by this work) were performed, as this study proposed in one of its initial objectives. However, the analysis revealed a shorter surgical cut, in terms of extension, than the original Delalande procedure, which may indicate a possible shorter surgical time and better clinical-surgical outcomes, given that a longer surgical procedure time is linked to higher risks to the patient and a worse prognosis, as previously seen in this work.

It is important to emphasize that there was no separation, choice, or determination regarding the sex, gender, and/or age of the individuals whose brains were used in the project. Only the application of the exclusion criteria was used, which makes it impossible to evaluate possible differences that may arise in the results and analyses due to these variations.

The fact that it was performed on post-mortem brains limits the associations and correlations that can be made about the results obtained and a real scenario of neurosurgery. It is not possible to predict whether there are better clinical repercussions in the procedure presented by this work, even though it is of notable probability, since there is less brain tissue affected by the proposed method. Another point to note is that as the

Table 1. Comparative analysis of 5 selected measurements between both procedures.

	Procedure	Corpus Callosum thickness	Straight incision – pericallosal distance	Continuous incision-pericallosal distance	Straight incision-insula distance	Continuous incision-insula distance	Total distance
N	Present work	6	6	6	6	6	6
	Delalande	6	6	6	6	6	6
Mean	Present work	5,83	7,67	7,67	29,8	41,2	59,0
	Delalande	5,83	46,2	66,8	43,3	51,3	74,3
Median	Present work	5,50	8,00	8,00	31,5	42,00	63,0
	Delalande	5,50	45,00	66,00	41,5	53,00	68,5
Standard deviation	Present work	1,47	1,51	1,51	3,82	3,54	9,23
	Delalande	1,17	6,05	9,60	7,28	7,55	14,5
Minimum	Present work	4	5	5	25	36	45
	Delalande	5	39	54	34	40	62
Maximum	Present work	8	9	9	33	45	68
	Delalande	8	53	80	53	59	98

Caption: Corpus callosum – thickness of the corpus callosum; Pericallosal artery (straight) – straight distance measured between the incision and the pericallosal artery; Pericallosal artery (continuous) – distance following the procedure's path between the incision and the pericallosal artery; Insula (straight) – straight distance measured between the incision and the insula; Insula (continuous) – distance following the procedure's path between the incision and the insula; Total distance – total length of the procedure's path. All measurements are in millimeters (mm).

Table 2. Presence of pericallosal artery lesion in both methods.

Procedure	No lesion	With lesion	Total
Present work	5	1	6
Delalande	5	1	6
Total	10	2	12

Table 3. Comparison of the length traveled in each procedure.

Group	N	Mean	Median	Standard deviation	Standard error
Distance in present work	6	59,0	63,0	9,23	3,77
Distance in Delalande	6	74,3	68,5	14,5	5,91

Table 4. Independent samples t-test – Comparison between distances traveled by each procedure under Student's t-test, assuming that the proposed method is smaller than the traditional method, which is confirmed by having the p-value below 0.05.

	Estatística	gl	p
Distance traveled on Student's T test	-2,19	10,0	0,027

Score: Ha μ proposed < μ Delalande.

Table 5. Normality Test (Shapiro-Wilk) – Reveals a p-value above 0.05, which along with the values from the study, which are quantitative, indicates a better applicability of the Student's t-test.

	W	p
Distance traveled	0,931	0,387

Note: A small p-value suggests a violation of the normality assumption.

work was done on brains subjected to coronal cuts, an element that will not be present in a real procedure, it is not possible to discuss the differences in the surgical characteristics of both procedures.

The results obtained and analyzed regarding the procedure proposed by this project demonstrate the same disconnections as the original Delalande procedure, indicating and ensuring similarity between the procedures, maintaining comparable characteristics between the two interventions.

5. CONCLUSION

In conclusion, the procedure proposed with this work can indicate a new approach over the hemispherectomy proposed by Delalande that, even though it does not show, in the number of procedures performed, a decreased likelihood of injury to the pericallosal artery (as initially theorized), it does in fact provide increased benefits to the patient as it has a smaller incision extent and, therefore, has a decreased procedure time and consequently a superior prognosis and safety, both to the physician and the patient.

On another note, further studies are needed with a larger number of brains, greater similarity to a real neurosurgical scenario, and a greater number of characteristics to be analyzed and compared, such as variations between age groups, ethnicities, and sex, and the possible repercussions these elements may have on the results. WIth that, it will be possible to fully test this new approach's potential, and its efficacy on future surgeries to come, so that patients with refractory epilepsy can have an even safer surgical treatment option, with better recovery and prognosis.

ACKNOLEDGMENTS

Work funded by the PIBIC-CNPq scholarship, without specific areas of investment and have no declarations of interest.

REFERENCES

1. Fisher RS, Acevedo C, Arzimanoglou A, Bogacz A, Cross JH, Elger CE, et al. ILAE Official Report: A practical clinical definition of epilepsy. Epilepsia. 2014 Apr;55(4):475–82. https://doi.org/10.1111/epi.12550.
2. Guerreiro CAM, Guerreiro MM, Cendes F, Lopes-Cendes I. Epilepsia. São Paulo: Lemos Editorial; 2002.
3. Aguiar PH, Leal A, Ramina R. (EDS.). Tratado de neurologia clínica e cirúrgica. 1ª edição ed. [s.l.] Atena Editora, 2022.
4. Fiest KM, Sauro KM, Wiebe S, Patten SB, Kwon CS, Dykeman J, et al. Prevalence and incidence of epilepsy. Neurology. 2017 Jan 17;88(3):296–303.
5. Murray CJL, Vos T, Lozano R, Naghavi M, Flaxman AD, Michaud C, et al. Disability-adjusted life years (DALYs) for 291 diseases and injuries in 21 regions, 1990–2010: a systematic analysis for the

Global Burden of Disease Study 2010. The Lancet [Internet]. 2012 Dec https://doi.org/10.1016/s0140-6736(12)61689-4
6. Tedrus GM de AS, Fonseca LC, Carvalho RM. Epilepsy and quality of life: socio-demographic and clinical aspects, and psychiatric co-morbidity. Arquivos de Neuro-Psiquiatria. 2013 Jun;71(6):385–91. https://doi.org/10.1590/0004-282x20130044
7. Bell GS. Predictive value of death certification in the case ascertainment of epilepsy. Journal of neurology, neurosurgery and psychiatry. 2004 Dec 1;75(12):1756–8. https://doi.org/10.1136/jnnp.2003.029918.
8. Thijs RD, Surges R, O'Brien TJ, Sander JW. Epilepsy in adults. The Lancet [Internet]. 2019 Feb;393(10172):689–701. https://doi.org/10.1016/s0140-6736(18)32596-0
9. Almeida AN de, Marino R, Marie SK, Aguiar PH, Teixeira MJ. Factors of morbidity in hemispherectomies: Surgical technique×pathology. Brain and Development. 2006 May;28(4):215–22. https://doi.org/10.1016/j.braindev.2005.08.005
10. De Ribaupierre S, Delalande O. Hemispherotomy and other disconnective techniques. Neurosurgical Focus. 2008 Sep;25(3):E14. https://doi.org/10.3171/foc/2008/25/9/e14
11. Costa JC da. Tratamento Cirúrgico das Epilepsias na Criança. Journal of Epilepsy and Clinical Neurophysiology. 2006 Mar;12(1 suppl 1):5–5. https://doi.org/10.1590/s1676-26492006000200001
12. Daniel, R.T., Villemure J. Hemispherotomy Techniques. Journal of Neurosurgery, v. 98, n. 2, 1 fev. 2003.
13. Fonseca LF, Melo RP de, Cukiert A, Burattini JA, Mariani PP, Brandão R, et al. Hemisferectomia funcional precoce na hemimegalencefalia associada à epilepsia refratária. Arquivos de Neuro-Psiquiatria. 2004 Dec;62(4):1063–7. https://doi.org/10.1590/s0004-282x2004000600024
14. Lew SM, Koop JI, Mueller WM, Matthews AE, Mallonee JC. Fifty Consecutive Hemispherectomies. Neurosurgery. 2013 Oct 30;74(2):182–95. https://doi.org/10.1227/neu.0000000000000241
15. Moosa ANV, Gupta A, Jehi L, Marashly A, Cosmo G, Lachhwani D, et al. Longitudinal seizure outcome and prognostic predictors after hemispherectomy in 170 children. Neurology. 2012 Dec 5;80(3):253–60. https://doi.org/10.1212/wnl.0b013e31827dead9
16. Obeid M, Wyllie E, Rahi AC, Mikati MA. Approach to pediatric epilepsy surgery: State of the art, Part I: General principles and presurgical workup. European Journal of Paediatric Neurology. 2009 Mar 1;13(2):102–14. https://doi.org/10.1016/j.ejpn.2008.05.007
17. Cats EA, Kuan Hua Kho, Onno Van Nieuwenhuizen, Veelen V, Gosselaar PH, Van PC. Seizure freedom after functional hemispherectomy and a possible role for the insular cortex: the Dutch experience. Journal of neurosurgery. 2007 Oct 1;107(4):275–80. https://doi.org/10.3171/ped-07/10/275
18. Lew, S. M. Hemispherectomy in the treatment of seizures: a review. Translational pediatrics, v. 3, n. 3, p. 208–17, 2014.
19. Lew, S. M. et al. Posthemispherectomy hydrocephalus: Results of a comprehensive, multiinstitutional review. Epilepsia. 2012 Oct 25; v. 54, n. 2, p. 383–389.
20. Chandra, S. P. et al. Endoscopic-Assisted (Through a Mini Craniotomy) Corpus Callosotomy Combined With Anterior, Hippocampal, and Posterior Commissurotomy in Lennox-Gastaut Syndrome: A Pilot Study to Establish Its Safety and Efficacy. Neurosurgery. 2016 May 1; v. 78, n. 5, p. 743–751.
21. Chandra S, Tripathi M. Endoscopic epilepsy surgery: Emergence of a new procedure. Neurology India. 2015;63(4):571. https://doi.org/10.4103/0028-3886.162056
22. Chandra S, Tripathi M. Epilepsy surgery: Recommendations for India. Annals of Indian Academy of Neurology. 2010;13(2):87. https://doi.org/10.4103/0972-2327.64625
23. Chandra PS, Kurwale N, Garg A, Dwivedi R, Malviya SV, Tripathi M. Endoscopy-Assisted Interhemispheric Transcallosal Hemispherotomy. Neurosurgery. 2015 Feb 12;76(4):485–95. https://doi.org/10.1227/neu.0000000000000675
24. Tripathi M, Chandra P, Padma V, Shailesh G, Chandreshekar B, Sarkar C. Hemispherotomy for intractable epilepsy. Neurology India. 2008;56(2):127. https://doi.org/10.4103/0028-3886.41988
25. Jonas R, Nguyen S, Hu B, Asarnow RF, Lopresti C, Curtiss S, et al. Cerebral hemispherectomy: Hospital course, seizure, developmental, language, and motor outcomes. Neurology. 2004 May 25;62(10):1712–21. https://doi.org/10.1212/01.wnl.0000127109.14569.c3
26. Kossoff EH, Vining EPG, Pillas DJ, Pyzik PL, Avellino AM, Carson BS, et al. Hemispherectomy for intractable unihemispheric epilepsy Etiology vs outcome. Neurology. 2003 Oct 13;61(7):887–90. https://doi.org/10.1212/01.wnl.0000090107.04681.5b
27. Limbrick DD, Narayan P, Powers AK, Ojemann JG, Tae Sung Park, Bertrand ME, et al. Hemispherotomy: efficacy and analysis of seizure recurrence. Journal of neurosurgery. 2009 Oct 1;4(4):323–32. https://doi.org/10.3171/2009.5.peds0942

28. Michael Anthony Ciliberto, Limbrick D, Powers A, Titus JB, Munro R, Smyth MD. Palliative hemispherotomy in children with bilateral seizure onset. Journal of neurosurgery. 2012 Apr 1;9(4):381–8. https://doi.org/10.3171/2011.12.peds11334
29. Greiner HM, Park YD, Holland K, Horn PS, Byars AW, Mangano FT, et al. Scalp EEG does not predict hemispherectomy outcome. Seizure. 2011 Dec;20(10):758–63. https://doi.org/10.1016/j.seizure.2011.07.006
30. Salamon N, Andres M, Chute DJ, Nguyen ST, Chang JW, Huynh MN, et al. Contralateral hemimicrencephaly and clinical–pathological correlations in children with hemimegalencephaly. Brain. 2005 Nov 16;129(2):352–65. https://doi.org/10.1093/brain/awh681
31. Vera Cristina Terra-Bustamante, Luciana Midori Inuzuka, Maria R, Escorsi-Rosset S, Lauro Wichert-Ana, Alexandre V, et al. Outcome of hemispheric surgeries for refractory epilepsy in pediatric patients. Childs Nervous System. 2006 Nov 7;23(3):321–6. https://doi.org/10.1007/s00381-006-0212-6
32. Wyllie E, Deepak Lachhwani, Gupta A, Anil Chirla, Cosmo G, Worley S, et al. Successful surgery for epilepsy due to early brain lesions despite generalized EEG findings. 2007 Jul 24;69(4):389–97. https://doi.org/10.1212/01.wnl.0000266386.55715.3f
33. Lupashko S, Malik S, Donahue D, Hernandez A, M. Scott Perry. Palliative functional hemispherectomy for treatment of refractory status epilepticus associated with Alpers' disease. Childs Nervous System. 2011 Jun 1;27(8):1321–3. https://doi.org/10.1007/s00381-011-1495-9
34. Brotis, A. G. Hemispherectomy: Indications, Surgical Techniques, Complications, and Outcome. Journal of Neurology & Neurophysiology. 2015; v. 06, n. 04.
35. Fountas KN, Smith JR, Robinson JS, Tamburrini G, Pietrini D, Di Rocco C. Anatomical hemispherectomy. Child's Nervous System. 2006 Jun 30;22(8):982–91. https://doi.org/10.1007/s00381-006-0135-2
36. Krynauw RA. Infantile hemiplegia treated by removing one cerebral hemisphere. Journal of Neurology, Neurosurgery & Psychiatry. 1950 Nov 1;13(4):243–67. https://doi.org/10.1136/jnnp.13.4.243
37. Dandy WE. Removal of right cerebral hemisphere for certain tumors with hemiplegia. Journal of the American Medical Association. 1928 Mar 17;90(11):823. https://doi.org/10.1001/jama.1928.02690380007003
38. Nogueira A, Marino R, Aguiar PH, Teixeira MJ. Hemispherectomy: a schematic review of the current techniques. Neurosurgical Review. 2006 Feb 7;29(2):97–102. https://doi.org/10.1007/s10143-005-0011-7
39. Villemure, JG. Anatomical to functional hemispherectomy from Krynauw to Rasmussen. Epilepsy research Supplement. 1992 Jan 1; v. 5, p. 209–215.
40. Villemure J, Rasmussen Th. Functional Hemispherectomy in Children. Neuropediatrics. 1993 Feb;24(01):53–5. https://doi.org/10.1055/s-2008-1071514
41. Rasmussen T. Hemispherectomy for Seizures Revisited. Canadian Journal of Neurological Sciences / Journal Canadien des Sciences Neurologiques. 1983 May;10(2):71–8. https://doi.org/10.1017/s0317167100044668
42. Binder DK, Schramm J. Transsylvian functional hemispherectomy. Child's Nervous System. 2006 Jun 9;22(8):960–6. https://doi.org/10.1007/s00381-006-0131-6
43. Villemure JG, Daniel RT. Peri-insular hemispherotomy in paediatric epilepsy. Child's Nervous System. 2006 Jun 29;22(8):967–81. https://doi.org/10.1007/s00381-006-0134-3
44. Martínez, F. et al. Bases anatómicas de la hemisferotomía periinsular. Rev. méd. Urug. 2004; p. 208–214.
45. Villemure JG, Mascott CR. Peri-insular Hemispherotomy. Neurosurgery. 1995 Nov 1;37(5):975–80. https://doi.org/10.1227/00006123-199511000-00018
46. De Ribaupierre, S. et al. Contralateral frontal and cerebellar haemorrhages after peri-insular hemispherotomy. Acta Neurochirurgica. 2004 Jul 1; v. 146, n. 7, p. 743–744.

IJAE
ITALIAN JOURNAL OF ANATOMY AND EMBRYOLOGY

Firenze University Press
www.fupress.com/ijae

OPEN ACCESS

Citation: de Palma Gomes, N., dos Reis Zuniga, R. D., Bobato Licciardi, R., Araujo Dal Fabbro, E. & Pires de Aguiar, P. H. (2025). Middle cerebral artery: a systematic review and meta-analysis. *Italian Journal of Anatomy and Embryology* 129(1): 67-74. doi: 10.36253/ijae-16050

© 2024 Author(s). This is an open access, peer-reviewed article published by Firenze University Press (https://www.fupress.com) and distributed, except where otherwise noted, under the terms of the CC BY 4.0 License for content and CC0 1.0 Universal for metadata.

Data Availability Statement: All relevant data are within the paper and its Supporting Information files.

Competing Interests: The Author(s) declare(s) no conflict of interest.

ORCID:
NdPG: 0009-0004-3732-5754
RDZdR: 0000-0001-6860-2647
RBL: 0009-0007-7274-4059
EADF: 0009-0009-3960-8463
PHPdA: 0000-0002-9059-4978

Middle cerebral artery: a systematic review and meta-analysis

Nicole de Palma Gomes[1]*, Rubén David dos Reis Zuniga[1], Rafael Bobato Licciardi[1], Esther Araujo Dal Fabbro[1], Paulo Henrique Pires de Aguiar[2]

[1] *Faculty of Medicine of ABC, Santo André, São Paulo, Brazil*
[2] *Department of Morphophysiology, Faculty of Medicine of ABC, Santo André, São Paulo, Brazil*
*Corresponding author. E-mail: nicolepalma2002@gmail.com

Abstract. The middle cerebral artery is the largest and most intricate artery in the brain, making a thorough understanding of its anatomical variations and anomalies crucial. Despite its importance, considerable debate surrounds the classification of these variations, the existence of anomalies, and their prevalence. This study seeks to elucidate the prevalence of anatomical variations and anomalies in the middle cerebral artery and, as a secondary objective, to examine their correlation with clinically significant events, such as aneurysms. *Methods:* A systematic review was conducted in accordance with PRISMA guidelines, using databases such as PubMed, Embase, BVS, and Cochrane. Relevant terms from MeSH, DeCS, and Emtree were used alongside the "Open Grey" platform. A meta-analysis was carried out to determine the overall prevalence of anomalies, along with a subgroup analysis based on the methods used for the inspection and detection of arterial anomalies. *Results:* The overall prevalence of anomalies was found to be 1.4%. Through subgroup analysis, studies utilizing colored material injection revealed an almost-7 fold higher prevalence of anomalies than imaging techniques studies, and this was statistically significant (3.9% vs 0.5%, p <0.01). *Conclusion:* Imaging techniques may not adequately detect all anatomical variations of the middle cerebral artery. Longitudinal observational studies are necessary for better understanding of our findings.

Keywords: middle cerebral artery, neuroanatomy, cerebral arteries, cerebral arterial diseases, cerebrovascular disorders.

1. INTRODUCTION

The middle cerebral artery (MCA) is the largest and most complex artery in the brain [1]. Its vascular territory includes important areas, such as the basal ganglia, descending and corticospinal tracts, and cortical regions, essential for motor and sensory functions [2]. Considering that a great part of the brain hemisphere is nurtured by the MCA, this artery is frequently used in surgical interventions [3], making the understanding of its anatomical variations vital.

Typically, between days 32 and 40 of embryonic development, the MCA develops from the primitive internal carotid artery near the anterior cerebral

artery. By days 47–48, it becomes more prominent and develops branches that supply areas of the cerebral hemispheres. Alterations in this process can result in anomalies such as duplications, fenestrations, and accessory arteries. Although the embryological origin and prevalence of MCA are poorly understood [4], these anomalies are associated with various clinical presentations, including aneurysms [5].

The MCA is the major site of a third of all cerebral aneurysms with diverse morphological traits. [6]. Anatomical modifications, such as in M1 segment length, may be correlated with this type of vascular event [7], which is estimated to be present in 3.2% of the population around 50 years of age [8].

Despite the significance of the MCA, its patterns and abnormalities remain unclear and no controversies exist about the classification criteria for different presentation forms [2]. The prevalence and characteristics of its various presentations, including bifurcation, trifurcation, and tetrafurcation, remain inadequately addressed in the literature. Approximately 50% of MCA aneurysms lead to rupture, and half of the individuals who experience subarachnoid hemorrhages due to these ruptures suffer severe long-term effects [9]. These insights underscore the necessity for different therapeutic strategies, highlighting the importance of anatomical studies of the MCA and its variations. This review aims to summarize collected data related to the MCA and its pattern identification, based on literature, aiming to impact the initial diagnosis and patient management.

2. LITERATURE REVIEW

The MCA is a critical vascular structure that supplies a substantial portion of the cerebral cortex [10]. Despite its significance, current literature reveals that variations in branching patterns and associated abnormalities of the MCA remain inadequately understood, and a consensus on classification is yet to be achieved [2].

The branching patterns of the MCA are defined by the number of blood vessels in which the main trunk of the artery divides. Many variations exist between branching patterns, however literature determined the segment M1 bifurcates into two main trunks in approximately 69.9% of the cases [11]. The artery can also divide into three trunks (trifurcation), four trunks (tetrafurcations), or maintain the permanence of the main trunk without ramification (monofurcation). Kashtiara et al. estimates that the prevalence of tetrafurcation, monofurcation, and trifurcation to be 1%, 1.9% and 27%, being the trifurcation the most common branching after bifurcation.

It also outlined uncommon variations, classified as abnormalities. Literature estimates that the occurrence of these presentations on the MCA is lower than that of other important cerebral arteries [2]. Its most frequent abnormalities are accessory artery, duplication, and fenestration. The accessory MCA is a vessel that originates from the anterior cerebral artery and goes through the sylvian fissure along with the MCA [11], having a prevalence estimated at 0.03% [2]. Duplication of the MCA is an abnormality represented by an artery that originated from the internal carotid artery, independently from its extent [12], having a prevalence estimated at 0.17% [2]. MCA fenestration or segment duplication has a prevalence estimated at 0.28% [13].

Despite the recognition of these variations, the prevalence rates reported in literature remain inconsistent. This discrepancy underscores the necessity for further research to provide in-depth understanding and consolidate the existing body of knowledge regarding MCA anatomy and its variations.

3. METHODOLOGY

3.1. Search Strategies

This review was conducted in accordance with the guidelines set forth by the Preferred Reporting Items for Systematic Reviews and Meta-Analyses (PRISMA) [14]. This review´s guiding question was defined based on the "PICOS" method, in which: P (population) represents patients without neurological previous diseases; I, anatomical aspects; C, -; O (outcome), MCA pathologies predictability; S (study), observational study. The selection was conducted in August 2024.

This research is based on electronic data from PubMed, Embase, BVS, and Cochrane, according to MeSH (PubMed, Cochrane), Decs (BVS), and Entree (Embase), using the most sensible and specific terms possible, along with boolean operators, shown in the Table 1.

Table 1. Descriptors used for each database.

Data Base	Descriptors
Embase	('Middle Cerebral Artery'/exp OR 'mca') AND anatomy AND ('variations' OR 'anomalies' OR 'patterns')
Pubmed	("Middle Cerebral Artery"[Mesh]) AND "abnormalities" [Subheading]
Cochrane	"middle cerebral artery" AND "anatomy"
BVS	(Middle Cerebral Artery) AND (anatomy) AND (sh:(abnormalities))
Open Grey	" Middle Cerebral Artery"

OpenGrey was used for gray literature. We used the Rayann platform to screen and organize studies [15]. A flowchart with a summary of the selected articles is presented in Figure 1.

3.2. Inclusion and Exclusion Criteria

The articles selected for this review are those that specifically addressed MCA anatomy variations in patients without previous neurological conditions . The exclusion criteria were: articles without the pertinent issue and lack of substantial information regarding MCA

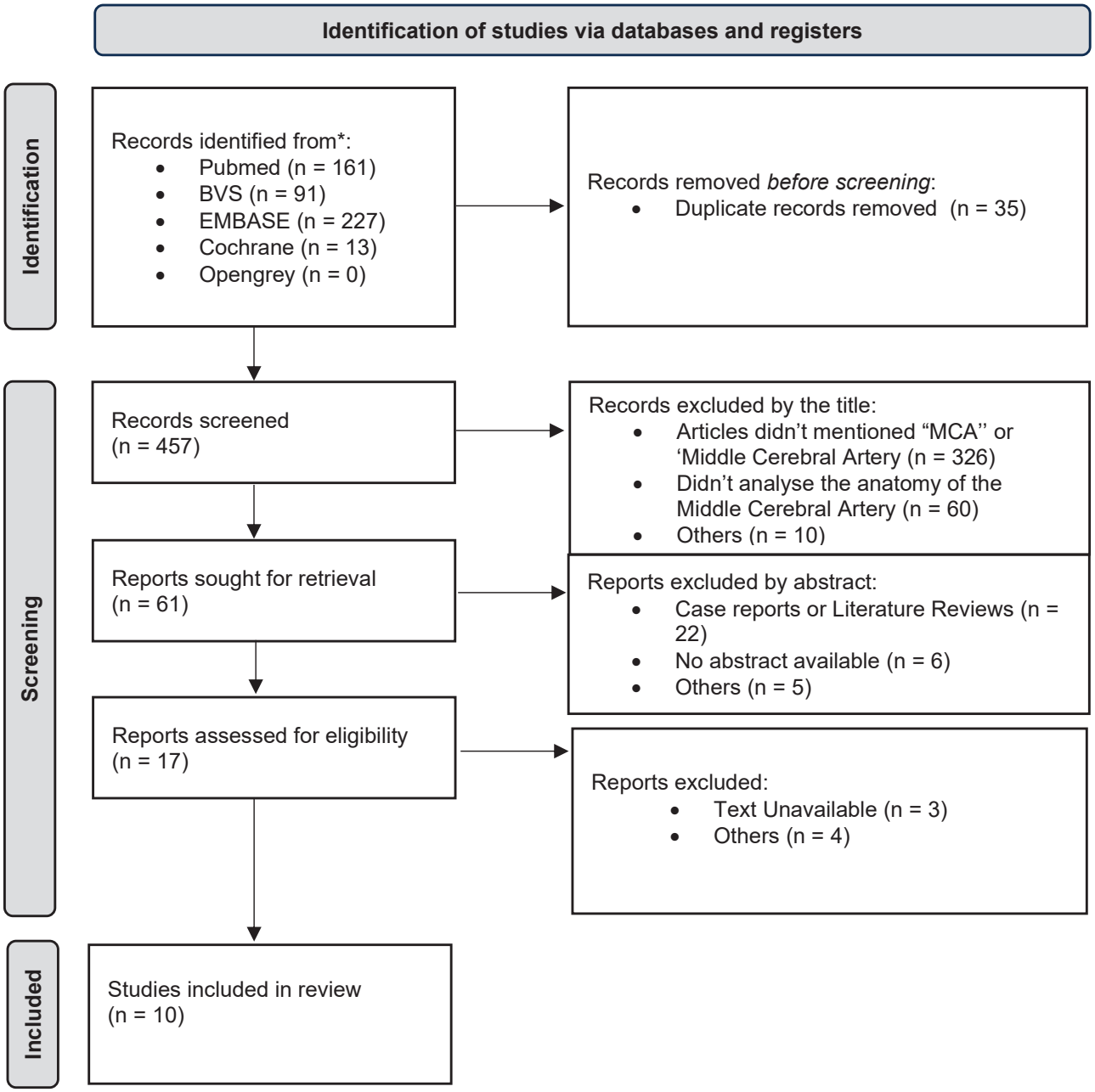

Figure 1. PRISMA flowchart.

variations. Additional exclusions encompassed abstracts, opinion pieces, narrative reviews, case reports, systematic reviews, and meta-analyses.

4. DATA ANALYSIS

A prevalence meta-analysis was conducted based on the selected studies. The extracted variable for this meta-analysis was the overall percentage of anomalies (including duplication, accessory, and fenestration) observed in the MCA. A random effects model was used for the analysis.

In addition, a subgroup analysis was carried out based on the method used to detect artery anomalies. The results of the meta-analysis are illustrated using a forest plot graphic. All analyses were performed using the R program, version 4.3.1 (2023).

5. RISK OF BIAS

The ROBINS-E platform was used to assess the risk of bias across studies [16]. Figure 2 illustrates the risk of bias, delineating distinct domains within the evaluated literature.

Studies differed in their risk of bias due to confounding factors. In some cases, as seen in a study by Brzegowy and Sharma, the variable control of age and sex was inadequate, raising concerns and moderate to high risk. In other studies, the measure of exposure presented a moderate risk due to lack of details of the instrument's precision or pattern.

Participant selection bias was higher in studies that used small or representative samples, as seen on Celliers, that did not detail the choice criteria for selecting the cerebral hemispheres to be studied. No risk of post-exposure intervention was observed in studies that did not include it. The risk of bias due to the absence of data was moderate in some studies, mainly regarding treatment. The outcome measure bias varied from low to moderate. The result selection reported bias was considered low to moderate risk, with some concerns regarding the selectivity in reporting only significant findings. In general, the graphic highlights that multiple studies present bias to some extent.

6. RESULTS:

Based on the information presented, 492 articles were initially filtered, with 35 excluded because of duplication. Following an analysis of titles and abstracts, 17 articles remained. After a complete study of the articles, only 10 met the inclusion criteria.

The selected articles, presented in Table 2, were published between 1984 and 2023, and the number of arteries analyzed in these studies ranged from 20 to 6,982. Among the methods used, four articles utilized colored substances for arterial infusion, one article implemented

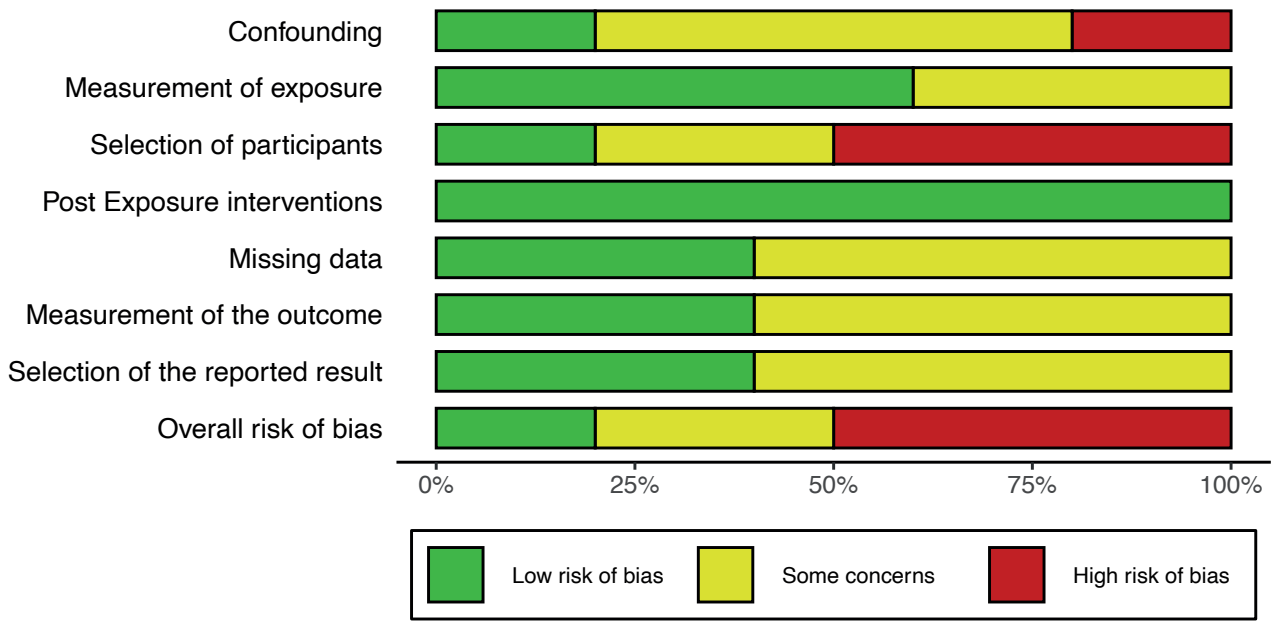

Figure 2. ROBINS-E assessment representation.

Table 2. Studies selected for the review.

Study	Age (mean)	Nº of arteries	Method	Anomalies	Branching patterns	Length of the main trunk
Celliers K, 2016	-	20	Arteries perfused with colored silicone and dissected.	Not evaluated.	5% presented monofurcation; 80% bifurcation; 15% trifurcation.	-
Uchino A et al, 2012.	-	6982	Magnetic resonance angiographies.	0.057% presented duplication; 0.043% presented fenestration.	They were not evaluated.	-
Umansky F et al, 1984.	adult individuals	70	Arteries injected with colored polyester and microsurgically dissected.	3% presented accessory artery.	6% presented monofurcation; 64% bifurcation; 29% trifurcation; 1% tetrafurcation.	15.35
Brzegowy P et al, 2017.	52.1	500	Angiotomography.	1% presented duplication; 0,4% accessory artery; 0,2% fenestration.	82,2% presented bifurcation; 13,8% trifurcation; 0,4% tetrafurcation.	15.8
Oo EM et al, 2021.	-	100	Fresh brains with microsurgical dissection.	Not evaluated.	12% presented monofurcation; 72% bifurcation; 16% trifurcation.	20.6
Pai SB et al, 2005.	-	10	Fresh brains with microsurgical dissection.	Not evaluated.	80% presented bifurcation; 20% trifurction.	20
Umansky F et al, 1988.	adult individuals	104	Arteries injected with colored polyester and microsurgically dissected.	1% presented duplication; 2% accessory artery; 1% fenestreation.	4% presented monofurcation; 60% bifurcation; 26% trifurcation; 4% tetrafurcation.	-
Tanriover N et al, 2003.	adult individuals	50	Arteries injected with colored latex.	2% presented duplication; 4% accessory artery.	88% presented bifurcation; 12% trifurcation.	17.82
Sharma U et al, 2023.	43.9	578	Angiotomography.	0.34% presented duplication; 0.17% presented fenestration.	0,17% presented monofurcation; 97,75% bifrucation; 1,04% trifurcation.	-
Rogge A et al, 2015.	42	100	Transcranial ultrasound with Doppler.	Not evaluated.	63% presented bifurcation; 32% trifurcation.	19.0

antiresonance techniques, two articles explored nanotomography, two used fresh brain specimens, and one used transcranial ultrasonography.

In terms of absolute data, the literature reported a variation in the occurrence of anomalies between 0.11% and 2%. The occurrence of MCA fenestration ranged from 0.20% to 1%, with a weighted average of 0.22%. For duplications, the weighted average occurrence was 0.2%, while that of related accessory arteries was 1.1%.

In terms of division patterns, segment M1 predominantly exhibits bifurcation with reported occurrences in the literature ranging from 64% to 97.75% and a weighted average of 84%, as detailed in Table 2. The second most common pattern is trifurcation, showing a prevalence between 1.04% and 32%, with a weighted average of 19%. Other patterns include monofurcation, which has a prevalence between 0.17% and 12%, yielding a weighted average of 2.5%, and tetrafurcation, which was a prevalence ranging from 0.4% to 4% and a weighted average of 1% (Table 3).

Furthermore, regarding length, the literature indicates a variation between 15.3 mm and 20.6 mm, with a weighted average length of 16.9 mm for segment M1.

The observed presence of anomalies was quantified at 1.4% (heterogeneity [I^2]= 89.5%; [τ^2] = 0.0055; $p < 0.0001$), as shown in Figure 3. Heterogeneity was expected, particularly due to Uchino's study [13] acting as an outlier. Application of the random effects model served to mitigate the influence of this disparity in the overall analysis.

Subsequently, a subgroup meta-analysis was performed to compare two groups using the anomaly evaluation method (infusion of colored material versus imaging study). The findings indicated a statistically significant difference in prevalence between the two methods ($\chi^2_1 = 9.74$; df = 1; $p = 0.0018$).

Regarding the heterogeneity within each group, arteries assessed by the infusion of colored material exhibited an overall anomaly prevalence of 4.0% ($I^2 = 0\%$; $\tau^2 = 0$; $p = 0.69$), suggesting no heterogeneity among the studies. In contrast, arteries evaluated through imaging studies revealed a significantly lower prevalence of 1% ($I^2 = 90.5\%$; $\tau^2 = 0.0055$; $p < 0.0001$), indicating considerable heterogeneity and underscoring the discrepancies between the methodologies employed, as demonstrated in Figure 4.

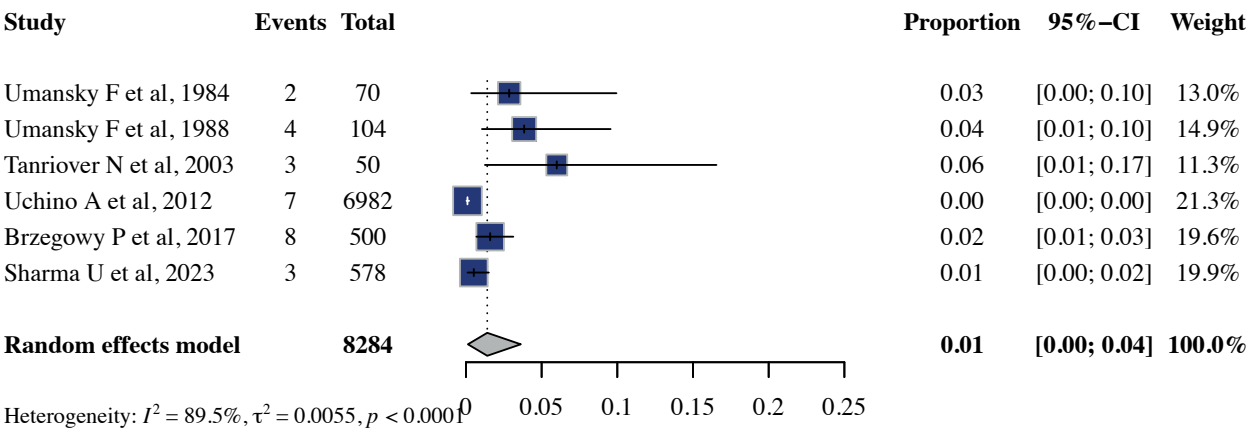

Figure 3. Forrest Plot presenting the overall prevalence of the anomalies.

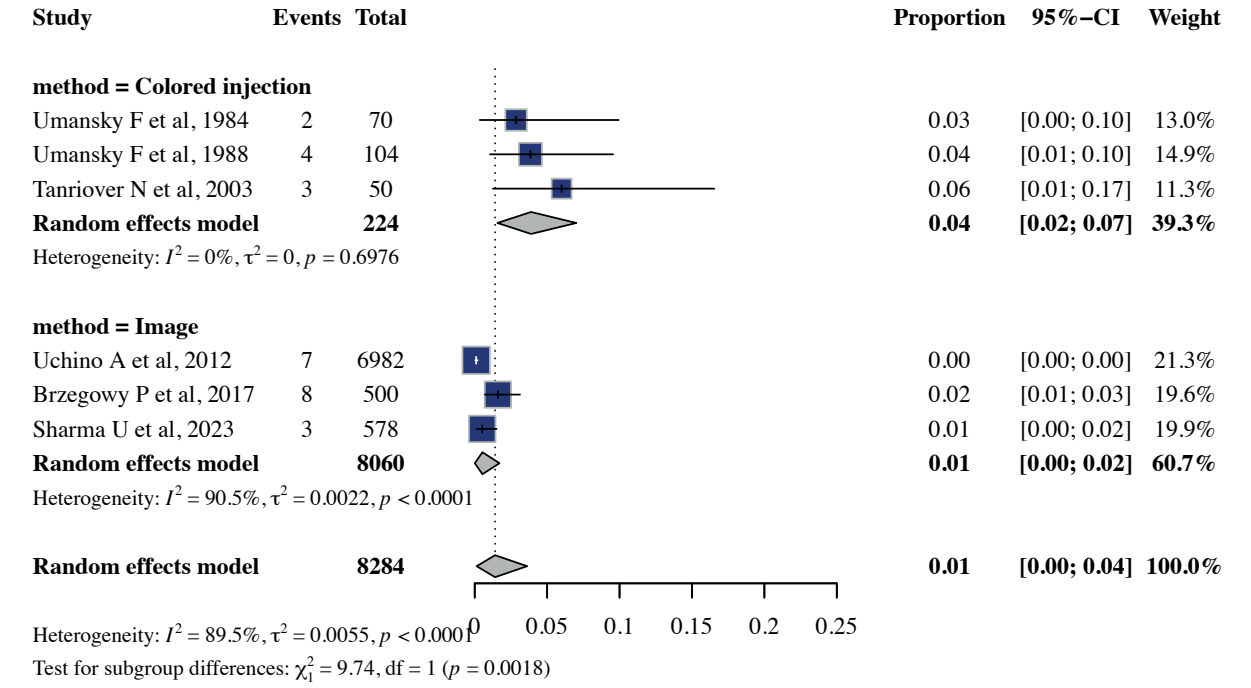

Figure 4. Subgroup meta-analysis anomaly evaluation method.

7. DISCUSSION

Detecting anatomical variations through the MCA is essential to ensure the safety of neurosurgical interventions, particularly in the context of aneurysm management. A thorough understanding of these variations contributes to more precise surgical planning and minimizes intraoperative risks.

This systematic review emphasizes the prevalence of various branching patterns, with bifurcation being the most common, occurring in approximately 84% of cases. Trifurcation represents the second most frequent variation, found in approximately 19% of cases. Additionally, less common variations such as monofurcation and tetrafurcation have been documented, although they appear in smaller proportions. Understanding whether different types of presentation of this artery are a risk factor in the development of some pathology remains necessary.

Anomalies, including duplications, accessory arteries, and fenestrations, can alter and potentially cause damage to blood flow. In cases with fenestrations, some evidence suggests that increased hemodynamic stress causes a increased prevalence of intracranial aneurysms in patients [11].

Among all selected studies, the estimated prevalence of these anomalies was 1.4%. However, a subgroup meta-analysis focusing exclusively on studies utilizing imaging methods indicated a prevalence of 0.5%. In contrast, studies that used colored injection techniques reported a higher prevalence of 3.9%.

This discrepancy (6.8 times higher in the colored injection technique) raises important questions regarding the capacity of imaging methods to capture more subtle anatomical details since this study indicates that traditional imaging methods may underestimate the prevalence of these variations. While imaging techniques such as magnetic resonance imaging (MRI) and computed tomography are commonly used to assess the MCA, they may not adequately detect the full range of anatomical variations . Although these imaging methods are convenient and broadly applicable, their limitations in identifying the complete spectrum of MCA anomalies need to be considered.

8. ACKNOWLEDGEMENTS

The author would like to thank all patients who somehow collaborated with scientific research and *Editage* for English language editing.

9. REFERENCES

1. Gibo H, Carver CC, Rhoton AL Jr, Lenkey C, Mitchell RJ. Microsurgical anatomy of the middle cerebral artery. J Neurosurg. 1981 Feb;54(2):151-69. https://doi.org/10.3171/jns.1981.54.2.0151. PMID: 7452329.
2. Fauzi AA, Gunawan R, Suroto NS. Neuroangiography patterns and anomalies of middle cerebral artery: A systematic review. *Surgical Neurology International*, v. 12, p. 235, 25 maio 2021.
3. Cilliers K, Page BJ. Anatomy of the middle cerebral artery: cortical branches, branching pattern and anomalies. *Turkish Neurosurgery*, v. 27, n. 5, p. 671-681, 2017. https://doi.org/10.5137/1019-5149.JTN.18127-16.1.
4. Okahara M, Kiyosue H, Mori H, Tanoue S, Sainou M, Nagatomi H. Anatomic variations of the cerebral arteries and their embryology: a pictorial review. *European Radiology*, v. 12, n. 10, p. 2548–2561, 21 mar. 2002.
5. Oo EM; Saw KEE, Oo HN, Than T, Thida K. Variable Anatomy of the Middle Cerebral Artery from Its Origin to the Edge of the Sylvian Fissure: A Direct Fresh Brain Study. *The Scientific World Journal*, v. 2021, p. 1–7, 9 mar. 2021. https://doi.org/10.1155/2021/6652676.
6. Estevão IA, Camporeze B, Araujo Jr AS, Nery B, Antunes ÁCM, Smith TR, Aguiar PHP. Middle cerebral artery aneurysms: aneurysm angiographic morphology and its relation to pre-operative and intraoperative rupture. *Arquivos de Neuro-Psiquiatria*, v. 75, n. 8, p. 523–532, ago. 2017.
7. Da Cunha CEG, Da Cunha Correia C. Middle cerebral artery extension and the risk for aneurysmal disease. *Journal of the Neurological Sciences*, v. 390, p. 219–221, 15 jul. 2018.
8. Galvão J, Lima DD, Haas LJ. Prevalência de aneurismas cerebrais incidentais entre homens e mulheres. *Saúde e Pesquisa*, v. 13, n. 2, p. 309–316, 12 jun. 2020.
9. Zhang W, Wang J, Li T, Mei M. Morphological parameters of middle cerebral arteries associated with aneurysm formation. *Neuroradiology*, v. 63, n. 2, p. 179–188, fev. 2021. https://doi.org/10.1007/s00234-020-02521-w.
10. Ring BA. Middle cerebral artery: Anatomical and radiographic study. *Acta Radiologica*, v. 57, n. 4, p. 289–300, 1962. https://doi.org/10.3171/jns.1981.54.2.015110.3109/00016926209171758.
11. Kashtiara A, Beldé S, Schollaert J, Menovsky T. Anatomical Variations and Anomalies of the Middle Cerebral Artery. World Neurosurg. 2024 Mar;183:e187-e200. https://doi.org/10.1016/j.wneu.2023.12.052. Epub 2023 Dec 14. PMID: 38101539.
12. Teal JS, Rumbaugh CL, Bergeron RT, Segall HD. Anomalies of the middle cerebral artery: accessory artery, duplication, and early bifurcation. Am J Roentgenol Radium Ther Nucl Med. 1973 Jul;118(3):567-75. https://doi.org/10.2214/ajr.118.3.567. PMID: 4723180.
13. Uchino A., Saito N, Okada Y, Nakajima R. Duplicate origin and fenestration of the middle cerebral artery on MR angiography. *Surgical and Radiologic Anatomy*, v. 34, p. 401–404, 2012.
14. Page MJ, McKenzie JE, Bossuyt PM, Boutron I, Hoffmann TC, Mulrow CD, Shamseer L, Tetzlaff JM, Akl EA, Brennan SE, Chou R, Glanville J, Grimshaw JM, Hróbjartsson A, Lalu MM, Li T, Loder EW, Mayo-Wilson E, McDonald S, McGuinness LA, Stewart LA, Thomas J, Tricco AC, Welch VA, Whiting P, Moher D. The PRISMA 2020 statement: an updated guideline for reporting systematic reviews. BMJ. 2021 Mar 29;372:n71. https://doi.org/10.1136/bmj.n71. PMID: 33782057; PMCID: PMC8005924.
15. Ouzzani M, Hammady H, Fedorowicz Z, Elmagarmid A. Rayyan—a web and mobile app for systematic reviews. *Systematic Reviews*, v. 5, n. 1, dez. 2016..
16. Higgins JPT, Morgan RL, Rooney AA, Taylor KW, Thayer KA, Silva RA, Lemeris C, Akl EA, Bateson TF,

Berkman ND, Glenn BS, Hróbjartsson A, LaKind JS, McAleenan A, Meerpohl JJ, Nachman RM, Obbagy JE, O'Connor A, Radke EG, Savović J, Schünemann HJ, Shea B, Tilling K, Verbeek J, Viswanathan M, Sterne JAC. A tool to assess risk of bias in non-randomized follow-up studies of exposure effects (ROBINS-E). Environ Int. 2024 Apr;186:108602. https://doi.org/10.1016/j.envint.2024.108602. Epub 2024 Mar 24. PMID: 38555664; PMCID: PMC11098530.

17. Ministério da saúde. *Diretrizes Metodológicas: Sistema GRADE – manual de graduação da qualidade da evidência e força de recomendação para tomada de decisão em saúde*. Brasília: Ministério da Saúde, Secretaria de Ciência, Tecnologia e Insumos Estratégicos, Departamento de Ciência e Tecnologia, 2014.
18. Ministério da saúde. *Diretrizes metodológicas: elaboração de revisão sistemática e meta-análise de ensaios clínicos randomizados*. Brasília: Ministério da Saúde, Secretaria de Ciência, Tecnologia, Inovação e Insumos Estratégicos em Saúde, Departamento de Gestão e Incorporação de Tecnologias em Saúde, 2021.
19. Umansky F, Juarez SM, Dujovny M, Ausman JI, Diaz FG, Gomes F, Mirchandani HG, Ray WJ. Microsurgical anatomy of the proximal segments of the middle cerebral artery. J Neurosurg. 1984 Sep;61(3):458-67. https://doi.org/10.3171/jns.1984.61.3.0458. PMID: 6747682.
20. Umansky F, Dujovny M, Ausman JI, Diaz FG, Mirchandani HG. Anomalies and variations of the middle cerebral artery: a microanatomical study. Neurosurgery. 1988 Jun;22(6 Pt 1):1023-7. https://doi.org/10.1227/00006123-198806010-00008. PMID: 3047592.
21. Rogge A, Doepp F, Schreiber S, Valdueza JM. Transcranial color-coded duplex sonography of the middle cerebral artery: more than just the M1 segment. J Ultrasound Med. 2015 Feb;34(2):267-73. https://doi.org/10.7863/ultra.34.2.267. PMID: 25614400.
22. Tanriover N, Kawashima M, Rhoton AL Jr, Ulm AJ, Mericle RA. Microsurgical anatomy of the early branches of the middle cerebral artery: morphometric analysis and classification with angiographic correlation. J Neurosurg. 2003 Jun;98(6):1277-90. https://doi.org/10.3171/jns.2003.98.6.1277. PMID: 12816276.
23. Sharma U, Verma S, Aditham S. Variations in branching pattern of middle cerebral artery using CT angiography in South Indian population. *European Journal of Anatomy*, v. 27, n. 2, p. 155-164, 2023. https://doi.org/10.52083/EPCW5127.
24. Brzegowy P, Polak J, Wnuk J, Łasocha B, Walocha J, Popiela TJ. Middle cerebral artery anatomical variations and aneurysms: a retrospective study based on computed tomography angiography findings. Folia Morphol (Warsz). 2018;77(3):434-440. https://doi.org/10.5603/FM.a2017.0112. Epub 2017 Dec 13. PMID: 29235088.
25. Pai SB, Varma RG, Kulkarni RN. Microsurgical anatomy of the middle cerebral artery. *Neurology India*, v. 53, n. 2, p. 186-190, 2005. https://doi.org/10.4103/0028-3886.16406.

IJAE
ITALIAN JOURNAL OF ANATOMY AND EMBRYOLOGY

Firenze University Press
www.fupress.com/ijae

OPEN ACCESS

Citation: Melovitz-Vasan, C., Huff, S. & Vasan, N. (2025). Accessory diaphragm: Uncommon structure in partial anomalous pulmonary venous return (PAPVR) donor. *Italian Journal of Anatomy and Embryology* 129(1): 75-78. doi: 10.36253/ijae-15942

© 2024 Author(s). This is an open access, peer-reviewed article published by Firenze University Press (https://www.fupress.com) and distributed, except where otherwise noted, under the terms of the CC BY 4.0 License for content and CC0 1.0 Universal for metadata.

Data Availability Statement: All relevant data are within the paper and its Supporting Information files.

Competing Interests: The Author(s) declare(s) no conflict of interest.

Accessory diaphragm: Uncommon structure in partial anomalous pulmonary venous return (PAPVR) donor

Cheryl Melovitz-Vasan[1]*, Susan Huff[2], Nagaswami Vasan[3]

[1] *Department of Biomedical Sciences, Cooper Medical School of Rowan University, Camden, New Jersey, 08103, USA*
[2] *Medical Education Research Collaborator, Winston-Salem, North Carolina 27104, USA*
[3] *Department of Biomedical Sciences, Cooper Medical School of Rowan University, Camden, New Jersey 08103, USA*
*Corresponding author. E-Mail: Melovitz-Vasan@rowan.edu

Abstract. This study builds upon an earlier case report, where the authors briefly mentioned the accessory diaphragm. This report provides a more detailed analysis of the embryological origins of the accessory diaphragm malformation, its clinical features, and, importantly, its impact on lung development. Duplication of the diaphragm, a rare congenital anomaly typically found on the right side and often associated with lobar agenesis-aplasia complex, is commonly referred to as an "accessory diaphragm". The exact cause of diaphragm duplication is not fully understood. However, it is believed that this condition may result from a lack of coordination between the downward migration of the septum transversum and the development of the bronchial system. The accessory diaphragm is characterized as a delicate fibromuscular membrane lined with serosa that attaches to the anterior part of the diaphragm. This membrane extends in a posterosuperior direction to connect with the posterior chest wall, effectively dividing the right hemithorax into two distinct regions. Early formation of the bronchial system may lead to the developing septum transversum being cleaved as it encounters the developing lung. Literature on accessory diaphragms indicates that the associated pulmonary vascular malformations occur during this embryonic period. In all reported cases, aplasia or varying degrees of pulmonary hypoplasia occurred on the affected side. Consequently, the accessory diaphragm divides the right pleural cavity into two sections, trapping part or all of the right middle or lower lobes beneath it.

Keywords: accessory diaphragm, pseudo horseshoe lung, congenital cardiovascular and pulmonary anomaly, partial anomalous pulmonary venous return (PAPVR), embryology of diaphragm development.

INTRODUCTION

A previous case report, briefly stated the presence of an 'accessory diaphragm' in a donor body [12]. This follow-up report includes a more detailed analysis of the embryological reasons behind this malformation, its clinical features, and, its effect on the lung's development.

Duplication of the diaphragm, also known as 'accessory diaphragm,' is a rare congenital anomaly that is almost always located on the right side and frequently associated with lobar agenesis-aplasia complex [9]. In the normal development of the diaphragm, the 'central hiatus' allows the passage of blood vessels and bronchial structures [15]. When the central hiatus is considerably narrowed and the trapped lung is not aerated, it may appear as a solid mass. In contrast, when the trapped lung is aerated, the accessory diaphragm can be seen as a fissure-like structure in the right base, extending from the anterior aspect of the hemidiaphragm toward the posterior chest wall [15].

The exact cause of diaphragm duplication is not fully understood. However, it has been postulated that this anomaly may arise from a lack of synchronization between the caudal migration of the septum transversum and the development of the bronchial system [1, 5]. In gross pathology, the accessory diaphragm is described as a delicate fibromuscular membrane lined with serosa that is connected to the anterior part of the diaphragm. It extends in a posterosuperior direction to connect with the posterior chest wall, dividing the right hemithorax into two distinct regions. It often features a central hiatus medially, allowing the passage of vessels and bronchial structures [17]. While some patients may remain asymptomatic, most present with varying degrees of respiratory difficulties. Radiographic image features include a small lung with a shift of the mediastinum and a hazy border to the mediastinum.

Very early formation of the bronchial system may result in the developing septum transversum being cleaved as it contacts the developing lung. The associated pulmonary vascular malformations reported in cases of accessory diaphragm in the literature suggest that the pathogenic event occurs during the same embryonic period [2, 6]. An accessory diaphragm is a malformation more common in males, and most often right sided [1]. It can occur in isolation or in association with lung hypoplasia or other vascular malformations. Hashida and Sherman reported that the accessory diaphragm is not always lethal in the neonatal period and may be associated with chronic pulmonary infection in later life [11]. Priyadarshi et al. reported an accessory diaphragm associated with non-immune hydrops fetalis [14].

In all the reported cases, aplasia or some degree of pulmonary hypoplasia was evident on the affected side, as seen in our earlier report [12]. The accessory diaphragm thus separates the right pleural cavity into two parts, trapping part or all of the right middle or lower lobes beneath it [4], as seen in this case. If the lung trapped beneath the accessory diaphragm is aerated, as the previous study revealed [12], it will move with respiration [7]. Furthermore, a branch of the pulmonary artery supplied the 'sequestered' segments. Most interestingly, an accessory diaphragm separating the fused anterior and lateral basal segments could be aerated using an air pump, thus providing evidence that it was functional [12].

MATERIALS AND METHODS

The cadaveric specimen reported on previously and here was obtained from the willed body program intended for dissection by medical students. This case report is based on the cadaveric dissection of a 71-year-old Caucasian male donor who died of chronic obstructive pulmonary disease and hypertension [12). Observation revealed what appeared to be surgical interventions of the heart, lung, and vasculatures, possibly due to malformations and anomalous venous drainage. Since students performed most of the dissection, some vascular and other structures were not optimally preserved. Additionally, the surgical corrective procedures disturbed the natural architecture of the gross morphology.

OBSERVATIONS AND RESULTS

On the right side of the thoracic wall, we observed an incision extending from the parasternal region at the fourth intercostal level to the midaxillary line, apparently to address anomalies surgically. Considering the shape of the incision, the surgery was probably performed during the donor's childhood to correct problems in the thoracic viscera [12].

Respiratory System: Right Lung

The right lung seemed functional, but its physical morphology was abnormal. In the hypoplastic right lung, the oblique fissure separated the upper lobe from the lower lobe, and a horizontal fissure defining the small middle lobe was also observed. The inferior lobe was vastly disorganized and severely hypoplastic and showed uncharacteristic morphology. The superior bronchopulmonary segment was markedly hypoplastic; the posterior basilar and medial basal segments (P/M basal) were not only hypoplastic and fused but also formed a slender "tail" that extended to the left pulmonary cavity behind the heart/pericardium and in front of the esophagus and aorta. However, the fused, tail-like right segments did not fuse with the similar segments of the left lung, as seen in the "scimitar" lung [8]. Closer examina-

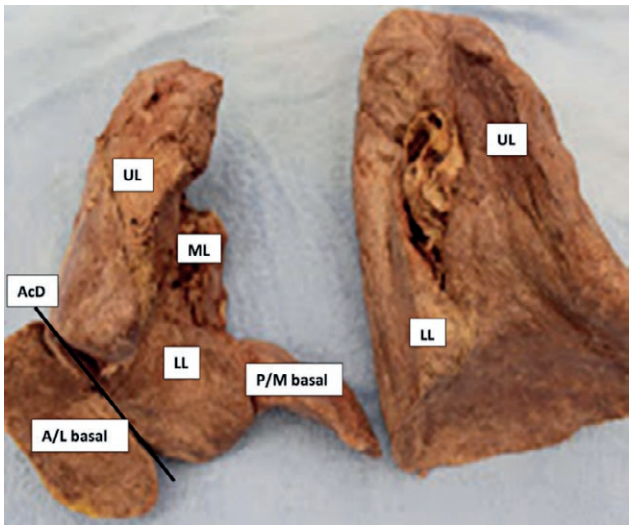

Figure 1. The accessory diaphragm is shown here by a line separating the fused anterior and lateral basal (A/L basal) segments. These fused anterior and lateral basal segments wedged between the true diaphragm and the accessory diaphragm were inflatable. The lungs of the donor show the hypogenetic right lung with anomalous morphology. The bronchopulmonary segments of the right upper (UL) and middle lobe (ML) were markedly hypoplastic but inflatable. The lower lobe was highly disorganized and severely hypoplastic and exhibited uncharacteristic morphology; the posterior basilar and medial basal segments were not only hypoplastic and fused, but also formed a slender "tail-like" morphology. UL: Upper Lobe; LL: Lower Lobe; ML: Middle Lobe; AcD: Accessory Diaphragm; A/L basal: Anterior and Lateral Basal fused segments; P/M basal: Posterior basilar and Medial basal fused segments.

tion of all the thoracic viscera, vasculatures, and surgical interventions revealed a hypogenetic right lung with partial anomalous pulmonary venous return (PAPVR) and a defined "accessory diaphragm." (Fig. 1).

The accessory diaphragm separated the fused anterior and lateral basal segments (Fig. 1). Additionally, the fused anterior and lateral basal segments, which were situated between the actual diaphragm and the accessory diaphragm, were inflatable. Although hypoplastic, the bronchi remained patent; we could inflate the superior and middle lung segments using an air pump. Notably, we could also inflate all the bronchopulmonary segments of the lower lobe and successfully pass a soft probe (such as a pipe cleaner) into the pulmonary arterial branches of these lower lobe segments.

The accessory diaphragm described and reported here is a rare congenital anomaly associated with pediatric patients having an atrial septal defect [13, 16]. It occurs mainly on the right side [3] and comprises fibromuscular tissue with a serosal lining [5]. In all documented cases, aplasia or some degree of pulmonary hypoplasia was evident on the affected side [3].

Heart and Vasculatures

The heart's morphology appeared normal; however, the heart and mediastinum were displaced more to the right side, as observed in previous studies [10, 12]. Evidence pointed to surgical procedures to correct the atrial septal defect and right superior pulmonary vein that reached into the superior vena cava.

DISCUSSION AND ANALYSIS

A person like the one in this report who has scimitar syndrome or partial anomalous pulmonary venous return (PAPVR), is often asymptomatic and may be unaware of the condition. However, the person (donor) in this report had surgical interventions at a young age to correct anomalous venous return and cardiac anomalies such as ASD.

Accessory Diaphragm

An accessory diaphragm is a thin fibromuscular membrane that appears to be related to the incomplete descent of the septum transversum [5]. This anomaly mainly occurs on the right side. Its cause remains unclear, but the timing difference in the growth of the two lung buds, as previously suggested, may provide an explanation [5]. In all the reported cases, aplasia or varying degrees of pulmonary hypoplasia were evident on the affected side, as also seen in the case presented here (Fig. 1). The accessory diaphragm separates the right pleural cavity into two parts, which can trap part or all of the right middle or lower lobes beneath it [4], as observed in the case presented here. If the lung located beneath the accessory diaphragm is aerated, as demonstrated in this report, it will move with respiration [7]. Interestingly, an accessory diaphragm separated the fused anterior and lateral basal segments; these segments could be aerated using a handheld cycle pump, thus providing evidence that it was functional. Additionally, the 'sequestered' segments received blood supply from a branch of the pulmonary artery.

CONCLUSION

In conclusion, in the follow-up of the case of the hypogenetic right lung, another unusual feature, the accessory diaphragm, is reported here. Very early formation of the bronchial system may result in the developing septum transversum being cleaved as it makes contact with the developing lung, which likely results in an accessory diaphragm. The associated pulmonary

vascular malformations reported in cases of accessory diaphragm in the literature suggest that the pathogenic event occurs during this embryonic period.

ACKNOWLEDGEMENTS:

The authors sincerely thank the donor and his family for their generosity, which made this study possible and facilitated scientific and medical innovations in patient care.

FUNDING

This study was supported by the Cooper Medical School of Rowan University research and innovation grant.

DISCLOSURE

Drs. Melovitz-Vasan and Vasan participated in the dissections. All authors participated in the article preparation. Dr. Melovitz-Vasan envisioned the project and edited the final manuscript along with Ms. Huff. All the authors approved the final form of the paper.

REFERENCES

1. Becmeur F, Horta P, Donato L, Christmann D, Sauvage P. (1995) Accessory diaphragm – review of 31 cases in the literature. Eur J Pediatr Surg. 5: 43–7, indexed in Pubmed: 7756236 https://doi.org/10.1055/s-2008-1066162.
2. Bellini C, Hennekam RCM. (2012) Non-immune hydrops fetalis: a short review of etiology and pathophysiology. Am J Med Genet A. 158A: 597–605, indexed in Pubmed: 22302731, https://doi.org/10.1002/ajmg.a.34438.
3. Cooper G. (1836) Case of malformation of the thoracic viscera consisting of imperfect development of the right lung and transposition of the heart. London Medical Gazette. 18: 600–602.
4. Currarino G, Williams B. (1985) Causes of congenital unilateral pulmonary hypoplasia: a study of 33 cases. Pediatr Radiol. 15(1): 15–24, indexed in Pubmed: 3969292, https://doi.org/10.1007/BF02387847,.
5. Davis WS, Allen RP. (1968) Accessory diaphragm. Duplication of the diaphragm. Radiol Clin North Am. 6(2): 253–263, indexed in Pubmed: 5667501.
6. Drake EH, Lynch JP. (1950) Bronchiectasis associated with anomaly of the right pulmonary vein and right diaphragm. J Thorac Surg. 19:433–37, indexed in Pubmed: 15410515.
7. Felson B. (1973) Chest roentgenology. Philadelphia, Saunders. 81–92.
8. Frank JL, Poole CA, Rosas G. (1986) Horseshoe lung: clinical, pathologic, and radiologic features and a new plain film finding. AJR Am J Roentgenol. 146(2): 217–226, indexed in Pubmed: 3484566, https://doi.org/10.2214/ajr.146.2.217.
9. Hart JC, Cohen IT, Ballantine TV, Varrano LF. (1981) Accessory diaphragm in an infant. J Pediatr Surg. 16; 947-949, indexed in Pubmed: 7338778, https://doi.org/10.1016/s0022-3468(81)80851-2.
10. Hartman T. Case 9 – Horseshoe lung. (2011) In: Hartman T (ed.). Pearls and Pitfalls in Thoracic Imaging: Variants and Other Difficult Diagnoses. Cambridge University Press, Cambridge. 22–23.
11. Hashida Y, Sherman FE. (1961) Accessory diaphragm associated with neonatal respiratory distress. J Pediatr. 59; 529-532, indexed in Pubmed: 13905178, https://doi.org/10.1016/s0022-3476(61)80236-9.
12. Melovitz-Vasan C, White A, Huff S, Vasan N. (2023) Hypogenetic right lung with partial anomalous pulmonary venous return and accessory diaphragm: a case of "scimitar lung." Folia Morphol (Warsz). 82(4): 980-987. https://doi.org/10.5603/FM.a2022.0098. Epub 2022 Dec 6. PMID: 36472398.
13. Olson MA, Becker GJ. (1986) The Scimitar syndrome: CT findings in partial anomalous pulmonary venous return. Radiology. 159(1): 25–26, https://doi.org/10.1148/radiology. 159.1.3952313, indexed in Pubmed: 3952313.
14. Priyadarshi A, Sugo E, Challis D, Bolisetty S. (2014) Accessory diaphragm associated with non-immune hydrops fetalis. BMJ Case Rep. Jul 4;2014:bcr2014204090. https://doi.org/10.1136/bcr-2014-204090. PMID: 25100808; PMCID: PMC4091454.
15. Restrepo R, Lee EY. (2008) The diaphragm. In: Slovis TL (ed.). Caffey's Pediatric Diagnostic Imaging (11th Edition). Mosby Elsevier, Philadelphia. 587-592.
16. van den Hoven AT, Chelu RG, Duijnhouwer AL, Demulier L, Devos D, Nieman K, Witsenburg M, van den Bosch AE, Loeys BL, van Hagen IM, Roos-Hesselink JW. (2017) Partial anomalous pulmonary venous return in Turner syndrome. Eur J Radiol. 95: 141–146, https://doi.org/10.1016/j. ejrad.2017.07.024, indexed in Pubmed: 28987660.
17. Wille L, Holthusen W, Willich E. (1975) Accessory diaphragm. Report of 6 cases and a review of the literature. Pediatr Radiol. 4; 14-20, indexed in Pubmed: 1233449, https://doi.org/10.1007/BF00978814.

IJAE
ITALIAN JOURNAL OF ANATOMY AND EMBRYOLOGY

Firenze University Press
www.fupress.com/ijae

OPEN ACCESS

Citation: Heyn, R. (2025). Use of figurative artwork in clinical anatomy as a valid teaching tool to train visual skills and critical thinking: a pictorial guide. *Italian Journal of Anatomy and Embryology* 129(1): 79-97. doi: 10.36253/ijae-15275

© 2024 Author(s). This is an open access, peer-reviewed article published by Firenze University Press (https://www.fupress.com) and distributed, except where otherwise noted, under the terms of the CC BY 4.0 License for content and CC0 1.0 Universal for metadata.

Data Availability Statement: All relevant data are within the paper and its Supporting Information files.

Competing Interests: The Author(s) declare(s) no conflict of interest.

Use of figurative artwork in clinical anatomy as a valid teaching tool to train visual skills and critical thinking: a pictorial guide

Rosemarie Heyn

Section of Human Anatomy, Department of Anatomy, Histological, Forensic, and Orthopedic Sciences (SAIMLAL), Sapienza University of Rome
E-mail: rose.heyn@uniroma1.it

Abstract. Observation has a key role in Anatomy; Art, in turn, is a powerful tool for training the "clinical eye" in medical undergraduate students. In the last years, different projects have been integrated into our three-semester course of human and clinical anatomy: webinars, conferences, videos, social media activities, and figurative artwork shown as clinical triggers. A practical guide to link artworks with body systems is herein proposed. Attention is given to choosing narrative paintings or sculptures suggesting anatomic details, malformations, and/or pathologies related to the several chapters treated along the anatomy course program. Good-resolution images can be uploaded from public-domain media file repositories. The teacher guides the students in trying to "read" and "decode" each artwork, not just looking at the main plane but also focusing on the background, color shades, textures, and body language. Free discussion, as well as critical and lateral thinking, should be encouraged. Students actively and enthusiastically participate, focusing on distinctive features of the artwork, thus rendering learning enjoyable and meaningful. The use of art positively impacts students' analytical and diagnostic skills, empathy, humanness, and mindfulness. Moreover, it promotes problem-solving and lateral thinking, all of which are essential in forming the person and a better future clinical performance. The benefits of using art in the anatomy course are clear, enhancing students' learning experience and preparing them for their future clinical practice.

Keywords: undergraduate medical education, medical humanities, artwork, lateral thinking, medical curriculum, visual skills.

INTRODUCTION

"Art teaches nothing except the significance of life" – Henry Miller.

Observation has a key role in Anatomy and is a key step preceding medical diagnosis, prognostication, and treatment (Bramstedt, 2016). Art, in turn, is a powerful tool for training the "clinical eye" in medical undergraduate students (Jasani and Saks, 2013; Srivastava et al., 2022). Clinical diagnosis includes observation, description, and interpretation of data coming from

medical imaging (radiographic, magnetic resonance imaging, computerized tomographic imaging, angiographies, and three-dimensional volume renderings). Careful patient observation is a skill that may be learned, but that is rarely explicitly taught (Bramstedt, 2016). Skills can be stimulated and trained through the medical humanities, in this case, through the analysis of figurative artworks, i.e., paintings or sculptures (Heyn, 2018). Moreover, Art as a visual narrative can show scenes of social reality and relationships and can catch the essence of life, old age, childhood, or illness. Art can show the human body in all its forms and actions (Powley and Higson, 2013).

USE OF ART IN MEDICAL EDUCATION

Anatomy teaching is undergoing significant changes. Social media are becoming increasingly prevalent as student learning aids in anatomy education. Therefore, a change in anatomy teachers' perceptions regarding the use of social media may be needed, given that most students consult online resources such as YouTube or Facebook rather than ask the educator to answer a question (Barry et al., 2016).

Many universities in the world offer -mostly elective- courses that focus on visual skills and the art of seeing (Naghshineh et al., 2008; Friedlaender and Friedlaender, 2013; Miller et al., 2013): Karolinska Institutet ("Visual Art Program", for Nursing); Yale University ("Enhancing Observational Skills"); Weill Cornell Medical College ("The Art of Observation"); McMaster University ("The Art of Seeing"); Harvard University ("Training the Eye: Improving the Art of Physical Diagnosis"). However, arts/medical humanities in general have not traditionally been part of European medical education.

During the last ten years, Sapienza University of Rome has been developing a pilot project to introduce artworks within the medical curriculum. Art has been integrated into the three-semester course of Human and Clinical Anatomy of the Faculty of Medicine and Psychology (one out of four medical faculties of Sapienza University of Rome). Students organized webinars, either online during the pandemic ("Training the Eye During the Pandemics with an Art Webinar") or hybrid after the pandemic ("Artists' Diseases in Art and Anatomy"). Students themselves chose the teachers to participate in these activities within a project called "Art and Disease. The gift of Art is the first step to caring for someone." Up until now, it has arrived in the second edition. In addition, asynchronous, pre-registered video tutorials covering clinical anatomy-related topics and subtopics have been uploaded to social media. These videos include short introductory remarks and legends. With this same aim, both a public, personally managed page of Facebook called *L'Anatomia nell'Arte: l'Arte di Osservare*; "Anatomy in Art: The Art of Observing" (https://www.facebook.com/arteanatomia/) as well as an academic channel of YouTube (https://www.youtube.com/channel/UCU1c-4GTyIXC8YH-1ZcicsA) are being used. Besides, the full video of a hybrid webinar entitled "Art and Genetics", which was organized by the medical students in 2023, was uploaded on a personal channel on YouTube (https://www.youtube.com/c/RosemarieHeyn).

Finally, figurative artworks are shown as clinical triggers or enhancers during traditional in-presence lessons. Artworks are chosen throughout a long time span, including Prehistory, the Classical period, the Late Middle Ages, the Renaissance (in particular, Flemish and Italian periods), Romanticism, Impressionism, and Modern times (Heyn, 2018). Attention is given to choosing narrative paintings, installations (i.e., Salvador Dalí's Mae West Room), or sculptures, suggesting anatomic details, malformations, and/or pathologies related to the main chapters treated along the course program.

Images of good resolution (possibly uploaded as a large format), mostly classical and representative paintings, sculptures, or photographs (especially if showing the artists), are chosen either directly from online world museums' collections, Google Arts & Culture (an online platform through which images may be obtained from partner cultural organizations in the world), or from Wikimedia Commons (an online collection of freely usable media files). In the case of most modern artists, like Frida Kahlo and Pablo Picasso, whose artworks are under the laws of copyright and not in the public domain, low-resolution images may be used, being certain that the images can be projected in the classroom without pixelation or blurring. Even a natural monument may well fit in a lesson on the eye, for example, the rock called "The Eye of the Sun" in the Monument Valley (Utah, USA). Alternatively, scientific journals may include artworks. Such is the case of the nice cover shown by Thorax (referring to the article of Ambrogi, 2014), illustrating a bronchial branching hidden in the Baby Jesus coral pendant (a detail of Piero della Francesca's artworks). In addition, the Journal of Endocrinological Investigation periodically publishes articles on Art, Anatomy, and health disorders.

Our course of Anatomy is divided into three semesters during the first two years as follows: musculoskeletal and cardiovascular systems (1st semester of the 1st year; Anatomy 1); splanchnology, including lymphatic; respiratory; digestive; urinary, and genital systems (2nd semester

of the 1st year; Anatomy 2); lastly, nervous system (central and peripheral systems as well as sense organs); integumentary (skin and its adnexa), and endocrine systems (1st semester of the 2nd year; Anatomy 3). After the first two semesters, the students get partial marks for Anatomy 1 and 2; the final mark is obtained with Anatomy 3.

Students are asked about the image they are seeing; the teacher guides the students during the lesson in trying to "read" and "decode" each artwork, not just looking to the main plane but also focusing on the background: color shades (i.e., pale; congestive, cyanotic, etc.); textures (i.e., smooth; irregular; swollen; wrinkled, etc.); body shape (i.e., dwarf; short; tall; giant; thin; overweight; obese), and body language (figure position and/or expression; emotions). A few minutes are allowed to observe and analyze the artwork properly before commenting. Even if having more than two hundred students in class may be challenging, one asks them what they see in the picture, what the picture represents to them, and what signs they see according to what they have just learned. Free discussion, as well as critical and lateral thinking, are encouraged, emphasizing that there are no "silly" questions but curiosity to find a collective -no single- truth with reasoning and imagination. An arrow or a circle may be drawn afterward to mark the detail in the picture, to look at it, and to read it again. Students replied with clearer and more focused answers; some of them gave written feedback by mail.

Thanks to the rich information regarding anatomy, health, and disease, given by the paintings and related discussions, there is a skill enhancement, training the clinical eye. The same artwork may be used more times to discuss various aspects of anatomy. For example, "The Three Graces" by Peter Paul Rubens, may be especially useful for discussing scoliosis; hyperlordosis; overweight; lateral deviation of the nipple; hyperextension of the metacarpal joints; flat feet; hallux valgus; signs of rheumatoid arthritis; cellulite or *panniculosis deformans*, and even locally advanced breast cancer with lymphadenopathy.

SUGGESTED ARTWORK

General introductory topics

General topics, such as classical anatomy lessons (Figure 1), the figure of the physician in Art, classical surgery lessons, usually taking place in medical amphitheaters, and old-style dissections, may be used within any introductory lesson. Table 1a shows a list of artworks associated with general introductory topics.

The concept of beauty, aging, and memento mori

The concepts of beauty and aging may be part of any anatomical chapter. The former is an abstract concept, elaborated by artists of all time, but not univocal in its form of representation. The idea of beauty changes according to the historical, cultural, economic, and social context in which artists live. Nevertheless, uni-

Table 1a. Examples of artworks associated with general introductory topics.

Topic	Period	Artist	Artwork
Anatomy lessons			
	1601-1603	Aert Pietersz	Anatomy Lesson of Dr. Sebastiaen Egbertsz
	1619	Nicolaes Eliaszoon Pickenoy	The Osteology Lesson of Dr. Sebastiaen Egbertsz
	1887	Pierre Aristide André Brouillet	A Clinical Lesson at the Salpêtrière
Physician	1926	Otto Dix	Portrait of Dr. Wilhelm Mayer-Hermann (laryngologist)
Surgery			
	c. 1494	Hieronymus Bosch	The Extraction of the Stone of Madness
	1628	Rembrandt	The Foot Operation
	1875	Thomas Eakins	Portrait of Dr. Samuel D. Gross (The Gross Clinic; thigh surgery)
	1889	Thomas Eakins	The Agnew Clinic (partial mastectomy in a medical amphitheater)
Dissection			
	1493	Johannes de' Ketham	The Dissection (woodcut)
	1632	Rembrandt	The Anatomy Lesson of Dr. Nicolaes Tulp
	1656	Rembrandt	The Anatomy Lesson of Dr. Deijman (brain dissection)
	1670	Adriaen Backer	Anatomy Lesson by Dr. F. Ruysch
	1683	Jan van Neck	The Anatomical Lesson of Frederik Ruysch

Figure 1. *Lesson of Anatomy.* The Osteology Lesson of Dr. Sebastiaen Egbertsz, Nicolaes Eliaszoon Pickenoy (1619). Rijksmuseum Amsterdam. Public domain, via Wikimedia Commons. https://en.m.wikipedia.org/wiki/File:Nicolaes_Eliasz._Pickenoy_The_Osteology_Lesson_of_Dr._Sebastiaen_Egbertsz.jpg

versal beauty may converge over the centuries through the representation of Venus, a symbol of fertility and femaleness. Examples are the prehistoric figurines Venus of Hohle Fels (Germany, Upper Paleolithic period) and Venus of Willendorf (Austria, Paleolithic period; Figure 14). More recent examples are the Venus de Milo (Aphrodite of Melos, Hellenistic period, c. 160-110 BCE) and the one painted by Sandro Botticelli in the "Birth of Venus" (mid 1480s).

On the other hand, brief remarks on aging and how ephemeral life is may be useful at any time of the course. Picturing the different ages of men and women was a favorite subject of the Renaissance artists, as the symbol of evanescence (Figure 2). Moreover, *memento mori* and *vanitas* were extremely popular in the 17th century, i.e., artworks designed to remind the viewer of their mortality (Figure 3), of the shortness and fragility of human life, earthly achievements, and pleasures. These paintings usually consist of a portrait with a skull and/or other symbols of mortality (hour glasses, clocks, guttering candles). Interestingly, Rembrandt Harmenszoon van Rijn (referred to as simply Rembrandt) left a legacy of about 80 self-portraits, allowing us to notice how his face changed with aging, from 1628 -in his early 20s- up to months before his death, in 1669, at 63 years old. Viewers have a unique insight into the life, character, and psychological development of the man and the artist, a perspective of which the artist was profoundly aware and that he intentionally gave the viewer, as though a more thoughtful and studied precursor to the modern selfie (Marder, 2020). Table 1b shows a list of artworks associated with beauty, aging, and *memento mori*.

The musculoskeletal system

Examples of the skeletal anatomy as well as musculoskeletal disorders are easy to be found throughout Art history: achondroplasia in court dwarves (Figure 4);

Table 1b. Examples of artworks associated with beauty, aging, and *memento mori*.

Topic	Period	Artist	Artwork
Beauty			
	Paleolithic (c. 25,000 -30,000 BCE)	Austria	Venus of Willendorf
	Mid 1480s	Sandro Botticelli	The Birth of Venus
Aging			
	c. 1512	Leonardo da Vinci (attributed)	Portrait of a Man in Red Chalk (self-portrait at about 60 years old)
	1544	Hans Baldung (Grien)	Die Sieben Lebensalter des Weibes ("The Seven Ages of Woman")
	1626-1669	Rembrandt	Self-portraits
	1835	Caspar David Friedrich	The Stages of Life
	1905	Gustav Klimt	The Three Ages of Woman
Memento mori			
	c. 1485-1490	Hieronymus Bosch	Death and the Miser
	c. 1509-1510	Hans Baldung (Grien)	Three Ages of the Woman and the Death (The Three Phases of Life and Death)
	1626-1628	Frans Hals	Young Man with a Skull
	c. 1671	Philippe de Champaigne	Still-Life with a Skull
	1885-1886	Vincent van Gogh	Head of a Skeleton with a Burning Cigarette

Figure 2. *Aging. Die Sieben Lebensalter des Weibes* ("The Seven Ages of Woman"), Hans Baldung (Grien), 1544. Museum of Fine Arts, Leipzig. Dguendel, own work, CC BY 4.0, Public domain, via Wikimedia Commons. https://en.wikipedia.org/wiki/The_Seven_Ages_of_Woman.

Figure 3. *Memento mori and vanitas.* Still-Life with a Skull, Philippe de Champaigne (c. 1671). Musée de Tessé (Le Mans). Public domain, via Wikimedia Commons. https://it.m.wikipedia.org/wiki/File:StillLifeWithASkull.jpg

Figure 4. *Musculoskeletal disorders: dwarfism.* The Dwarf, Giacomo Ceruti – "Pitocchetto" (c. 1720). In the background, a tiny subject is defecating in the middle of the street. Private collection. Public domain, via Wikimedia Commons. https://it.m.wikipedia.org/wiki/File:Giacomo_Ceruti_-_The_Dwarf_-_WGA4665.jpg

arachnodactyly (exaggerated length of ribs, extremities, and digits); polydactyly (supernumerary fingers); *hallux valgus*, i.e., lateral deviation of the hallux (Figure 5); prognathism due to consanguinity (Figure 6); connective tissue disorders, i.e., Marfan syndrome (Pyeritz, 2021); hand osteoarthritis and rheumatoid arthritis. A separate chapter is represented by genetic syndromes altering the musculoskeletal system. The famous large-format painting "The Family of King Philip IV" (better known as "Las Meninas") by Diego de Velázquez is an excellent example of characters suffering different genetic syndromes with skeletal abnormalities. Table 2a shows a list of artworks associated with the musculoskeletal system.

The cardiovascular system

The cardiovascular system may be triggered by the interesting self-portrait of Dick Ket, a Dutch painter who represents the New Realism in Art history. He suffered of cardiovascular problems and dextrocardia. In fact, a heart shadow is observed on the right part of his white t-shirt together with clubbing or "drumstick" fingers in his self-portrait of 1932). Besides, Frida Kahlo's self-portraits "Memory, the Heart" and "The Two Fridas" (Figure 7) show bleeding hearts, a symbol of her life struggles (she was divorcing from his hus-

Figure 5. *Musculoskeletal disorders: hallux valgus.* Christ at the Feast of Simon the Pharisee, Aelbrecht Bouts (c. 1490). Note the foot on the right angle. Royal Museums of Fine Arts of Belgium (Brussels). Public domain, via Wikimedia Commons. https://en.m.wikipedia.org/wiki/File:Albrecht_Bouts-Jesus_chez_Simon_le_Pharisien_IMG_1407.JPG

band, the famous Mexican painter Diego Rivera). On the other hand, Leonardo da Vinci performed many anatomical studies during his life, either as sketches or as drawings. Most of these drawings reside in the Royal Library at Windsor Castle (UK). His drawings and writings on the heart's anatomy and function are remarkably accurate, even if dated to the beginning of the 16th century. He described the heart's central function, noting that the "blood from the heart receives freshness and air in the lungs" and described the muscle meshwork architecture of the endocardium (Sterpetti, 2019). Table 2b shows a list of artworks associated with the cardiovascular system.

Figure 6. *Musculoskeletal disorders: mandibular prognathism (consanguinity).* Portrait of the Emperor Charles V, Lucas Cranach the Elder (1533). Museo Nacional Thyssen-Bornemisza (Madrid). Public domain, via Wikimedia Commons. https://en.m.wikipedia.org/wiki/File:Portrait_of_the_Emperor_Charles_V_(Lucas_Cranach_the_Elder).jpg

Splanchnology

When triggering the lymphatic system, a painting such as "Portrait of Daniel Lambert of Leicester" by Benjamin Marshall (1806) may be useful to illustrate lymphedema (besides obesity). Useful artworks illustrating the respiratory system, are those of Piero della Francesca (hidden details on the coral pendant). Salvador Dalí's installation of Mae West Room, particularly Mae West Lips, may be interesting to show for the oral cavity. Enhancing the concepts of "eating" or "swallowing" when talking about the esophagus or the stomach may be achieved by showing Vincenzo Campi's artworks, for example, *I Mangiatori di Ricotta* ("The Ricotta Eaters", c. 1585). Two curiosities of this nice painting are the artist's self-portrait (dressed in red) and a skull design on the ricotta as a *memento mori* symbol (Figure 8). A curious way of enhancing the topic "intestines" and "defecation reflex" is by showing Giacomo Ceruti's painting "The Dwarf" (Figure 4), asking the students not to focus on the first plane but on the background of the artwork. A tiny male character is observed in the typical position of defecation, in the middle of the street. Regarding the liver, the Bacchus paintings by Caravaggio show the artist himself with and without jaundice (a sign of hepatitis during and after healing). If talking, in turn, about the urinary system, Rembrandt's etching prints on micturition are illustrated funnily, with a man and a woman "making water." A famous, though tiny, landmark bronze fountain sculpture in central Brussels is the *Manneken Pis* depicting a little boy urinating into the fountain (Figure 9). Another example is "A Doctor Examining Urine," an artwork

Table 2a. Examples of artworks associated with the musculoskeletal system.

Topic	Period	Artist	Artwork
Proportions of the human body	c. 1492	Leonardo da Vinci	The Proportions of the Human Figure (after Vitruvius)
Skull			
Skull sectioned	c. 1489	Leonardo da Vinci	The skull sectioned and the seat of the "senso comune" (drawing)
Skull carving	Contemporary	Gregory Raymond Halili	Mother-of-pearl shell hand-carving
Musculoskeletal disorders			
Dwarfism	1465-1474	Andrea Mantegna	The Camera Picta
	1635-1645	Diego de Velázquez	Francisco Lezcano (El Niño de Vallecas)
	c. 1720	Giacomo Ceruti ("Pitocchetto")	The Dwarf
Gigantism	1605	Guido Reni	David with the Head of Goliath
	2001-2002	Ron Mueck	The Mask II (self-portrait)
Talipes equinovarus (clubfoot)	1642	José de Ribera ("Spagnoletto")	El Patizambo (The Clubfoot)
Hallux valgus	c. 1490	Aelbrecht Bouts	Christ at the Feast of Simon the Pharisee (the foot on the right)
Scoliosis	1625-1630	Pietro Paolini	Bacchic Concert
Scoliosis, hyperlordosis, and flat feet	1636	Peter Paul Rubens	The Three Graces
Mandibular prognathism	1533	Lucas Cranach the Elder	Portrait of the Emperor Charles V (consanguinity)
Connective tissue disorders	1534-1540	Parmigianino	Madonna with the Long Neck
Pectus excavatum, kyphosis, connective tissue disorders	1929	Christian Schad	Agosta, the Pigeon-Chested Man, and Rasha, the Black Dove
Paget's disease of bone	c. 1513	Quentin Matsys	The Ugly Duchess (aka "A Grotesque Old Woman")
Genetic syndromes	1656	Diego de Velázquez	The Family of King Philip IV (aka "Las Meninas")
Polydactyly	1912-1913	Marc Chagall	Self-portrait with Seven Digits
Hand osteoarthritis	c. 1540	Jacopino Del Conte	Michelangelo's portrait
Rheumatoid arthritis	1483	Sandro Botticelli	Portrait of a Young Man (Portrait of a Youth)

Table 2b. Examples of artworks associated with the cardiovascular system.

Topic	Period	Artist	Artwork
Studies of the major organs and vessels	c. 1480-1482	Leonardo da Vinci	Drawing
Studies of the stomach and heart	c. 1508-1509	Leonardo da Vinci	Drawings
Anatomy of a woman, showing the cardiovascular system and principal organs	c.1509-1510	Leonardo da Vinci	Drawing
Studies of the chambers of the heart	c. 1513	Leonardo da Vinci	Drawings
Heart	1982	Keith Haring	Untitled (painting of a radiating heart)
Bleeding heart	1937	Frida Kahlo	Memory, the Heart
	1939	Frida Kahlo	The Two Fridas
Heart, death, autopsy	1890	Enrique Simonet y Lombardo	Anatomy of the Heart (aka And She Had a Heart! or The Autopsy)
Dextrocardia and clubbing ("drumstick") fingers	1932	Dick Ket	Self-portrait

by Trophime Bigot, the Candlelight Master, illustrating urine analysis. Triggers for the genital system are well represented by Leonardo da Vinci's drawings as well as sculptures of female (uterus) and male (penis and scrotum) genital organs, especially as terracotta votive offerings coming from the Etruscan culture (Figure 10). Indeed, it was common in ancient Greek and Roman cultures to dedicate anatomical votive offerings to testify or acknowledge God's power (Oberhelman, 2014). Finally, suggested works for beauty and aging may be used when discussing menopause (Figures 2-3). Table 3a shows a list of artworks associated with the lymphatic system and splanchnology.

Figure 7. *Cardiovascular system: bleeding heart.* The Two Fridas, Frida Kahlo (1939). Museo de Arte Moderno (Mexico City). Public domain (low resolution), via Wikimedia Commons. https://en.wikipedia.org/wiki/The_Two_Fridas

Figure 9. *Urinary system: micturition.* Manneken Pis, Brussels landmark fountain sculpture (1965). Public domain, via Wikimedia Commons. https://commons.wikimedia.org/wiki/File:Manneken_Pis,_Brussels_(DSCF4466-crop).jpg

Figure 8. *Splanchnology: digestive system (eating, swallowing). I Mangiatori di Ricotta* ("The Ricotta Eaters"), Vincenzo Campi (c. 1585). Musée des Beaux-Arts (Lyon). Public domain, via Wikimedia Commons. https://it.m.wikipedia.org/wiki/File:The_Ricotta_eaters-Vincenzo_Campi-MBA_Lyon_H673-IMG_0324.jpg

Figure 10. *Female genital system: uterus.* "Votive uterus, 2000-344" (terracotta), Etruscan culture (3rd-2nd century BCE). Princeton University Art Museums collections online, April 7th, 2024. https://artmuseum.princeton.edu/collections/objects/5840

The mammary gland

The mammary gland is treated at various times according to the faculty we consider. In our case, it is traditionally linked to the female genital system: in other courses, in turn, it goes together with the integumentary system. The history of art provides examples of normal, active, and pathological mammary glands in young or aging women. The world's most famous statue of Juliet in Verona (Italy) has been remade several times due to

Table 3a. Examples of artworks associated with the lymphatic system and splanchnology.

Topic	Period	Artist	Artwork
Lymphatic system (lymphedema; obesity)	1806	Benjamin Marshall	Portrait of Daniel Lambert of Leicester
Respiratory system (bronchial branching)	1470-1485	Piero della Francesca	*Madonna of Senigallia* and *Brera Madonna* (Montefeltro Altarpiece; details)
Digestive system			
Oral cavity	1650	Joos van Craesbeeck	The Temptation of Saint Anthony
	1938	Salvador Dalí	Mae West Lips Sofa (installation)
Eating, swallowing; *memento mori*	c. 1585	Vincenzo Campi	*I Mangiatori di Ricotta* ("The Ricotta Eaters"; with a self-portrait)
Defecation reflex	1720	Giacomo Ceruti ("Il Pitocchetto")	*Il Nano* ("The Dwarf"; detail)
Jaundice (during illness)	1594	Caravaggio	Young Sick Bacchus (self-portrait)
Jaundice (healing)	1596	Caravaggio	Bacchus (self-portrait)
Urinary System			
Micturition (child)	1619; 1965*	Brussels landmark	*Manneken Pis* ("Little Pissing Man"); bronze fountain sculpture
Micturition (man)	1630	Rembrandt	A Man Making Water (etching print)
Micturition (woman)	1631	Rembrandt	A Woman Making Water (etching print)
Urine analysis	1630-1633	Trophime Bigot (Candlelight Master)	A Doctor Examining Urine
Genital system			
Female genital system: uterus	3rd-2nd century BCE	Etruscan culture	Votive terracotta uteri
The foetus in the womb and other studies on reproduction	c. 1509-1516	Leonardo da Vinci	Drawings
Male genital system: penis and scrotum	3rd-1st century BCE	Etruscan culture	Votive terracotta penis and scrotum
	1506–1508	Leonardo da Vinci	Weimar sheet (drawings)
Coitus (anatomical studies)	1490-1493	Leonardo da Vinci	Sketch

* This is a copy; the original one (1619) is kept at the Brussels City Museum.

erosion caused by the tradition of rubbing her breasts for good luck. The erosion opens holes in the metal as cancer marks the women's breasts. A mention of mastectomy may enrich the discussion on the personal life and human aspects of the women depicted. A good example of mastectomy is the martyrdom of Saint Agatha, like the ones illustrated in the artworks by Piero della Francesca and Francisco de Zurbarán (Figure 11). Table 3b shows a list of artworks associated with the mammary gland.

The nervous system

Some interesting artworks regarding pathologies of the nervous system, which allow a rich discussion, may be found in the last century (Radonjic, 2020), especially because with advancing medical technology many pathologies that were unknown or unidentified before, are now well described. Sometimes, we even know details on the clinical history of the figures illustrated in the artworks (i.e., Christine's World by Andrew Wyeth, 1948). If talking, in turn, about the sense organs, Art offers a wide choice with allegorical paintings on the senses, especially the series done by Peter Paul Rubens together with Jan Brueghel the Elder during the 17th century (Figure 12). Delicate, realistic tears can be found in the painting "The Descent from the Cross" ("Deposition of Christ", Figure 13) by one of the greatest Early Flemish artists ("Flemish Primitives"), Rogier van der Weyden, who lived in the 15th century. Table 4a shows a list of artworks associated with the nervous system.

The endocrine system

Obesity and the related metabolic syndrome may be illustrated by choosing a Venus sculpture, like the Paleolithic Venus of Willendorf (Figure 14), or any of the characteristic artworks of the Colombian artist, Fernando Botero. Concerning the thyroid gland and its dis-

Figure 11. *The mammary gland: mastectomy. Santa Águeda* ("Saint Agatha"), Francisco de Zurbarán (1630). Musée Fabre (Montpellier). Public domain, via Wikimedia Commons. https://commons.wikimedia.org/wiki/File:Francisco_de_Zurbar%C3%A1n_031.jpg

orders, in turn, religious images show evident thyroid enlargements (Figures 15-16), i.e., hypothyroidism or a goiter (Traversari et al., 2017; Buta, 2021; Ashrafian, 2023, 2024). In that period, an enlarged or fat neck was considered a sign of beauty and prosperity (Sterpetti et al., 2015). Goiter is characterized by the loss or shallowing of the suprasternal notch recess or craniocervical neck flexion accentuating thyroid enlargement (Ashrafian, 2024). Interestingly, Michelangelo Buonarotti and Artemisia Gentileschi painted their self-portraits evidencing goiter. In addition, Artemisia Gentileschi's famous painting "Judith and Her Maidservant" shows a goitrous neck (Christopoulou-Aletra et al., 2007). On the other hand, Piero della Francesca (1412-1492) painted two huge artworks showing himself with an evident lump or swelling in the middle of the anterior region of the neck, representing a thyroglossal duct cyst (Sterpetti et al., 2015).

Cushing's syndrome is a pathology of the adrenal glands characterized by the so-called "moon face." Two paintings of Hans Holbein the Younger, a German-Swiss artist, member of the Northern Renaissance style, and one of the greatest portraitists of the 16th century, may be good examples in this case. Table 4b shows a list of artworks associated with the endocrine system.

The integumentary system

When teaching this subject, one should first point to the characteristics of normal skin and its changes with aging. In this way, students get used to distinguishing skin physiological changes (blush, pallor, wrinkles). Alexander Kucharski's painting "Marie Antoinette in the Temple Prison" (c. 1793) points out the French Queen's pallor while imprisoned in the Tower of the Temple (Figure 17), before her execution by guillotine.

Abnormalities, like cyanosis or texture changes (i.e., rhinophyma, a complication of rosacea) may also be considered. Domenico Ghirlandaio shows a magnificent example of rhinophyma in his painting "An Old Man and His Grandson" (c. 1490, Figure 18). When talking about skin adnexa, in particular, the hair follicle, artworks showing subjects with thick beards, hypertrichosis, or alopecia, may be useful. As a curiosity, the first recorded case of hypertrichosis was described in 1580; it corresponded to Petrus Gonsalvus, a gentleman in the court of Henry II of France. On the other hand, examples of pseudoalopecia and true frontal alopecia may be observed in paintings from the 15th to the 17th centuries (Fernandez-Flores et al., 2020). A good example of how to illustrate alopecia is represented by Jan Vermeer's famous painting "The Milkmaid" (1658). Table 4c shows a list of artworks associated with the integumentary system.

Artists' disease

In the case of artists' diseases, many are the examples to be suggested, which can be properly included along the whole human and clinical anatomy course

Table 3b. Examples of artworks associated with the mammary gland.

Topic	Period	Artist	Artwork
Normal gland			
Young gland	1484	Sandro Botticelli	*La Nascita di Venere* ("The Birth of Venus")
Lactating gland	1320-1325	Ambrogio Lorenzetti	*Madonna del Latte* ("Madonna of Milk")
	1937	Frida Kahlo	*Mi Nana y Yo* ("My Nurse and I")
Aging gland	1507	Albrecht Dürer	Avarice (Old Woman with a Purse)
Abnormal gland			
Abnormal anatomical position	1487-1490	Hans Memling	The Virgin Mary Nursing the Child Christ
Breast cancer			
	1969; 1972; 2014*	Nereo Costantino	Juliet statue (Juliet's house, Verona)
	c. 1516	Raffaello Sanzio	*La Fornarina*
	1654	Rembrandt	Bathsheba Holding King David's Letter
Mastectomy	1460-1470	Piero della Francesca	*Sant'Agata* ("Saint Agatha")
	1630	Francisco de Zurbarán	*Santa Águeda* ("Saint Agatha")

*Different copies of the statue have been made due to the continuous erosion caused by tourists rubbing Juliet's breast.

Figure 12. *The sense organs: smell*. Allegory of Smell, Peter Paul Rubens and Jan Brueghel the Elder (1617-1618). Museo del Prado (Madrid). Public domain, via Wikimedia Commons. https://upload.wikimedia.org/wikipedia/commons/2/26/Jan_Brueghel_I_%26_Peter_Paul_Rubens_-_Smell_%28Museo_del_Prado%29.jpg

Figure 13. *The sense organs: eyes (tears)*. The Descent from the Cross (detail *Stabat Mater*, Mary, left), Rogier van der Weyden (before 1443). Museo del Prado (Madrid). Public domain, via Wikimedia Commons. https://upload.wikimedia.org/wikipedia/commons/a/ac/Weyden%2C_Rogier_van_der_-_Descent_from_the_Cross_-_Detail_women_%28left%29.jpg

program, as well as in *ad hoc* conferences or webinars. Besides their famous self-portraits, modern artists were also depicted in their daily lives through paintings or photographs. At times, their precious legacies of letters and poems provide insight into the struggles they faced. The self-portrait of a diseased Goya with his friend and physician, Dr. Arrieta (1820), well illustrates the bad painter's conditions at that moment (note the painting's background, which features various ghostly figures that suggest the artist's hallucinations). Moreover, his work is divided into two main periods, light, and darkness, before and after his diseases.

Henri Marie Raymond de Toulouse-Lautrec-Monfa, better known as Henri de Toulouse-Lautrec (1864–1901), had pycnodysostosis (Maroteaux-Lamy syndrome), a recessive autosomal dysplasia characterized by alteration of the bone matrix and bone fragility (he broke his legs at 13 and 14 years old); short stature (1,54 m), with an adult thorax and child inferior limbs. His skull was deformed, with a broad forehead. For the above reasons, he walked with great difficulty and suffered from recurrent pain (Markatos et al., 2018). He had to move with a cane and

Table 4a. Examples of artworks associated with the nervous system.

Topic	Period	Artist	Artwork
Nervous system			
Poliomyelitis	18th Egyptian Dynasty	Egyptian ancient art	The Doorkeeper (polio victim in an Egyptian stele)
Charcot-Marie-Tooth disease (hereditary motor and sensory neuropathy)	1948	Andrew Wyeth	Christina's World
Sense Organs			
Senses (sight, hearing, smell, taste, touch)	1617-1618	Peter Paul Rubens and Jan Brueghel the Elder	The Five Senses (allegorical series)
Hearing	17th century	Jan van Kessel the Elder	Allegory of Hearing
Ear			
	1889	Vincent van Gogh	Self-Portrait with Bandaged Ear (self-mutilation)
	20th century	Antonio Ligabue	Self-portraits series
Ear pathology: cauliflower ear	late 4th–2nd century BCE	Greek, Hellenistic period	The Boxer at Rest (bronze statue)
Taste	1645-1650	Bartolomé Esteban Murillo	Children Eating Grapes and a Melon
Eyes			
	-	Natural, Monument Valley (Utah, USA)	The Eye of the Sun (rock)
	5th century BCE or later	Classical Greek culture	Pair of stone eyes (designed for a statue)
	12th century	Roman	Mosaic of Ecclesia Romana (polychrome mosaic, Old St. Peter's Basilica apse)
Eyes (tears)	Before 1443	Rogier van der Weyden	The Descent from the Cross (detail *Stabat Mater*, Mary, left)
Red eyes	1480-1500	Dieric Bouts	*Mater Dolorosa* (Sorrowing Virgin)
	1928	René Magritte	The False Mirror

Figure 14. *The endocrine system: obesity/metabolic disorder*. The Venus of Willendorf, Austria (Paleolithic, c. 25,000 -30,000 BCE). Naturhistorisches Museum (Vienna). Bjørn Christian Tørrissen, CC BY-SA 4.0, Public domain, via Wikimedia Commons. https://commons.wikimedia.org/wiki/File:Venus_of_Willendorf_-_All_sides.jpg

always wore a hat (Figure 19). Besides, he got syphilis and cerebral alcoholism. He died at 36 years old from a stroke. Curiously, his short stature helped him in his unique artistic style, the "cut-off" technique, subsequently adopted by other painters, where objects and figures appear cut off from the edge of the frame and from unusual angles.

Vincent van Gogh, in turn, was treated with digitalis by his physician for presumed neuropsychiatric diseases. This substance was considered in the 19th century as one of the treatments for epilepsy as well as for some psychiatric illnesses. One of the well-known side effects of systemic digitalis treatment is a disturbance in yellow-blue vision (xanthopsia). Due to digitalis-induced xanthopsia, van Gogh may have perceived the world with a yellow tint, which also resulted in the predominance of colored haloes around light sources in some of his famous works. Alternatively, the haloes in his works may be caused by glaucoma (Dahan and Shoenfeld, 2017). In an analogous way, when analyzing Claude Monet's paintings (19th to 20th centuries), a change in color shades and focus of the water lilies series is noticed before and after cataracts surgery. Monet struggled to differentiate colors accurately and wrote about this to his friends. His letters provide a glimpse into the life of an artist who overcame such challenges to create masterpieces still revered today. Understanding his struggles can inspire us to appreciate his works on a deeper level.

Finally, two famous artists deserve attention. Firstly, Pierre-Auguste Renoir (1841-1919), secondly, Magdalena

Figure 15. *The endocrine system: goiter (hypothryroidism).* San Luca (Saint Luke), Jacopo Carucci (Pontormo, c. 1525). Decoration of the Capponi Chapel at Santa Felicita Church (Florence). Public domain (low resolution), via Wikimedia Commons. https://it.m.wikipedia.org/wiki/File:Jacopo_Pontormo_-_St_Luke_-_WGA18124.jpg

Figure 16. *The endocrine system: goiter (hypothryroidism).* Roger Freeing Angelica, Jean-Auguste-Dominique Ingres (1819). Louvre Museum. Public domain, via Wikimedia Commons. https://commons.wikimedia.org/wiki/File:Jean_Auguste_Dominique_Ingres_-_Roger_Delivering_Angelica.jpg

Carmen Frida Kahlo y Calderón, better known as Frida Kahlo (1907-1954). The former was a French artist, leader in the development of the Impressionist style. Around 1892, Renoir developed rheumatoid arthritis, worsened by cigarette smoking. He painted during the last twenty years of his life even after his rheumatoid arthritis severely limited his mobility. His hands were deformed and had also ankylosis of his right shoulder (Figure 20). The disease progressed in paralysis; as a consequence, the artist required a wheelchair in his last years. Nevertheless, Renoir remained able to grasp a brush, although he required an assistant to place it in his hand. The life of Renoir shows how disability cannot quell an artist's desire to create. When asked about his plight the disabled artist gave the amiable reply of "the pain passes, but the beauty remains" (Gandhi, 2019). Frida Kahlo is also an outstanding example of how strongly a person reacts to tragedy and illness. Unconventional and vital, she was marked from birth by pain and illness. She was born with spina bifida. At 18 years old she had a terrible accident, leaving her with severe polytraumatism, including her spine. She needed thirty-two orthopedic surgeries, the necessity of lying in bed for years. Consequently, she was unable to have a child. Her parents arranged a mirror above her bed so she could see herself. Consequently, her artwork is full of self-portraits and symbols, representing her feelings on physical and sentimental pain. The latter can be read everywhere in her famous painting "The Broken Spine" (*La Columna Rota*, Figure 21) painted in 1944, shortly after she had spinal surgery to correct the ongoing consequences of the traffic accident. Her spine is replaced by an Ionic column, nails are placed all over her body, and a desertic, sterile background, represents her infertility. After the amputation of her leg, she wrote "Feet, what do I need you for when I have wings to fly?"

Table 5a shows a list of artworks associated with artists' diseases.

STUDENTS' OPINION

Class representatives from the first to fifth year of the medical undergraduate degree were asked to anonymously evaluate the use of artworks during Anatomy lessons, workshops, and conferences. Students may submit an adjective or sentence either by email or anonymously through chat. Tables 6-7 show a summary of their comments (for simplicity, comments are in alphabetical order).

DISCUSSION

From the medical student's point of view, Anatomy represents a hard and challenging discipline. It is a

Table 4b. Examples of artworks associated with the endocrine system.

Topic	Period	Artist	Artwork
Obesity, metabolic syndrome	Paleolithic (c. 25,000 -30,000 BCE)	Austria	Venus of Willendorf
	c.1680	Juan Carreño de Miranda	Eugenia Martínez Vallejo (*La Monstrua Vestida*)
	20th-21st centuries	Fernando Botero	All his artworks (for example, *Mujer Fumando Un Cigarrillo*, "A Woman Smoking", 1987, sculpture)
Goiter, hypothyroidism	1435-38	Rogier van der Weyden	Virgin and Child in a Niche
	1460	Andrea Mantegna	Virgin and Child
	1512	Michelangelo	The Creator Separating Light from Darkness (self-portrait); letters
	c. 1525	Jacopo Carucci (Pontormo)	*San Luca* (Saint Luke), decoration of the Capponi Chapel at Santa Felicita Church (Florence)
	1612-1613	Artemisia Gentileschi	Judith and Her Maidservant
	1819	Jean-Auguste-Dominique Ingres	Roger Freeing Angelica
Thyroglossal duct cyst	1450-1463	Piero della Francesca	Resurrection
	1463-65	Piero della Francesca	Polyptych of the Misericordia
Hyperthyroidism	1499	Albrecht Dürer	Self-portrait
Hirsutism	1631	José de Ribera	Magdalena Ventura with Her Husband and Son
Cushing's syndrome ("moon face")	1517	Hans Holbein the Younger	Adam and Eve
	c. 1540	Hans Holbein the Younger	Portrait of Henry VIII

three-semester course given during the first two years of the medical degree curriculum. Therefore, teachers need to constantly innovate to keep both interest and concentration high. The use of artworks at any point of the program represents a new experience that helps to make anatomy teaching lighter and even funnier, without disregarding quality or contents. Good resolution images are easily found without problems of licensing and with no cost at all. It is always suggested to cite the details of each artwork (title, author, period) as well as the resources where they were obtained from. This work intends to be only a guide to whoever decides to start innovating teaching with artworks. Moreover, the suggested artworks herein contained may be changed and/or mixed with other types of artworks or even forms of Art, according to the personal preferences, the kind of audience and the type of intervention (undergraduate or postgraduate lesson; duration of the lesson, conference, or online seminar). It is always a "work in progress", modelling the selection of artworks according to the main objectives of the lesson or talk.

Students actively and enthusiastically participated, and collaboratively communicated, both during in-presence lessons as well as during in-presence and online webinars. Guided by the teacher, they focused on distinctive features of the artworks shown, thus rendering learning enjoyable and meaningful. Discussions are rich and energetic, representing a unique opportunity to interact with faculty on a non-medical level. Students learned to disagree respectfully, appreciating other perspectives. Students learned to observe objectively, to navigate uncertainty, searching a collective and no single truth. It is highly recommended to enable anonymous chat during webinars, as it allows students to express their thoughts freely. When teaching, the teacher may encourage students, especially shy ones, to participate in class discussions or ask questions via email voluntarily. The feedback was positive, even if only part of the students replied, either directly or through their representatives.

Artistic creativity is one amazing feature of human uniqueness. Moreover, Art is a representation of human life experiences across different eras and times, intertwined with emotion and cultural expression. Artificial intelligence Art, in turn, lacks the human touch and is devoid of emotion and meaning.

According to the online Encyclopedia Britannica (2024), the term Art encompasses diverse media such as painting, sculpture, printmaking, drawing, decorative arts, photography, and installation. Art-based lessons or sessions tend to approach observation and pattern recognition, metaphorically, and symbolically. Artworks represent a powerful, easy-to-find resource to

Figure 17. *The integumentary system: pallor*. Marie Antoinette at the Temple Tower, Alexandre Kucharski (c. 1793). The Royal Castle in Warsaw. Public domain, via Wikimedia Commons. https://upload.wikimedia.org/wikipedia/commons/8/80/Kucharsky_Marie_Antoinette_in_the_Temple.jpg

Figure 18. *The integumentary system: rhinophyma*. An Old Man and His Grandson, Domenico Ghirlandaio (1490). Louvre Museum. Public domain, via Wikimedia Commons. https://commons.wikimedia.org/wiki/File:Ghirlandaio,_Domenico_-_An_Old_Man_and_His_Grandson_-_Louvre_-_Google_Art_Project.jpg

understand human body changes along life as well as the natural course of diseases. It is a useful teaching tool to refine visual skills and to build so-called visual literacy, in other words, the ability to reason anatomy, physiology, and pathophysiology from visual clues (Naghshineh et al., 2008; Bramstedt, 2016). Art has a positive impact on mindfulness, i.e., a state of mind that is open to new information, actively engaged in the present, aware of multiple perspectives (Langer, 2000). In a few words, students learn a broader conception of humanness and acquire a more complete "picture" of the subjects/patients.

A particular feature emerged after reading the students' opinions. Medical humanities are essential during undergraduate studies to develop the student-person-future physician. The fact that a teacher talks about Art in a medical course, making them to notice details of an artwork never seen before, changes their perspective, stimulating critical and lateral thinking, against the rigidity of a single medical diagnosis. Seeing is defined not only as observation of physical signs and features, but also a process of understanding both person and context. Art opens the mind to different parallel solutions, all of them valid, if properly discussed. Michelangelo was once asked how he went about the sculpting process; his answer was: "I saw the angel in the marble and carved until I set him free".

Finally, a crucial point to consider is "teaching the teachers". There are many ways to form medical educators: seminars, courses, or webinars, which can be organized without much complexity. Sapienza University of Rome, for example, thanks to the Committee for Medical Education, organizes periodical seminars and courses addressed to medical teachers within the context of a tutorial on medical humanities.

CONCLUSIONS

An Art-based approach to teaching and training visual skills should be included continuously within the medical curriculum. It is our duty to stimulate a formal

Table 4c. Examples of artworks associated with the integumentary system.

Topic	Period	Artist	Artwork
Skin			
Skin as a whole	1562	Marco d'Agrate	St. Bartholomew Flayed (Duomo of Milan; sculpture)
Epidermis (normal)			
Infant (blush)	1836	Friedrich von Amerling	Portrait of Princess Maria Franziska von Liechtenstein Aged Two
Adult	c. 1460	Rogier van der Weyden	Portrait of a Lady
Adult (pallor)	c. 1793	Alexandre Kucharski	Marie Antoinette in the Temple Prison
Family	1840	Ferdinand Georg Waldmüller	Young Peasant Woman with Three Children at the Window
Old (wrinkles)			
	c. 1450	Giorgio Schiavone (Juraj Culinovic)	Saint Bernardino of Siena
	Before 1768	Christian Seybold	Portrait of an Old Woman with a Green Scarf
Adnexa: hair			
	1645	Govern Flinck	Bearded Man with a Velvet Cap
	1979	Andrew Wyeth	Braids (The Helga Pictures series)
Skin disorders			
Rhinophyma (complication of rosacea)	1490	Domenico Ghirlandaio	An Old Man and His Grandson
Alopecia	1658	Jan Vermeer	The Milkmaid
Hypertrichosis	c.1580	Unknown	Portrait of Petrus Gonsalvus

Figure 19. *Artists' disease: Henri de Toulouse-Lautrec.* Mr. Toulouse paints Mr. Lautrec. Photomontage of the artist as painter and model showing pycnodysostosis (c. 1891). Maurice Guibert (1856-1913), Public domain, via Wikimedia Commons. https://commons.wikimedia.org/wiki/File:Guibert_2.jpg

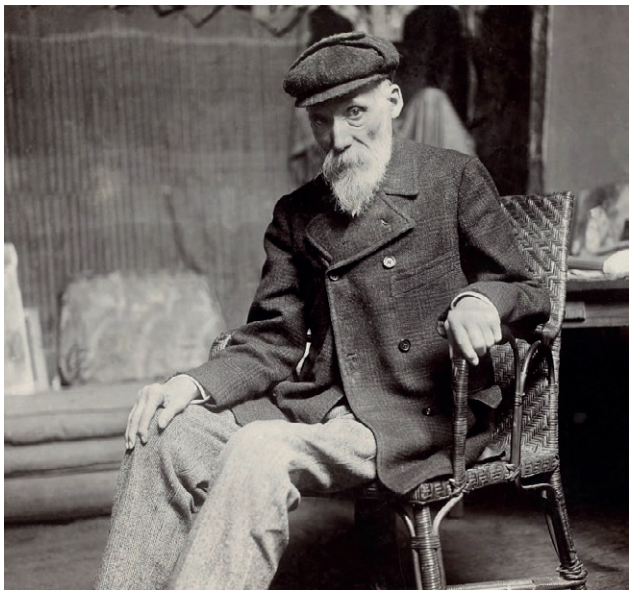

Figure 20. *Artists' disease: Pierre-Auguste Renoir.* Portrait of the artist showing the effects of advanced rheumatoid arthritis (c. 1910). Dornac, Public domain, via Wikimedia Commons. https://commons.wikimedia.org/wiki/File:Renoir,_Pierre-Auguste,_by_Dornac,_BNF_Gallica.jpg

commitment with medical humanities in any biomedical degree, including both students and colleagues. The use of figurative art has a positive impact on students' diagnostic skills, empathy, and mindfulness. Moreover, it favors critical and lateral thinking, as well as problem-solving, opening the mind to alternate ways of seeing. The natural consequence is to enhance students' abilities to observe more deeply and to better understand real clinical situations, thus training more empathic (future) physicians.

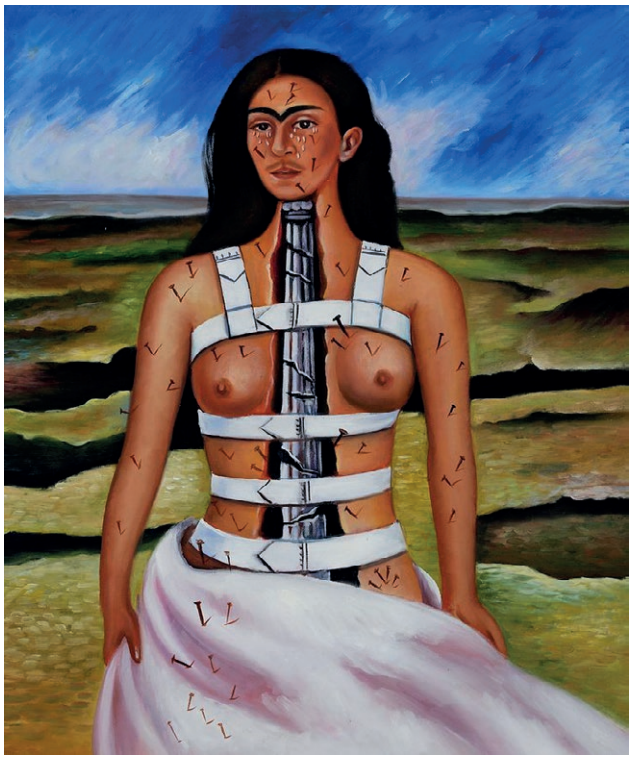

Figure 21. *Artists' disease: Frida Kahlo. La Columna Rota* ("The Broken Column"). Self-portrait of the artist symbolysing the physical and sentimental pain that signed her whole life. Frida Kahlo (1944). Museo Dolores Olmedo, Xochimilco (Mexico City). Public domain (low resolution), via Wikimedia Commons. https://en.wikipedia.org/wiki/File:The_Broken_Column.jpg#/media/File:The_Broken_Column.jpg

ACKNOWLEDGEMENTS

Thanks are due to Prof. G. Familiari for the ideas given.

REFERENCES

Ambrogi V. (2014) Piero della Francesca's coral pendants: the hidden bronchial anatomy. Thorax. 69: 1161. https://doi.org/10.1136/thoraxjnl-2014-205344

Ashrafian H. (2023) Goiters in the renaissance era: multiple cases of thyroid autoimmunity and iodine deficiency. Best Pract Res Clin Endocrinol Metab. 37(2): 101748. https://doi.org/10.1016/j.beem.2023.101748. Epub 2023 Feb 15.

Ashrafian H. (2024) Goiter in the paintings by Rogier van der Weyden (1399-1464). J Endocrinol Invest. 47(2):483-484. https://doi.org/10.1007/s40618-023-02108-1. Epub 2023 May 12.

Barry D.S., Marzouk F., Chulak-Oglu K., Bennett D., Tierney P., O'Keeffe G.W. (2016) Anatomy education for the YouTube generation. Anat Sci Educ. 9: 90-96. https://doi.org/10.1002/ase.1550

Bramstedt K.A. (2016) The use of visual arts as a window to diagnosing medical pathologies. AMA J Ethics. 18(8): 843-854. https://doi.org/10.1001/journalofethics.2016.18.8.imhl1-1608

Britannica, The Editors of Encyclopaedia (2024). "Art". Encyclopaedia Britannica, 29 Mar. 2024, https://www.britannica.com/art/visual-arts. Accessed April 3, 2024.

Buta M.G. (2021) Genetic diseases in religious paintings. Medicine and Pharmacy Reports 94(3): 382-389. https://doi.org/10.15386%2Fmpr-1996

Christopoulou-Aletra H., Papavramidou N., Pozzilli P. (2007) Goitrous beauty in Artemisia Gentileschi's Judit and her Maidservant. Thyroid. 17(1): 37-38. https://doi.org/10.1089/thy.2006.0223

Dahan S., Shoenfeld Y. (2017) A picture is worth a thousand words: Art and Medicine. IMAJ 19(12): 772-776.

Facebook https://www.facebook.com/arteanatomia/

Fernandez-Flores A., Marqués Serrano O., Serrano S., Fonseca E. (2020) True frontal alopecia in 17th-century paintings. Clinics in Dermatology 38: 574-579. https://doi.org/10.1016/j.clindermatol.2020.04.002

Friedlaender G.E., Friedlaender L.K. (2013) Art in science: enhancing observational skills. Clin Orthop Relat Res. 471: 2065-2067. https://doi.org/10.1007%2Fs11999-013-3000-0

Gandhi JS. (2019) The rheumatoid hands of Renoir. Am J Med. 132(5): 658-659. https://doi.org/10.1016/j.amjmed.2018.12.034. Epub 2019 Jan 16.

Google Arts & Culture https://artsandculture.google.com/

Heyn R. (2018) The art of observation, from visual artworks to medical diagnosis: initial experience at Sapienza University of Rome. In: Orefice C., Baños J.-E. Monographs 38. The role of humanities in the teaching of medical students; Dr. Antoni Esteve Foundation, Barcelona. Pp. 116-125.

Jasani S.K., Saks N.S. (2013) Utilizing visual art to enhance the clinical observation skills of medical students. Med Teach. 35(7): e1327-31. https://doi.org/10.3109/0142159X.2013.770131. Epub 2013 May 3.

Langer E.J. (2000) Mindful learning. Curr Dir Psychol Sci. 9: 220-223. https://doi.org/10.1111/1467-8721.00099

Marder L. (2020) Rembrandt's Self-Portraits. Retrieved from: ThoughtCo. Aug. 28, 2020, https://www.thoughtco.com/rembrandts-selfportraits-4153454 Accessed March 28, 2024.

Table 5. Examples of artworks associated with artists' diseases.

Artist	Period	Disease	Artwork
Piero della Francesca	15th century	Thyroglossal duct cyst	Self-portraits ("Polyptych of the Misericordia" and "The Resurrection")
Albrecht Dürer	15th-16th centuries	Hyperthyroidism	Self-Portrait at Twenty-Eight
Michelangelo Buonarroti	16th century	Goiter; hand osteoarthritis	Self-portraits, poems, and letters
Michelangelo Merisi "Caravaggio"	16th-17th centuries	Syphilis; jaundice (acute hepatitis)	Self-portraits (Bacchus paintings during illness and after healing)
Francisco José de Goya y Lucientes	18th-19th centuries	Encephalopathy caused by chronic lead poisoning (saturnism); labyrinthitis; deafness; hallucinations	A sharp difference in light and color is noticed in his artworks before and after his health problems; letters
Joseph Mallord William Turner	18th-19th centuries	Color blindness and cataracts	A change in color shades of his artworks is noticed with the progress of his eye problems
Vincent van Gogh	19th century	Alcoholism; xanthopsia; Mèniére syndrome; glaucoma; epilepsy	Self-portraits and letters
Henri de Toulouse-Lautrec	19th century	Pycnodysostosis (genetic dwarfism); alcoholism and syphilis	Photographs
Pablo Picasso	19-20th centuries	Dysmorphic mental disorder (body dysmorphic disorder)	Self-portraits
Claude Monet	19th-20th centuries	Myopia and bilateral cataracts	A change in color shades and focus of the water lilies series is noticed before and after cataracts surgery; letters
Pierre-Auguste Renoir	19th-20th centuries	Myopia, rheumatoid arthritis, and later paralysis	Self-portraits, letters, and photographs
Edgar Degas	19th-20th centuries	Myopia and retinopathy	A change in color shades and in the focus of his paintings is noticed along the years; letters
Frida Kahlo	20th century	Bifid spine; infertility; pain; polytraumatism; amputation; post-traumatic fibromyalgia	Self-portraits (*La Columna Rota*; "The Broken Column", 1944), letters, photographs

Markatos K., Mavrogenis A.F., Karamanou M., Androutsos G. (2018) Pycnodysostosis: the disease of Henri de Toulouse-Lautrec. Eur J Orthop Surg Traumatol. 28(8): 1569-1572. https://doi.org/10.1007/s00590-018-2233-8. Epub 2018 May 24.

Miller A., Grohe M., Khoshbin S., Katz J.T. (2013) From the galleries to the clinic: applying art museum lessons to patient care. J Med Humanit. 34: 433-438. https://doi.org/10.1007/s10912-013-9250-8

Naghshineh S., Hafler J.P., Miller A.R., Blanco M.A., Lipsitz S.R., Dubroff R.P., Khoshbin S., Katz J.T. (2008) Formal art observation training improves medical students' visual diagnostic skills. J Gen Intern Med. 23: 991-997. https://doi.org/10.1007%2Fs11606-008-0667-0

Oberhelman S.M. (2014) Anatomical votive reliefs as evidence for specialization at healing sanctuaries in the ancient Mediterranean world. AJH. 1(1): 47-62. https://doi.org/10.30958/ajh.1-1-4

Powley E., Higson R. (2013) The arts in medical education. A practical guide. Second edition. CRC Press, London, pp. 67-84.

Pyeritz R.E. (2021) Arachnodactyly represented in art. Am J Med Genet. 187C: 163-167. https://doi.org/10.1002/ajmg.c.31930. Epub 2021 May 22.

Radonjic A. (2020) The undiagnosed patient in Christina's world. Am J Med. 133(2): 253-254. https://doi.org/10.1016/j.amjmed.2019.09.013. Epub 2019 Oct 14.

Srivastava A.A., Cohen S., Hailey D., Khoshbin S., Katz J.T., Gaske I.M. (2022) Training the eye, virtually: adapting an art in medicine curriculum for online learning. SN Soc Sci. (2022) 2:158. https://doi.org/10.1007/s43545-022-00442-4

Sterpetti A.V. (2019) Cardiovascular research by Leonardo da Vinci (1452-1519). Circ Res. 124(2): 189-191. https://doi.org/10.1161/CIRCRESAHA.118.314253

Sterpetti A.V., De Toma G., De Cesare A. (2015) Thyroid swelling in the art of the Italian Renaissance. Am J Surg. 210: 591-596. https://doi.org/10.1016/j.amjsurg.2015.01.027

Traversari M., Ballestrieri R., Galassi F.M. (2017) A likely cause of goiter in the Madonna col Bambino dormiente (1465/1470) by Andrea Mantegna (1431-

Table 6. Students' comments to the introduction of artworks along their medical curriculum (Adjective).

– Admirable	– Brilliant	– Concrete
– Creative	– Cutting-edge	– Different
– Engaging	– Fascinating	– Funny
– Innovative/very innovative	– Interesting/very interesting	– Original
– Pleasant	– Stimulating/very stimulating	– Unexpected

Table 7. Students' comments on the introduction of artworks along their medical curriculum (Sentence).

- A cultural, interesting, and ludic way of reconstructing medicine along history.
- A deep point of reflection on the concept of disease and medicine as elements influencing daily aspects of life, including artistic expression.
- An enjoyable way to renew my art interest, especially if treating topics that we usually only see in textbooks.
- Behind artworks, we have artists as well as models with their clinical history, strictly dependent on their own historical, social, cultural, and scientific period. Moreover, talented artists (from Monet to Michelangelo, from Egyptians to Kahlo) became "common" persons, suffering from the aches and diseases of our times.
- Certain concepts are fixed easily and for a long time.
- I have never thought that art could be so helpful.
- It is helpful to develop lateral thinking to stimulate concentration during the lessons, especially at the beginning of the core curriculum.
- It helps to apply anatomical knowledge in daily life and helps to think "out of the schemes".
- I have appreciated references to mental diseases and how these have an impact on art.
- Anatomy, like philosophy and literature, brings me joy. They share the common denominator of getting to know oneself from different perspectives, all equally fascinating and intertwined.
- Medicine is a fusion of sensitivity and technique. It is art more than art itself.
- It is exciting to realize how medicine has influenced art.
- Makes us reflect.
- It offers an alternative perspective of artworks, a more medical one. It looks for and explains anatomical variations or pathologies, thus helping to fix these concepts immediately.
- It opens the mind.
- Perfect mix between art and medicine.
- It shows me what it really means to have passion for a discipline. It is uncommon for a professor to share their own life, thoughts, and hobbies. These professors will remain in our memory as students.
- It stimulates "photographic" memory, curiosity, and intuition.
- The use of art as a tool to stimulate the clinical eye is advantageous in that daily life experiences may complement formal study from textbooks.
- The use of artworks both during in-presence lessons and *ad hoc* webinars has allowed a pleasant moment of relaxation, in between so many university commitments. The university is too concentrated on the "lessons calendar" rather than on ludic or interactive activities, which may be able to improve a student's day.

1506). J Endocrinol Invest. 40: 237-238. https://doi.org/10.1007/s40618-016-0548-z
Wikimedia Commons https://w.wiki/Ns
YouTube https://www.youtube.com/channel/UCU1c-4GTyIXC8YH-1ZcicsA and https://www.youtube.com/c/RosemarieHeyn

Finito di stampare da
Logo s.r.l. – Borgoricco (PD) – Italia

IJAE
Italian Journal of Anatomy and Embryology
Vol. 129, N. 1 – 2025

Visual Thinking Strategies for medico-anatomical teaching and rheumatological diagnostics: the case of M. L. Greville Cooksey's Maria Virgo (1915) 3
Donatella Lippi, Daniele Cammelli, Elisa Zucchini, Linda Vignozzi, Francesco M. Galassi, Immacolata Belviso, Ferdinando Paternostro, Elena Varotto

An anatomical drawing by Leonardo as the matrix for the landscape of his Monna Lisa? An anatomical analysis 9
Jean-Yves Maigne, MD

Transduodenal Surgical Ampullectomy: technical considerations 17
Paolo Panaccio, Pierluigi Di Sebastiano

Radiographic detection of anatomical variations in the mental foramen position in a sample of Salahuddin province population 21
Ban Sedeeq, Ali G. Abdullah, Marwan Saad Azzubaidi

Effect of streptozocin-induced diabetes on the histomorphometry of the liver and kidneys of male sprague dawley rats 29
Pfarelo A. Mbelengwa, Matome L. Mpholwane, Nkosi Xhakaza

A case report of the right vertebral artery's origin as a unique 'trifurcation' involving the brachiocephalic trunk, right common carotid artery, and the right vertebral artery 41
Cheryl Melovitz-Vasan, Susan Huff, Nagaswami Vasan

Corpus callosum motor fibers dissection using Klingler's method and methylene blue 47
Paulo Henrique Pires de Aguiar, Carolina Simão Martini, Giulia Bassalo Canals Silva, Giovanna Zambo Galafassi, Jemaila Maciel da Cunha, Giovana Figueira Rodrigues Vieira Pessano, Ricardo Silva Centeno

Technical update of Delalande's hemispherectomy 55
Danilo T. Queiroz, João Luís A. Trentini, Ricardo S. Centeno, Paulo Henrique Pires de Aguiar

Middle cerebral artery: a systematic review and meta-analysis 67
Nicole de Palma Gomes, Rubén David dos Reis Zuniga, Rafael Bobato Licciardi, Esther Araujo Dal Fabbro, Paulo Henrique Pires de Aguiar

Accessory diaphragm: Uncommon structure in partial anomalous pulmonary venous return (PAPVR) donor 75
Cheryl Melovitz-Vasan, Susan Huff, Nagaswami Vasan

Use of figurative artwork in clinical anatomy as a valid teaching tool to train visual skills and critical thinking: a pictorial guide 79
Rosemarie Heyn

€ 26,00 (for Italy)